Numerical Modelling of Flow and Settling in Secondary Settling Tanks

Dahl, Claus Poulsen

Publication date:
1995

Document Version
Publisher's PDF, also known as Version of record

Hydraulics & Coastal Engineering Laboratory
Department of Civil Engineering
Aalborg University
SERIES PAPER No. 8

ISSN 0909-4296

Numerical modelling of flow and settling in secondary settling tanks

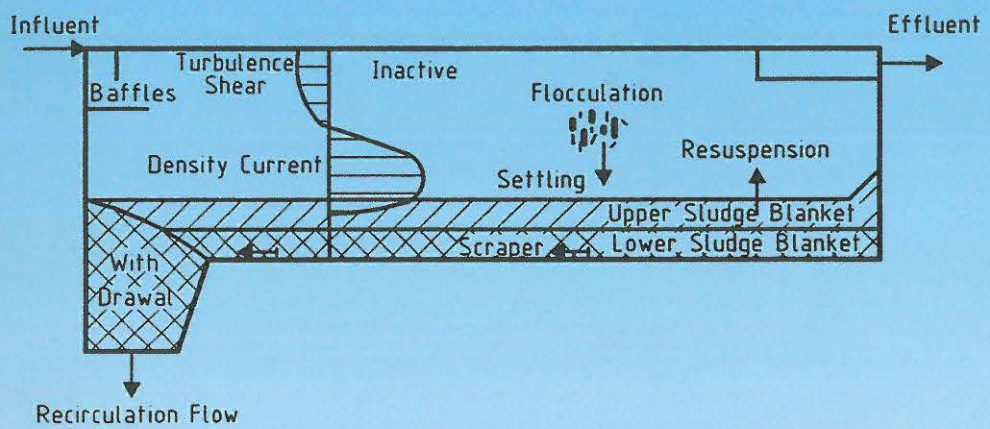

PH.D thesis, ATV project EF-359

Claus Dahl

Aalborg University - Denmark
Department of Civil Engineering

I. Krüger Systems AS
November 1993

Numerical modelling of flow and settling in secondary settling tanks

PH.D thesis, ATV project EF-359

Claus Dahl

Aalborg University - Denmark
Department of Civil Engineering

I. Krüger Systems AS
November 1993

Printed in Denmark by
REPRO, I. Krüger AS, January 1995
ISBN 97-90034-082

PREFACE

The present thesis has been prepared to fulfil one of the requirements for the Danish Ph.D. degree stipulated by the executive order of December 11, 1992 from the Danish Ministry of Education. The study was carried out as an industrial (Ph.D.) project with Professor Torben Larsen and Lecturer Ole Petersen as supervisors and was financially supported by ATV and I. Krüger Systems AS.

I would like to express my gratitude to Aalborg Øst wastewater treatment plant, to the Lynetten wastewater treatment plant and Slagelse wastewater treatment plant for their participation in the measurements.

I wish to thank my supervisors and the other members of my support group, Professor Poul Harremoës, Product Development Manager Keld Nymann Jensen, R&D Manager Erik Bundgaard, and Engineer Bente Nielsen for scientific guidance throughout the whole process.

I would also like to express my gratitude to Bodil Jensen for typing the thesis and correcting my written English and Marianne Beckmann for performing of the drawings.

Copenhagen, 8th November 1993

Claus Dahl

CONTENTS

RESUME

Denne afhandling omhandler udviklingen af en numerisk model til simulering af efterklaringstanke. Indledningsvis er beskrevet status for udviklingen inden for numeriske modeller for efterklaring og den nuværende designpraksis. Resultatet af denne statusbeskrivelse er et behov for videre udvikling for at indføre numeriske modeller i design af efterklaringstanke og hermed forbedre efterklaringstanke i fremtiden.

I en systemanalyse er de styrende fysiske processer i efterklaringstanke præsenteret og diskuteret. Processerne er strømnings- og slamtransportprocesser, aktive slamflokkes specifikke egenskaber samt processer for slam i suspension. På baggrund af systemanalysen opstilles en syntese for udviklingen af den numeriske model. Syntesen indeholder en beskrivelse af de nødvendige modelvariable for at inddrage alle styrende fysiske processer i den numeriske model. De basale antagelser for den numeriske model er ligeledes beskrevet i syntesen.

De i syntesen udpegede modelvariable er indført i den matematiske formulering af den numeriske model via fire undermodeller for henholdsvis strømning, turbulens, transport og flokkulering. Herudover beskrives strategien for verificeringen, kalibreringen og valideringen af den numeriske model. I den matematiske formulering opstår sammenhænge mellem modelvariablerne, som skal fastlægges enten via direkte målinger eller via kalibrering. De udviklede målemetoder for måling af sedimentation af slam i fri og hindret sedimentation, flokkulering og densititen af suspensionen præsenteres.

Et modeltankmåleprogram udviklet til kalibrering og validering af den numeriske model beskrives. De målte resultater viste god overensstemmelse med beskrivelsen af de styrende fysiske processer i systemanalysen. Parametre i modelbeskrivelsen af en Bingham plastik suspension kalibreres ved en sammenligning mellem modelsimuleringer og modeltankmålinger. Der er en god overensstemmelse mellem de simulerede og målte resultater. En validering af den numeriske model er udført ved sammenligning af modelsimuleringer fra den kalibrerede model med nye modeltankmålinger med nye begyndelses og randbetingelser, og også her er der en god overensstemmelse.

Til den endelige validering af den numeriske model sammenlignes modelsimuleringer med fuldskalamålinger på efterklaringstanke fra to forskellige spildevandsrenseanlæg. Modelsimuleringerne kan kun simulere storskalabevægelserne, men ikke de rigtige værdier for alle modelvariablerne. Alligevel er den numeriske model anvendt til undersøgelse af ændrede udløbsrender i en eksisterende efterklaringstank og viste en relativ forbedret udløbskvalitet

ABSTRACT

This thesis discusses the development of a numerical model for the simulation of secondary settling tanks. In the first part, the status on the development of numerical models for settling tanks and a discussion of the current design practice are presented. A study of the existing numerical models and design practice proved a demand for further development to include numerical models in the design of settling tanks, thus improving the future settling tanks.

The prevailing physical processes in secondary settling tanks are presented and discussed in a system analysis. These processes are the flow and sludge transport processes, the specific characteristics of activated sludge flocs and processes for sludge in suspension. The outcome of this analysis is a synthesis of the development of the numerical model presenting the model variables required to allow the physical processes to be included. Furthermore, some of the basic numerical model assumptions are described in the synthesis.

The mathematical formulation of the numerical model includes the necessary model variables pointed out in the synthesis and is organised as four submodels for hydrodynamic, turbulence, transport and flocculation. A strategy for the verification, calibration and validation of the numerical model is described. The mathematical formulation establish some relationship between model variables which must be found either by direct measurement or calibration. The procedures developed for basic measuring of settling of sludge in free and hindered settling regimes, flocculation and density of suspension are presented.

For the calibration and validation of the numerical model, a model tank measurement was developed. The model tank measurements showed an agreement with the description of the physical processes in the system analysis. By calibrating parameters in the model description of a Bingham plastic suspension, the numerical model simulated the model tank measurements with a reasonable agreement. By comparing model simulation from the calibrated model with new model tank measurements the numerical model is validated and the model proved to be quite accurate in terms of measurement prediction.

The numerical model is then validated by comparing the model simulations with measurements from full scale settling tanks at two different wastewater treatment plants. The model simulation can predict the large-scale motion in the settling tanks but cannot predict the correct value of all the model variables. Despite the problems with model simulation of full-scale settling tanks, the numerical model is used to improve an existing settling tank by increasing the outlet area.

1. INTRODUCTION

Settling by gravity of suspended solid which is heavier than water, is one of the most common processes in wastewater treatment. Settling tanks are used for primary settling of raw wastewater and secondary settling of activated sludge suspension from an activated sludge process. Secondary settling tanks are usually the last treatment step before discharge of the treated wastewater to a recipient. The quality of the treated wastewater must meet official standards which for most recipients are very high. Therefore, the function and reliability of secondary settling tanks must meet these standards for every load of the wastewater treatment plant. Loads of treatment plants are transient due to variation in water consumption during a day and wet weather loads.

The present design practice for secondary settling tanks is based on one-dimensional approaches where experience and measurements are used for empirical solutions. In this design practice, the main emphasis is on the hydraulic load and the settling properties of the sludge. Other physical processes which are important to settling tanks, e.g. flocculation, turbulence and rheology of suspension are not used in the immediate design practice. Furthermore, in the design practice the empirical solutions are limited to a certain normal variation in the operation of settling tanks.

This thesis attempts to develop a numerical model where all the prevailing physical processes for the flow and sludge transport in secondary settling tanks are included in the numerical model. By means of the numerical model the effect of each physical process and other operational variations can be examined. The numerical model can thus be used to predict the effect of modifications, to improve the performance of existing settling tanks and to develop a new design practice for settling tanks.

The development of the numerical model was done in the following steps: First, in chapter 2 the status of numerical modelling of settling tanks and the present design practice are described. Chapter 3 describes, a system analysis where the physical processes in settling tanks are presented and discussed and a synthesis for the development of the numerical model is presented. Chapter 4 describes the mathematical formulation of the numerical model divided into 4 submodels for hydrodynamic, turbulence, transport and flocculation. Furthermore, the model formulation is verified.

Basic measurements for measuring relationships between model variables were developed and are described in chapter 5. The instrumentation used for measuring velocities, sludge concentration and tracer concentration is also described in chapter 5. Model tank measurements were developed for calibration and validation of the numerical model and are described in chapter 6. Finally, the numerical model was validated for measurement in

full scale settling tanks in chapter 7, and chapter 8 describes an attempt to improve of a settling tank by using the numerical model. The closing chapter contains a summary of the work and the conclusions that emerge from this thesis.

2. STATUS

2.1 Numerical modelling

The present understanding of the hydraulic and solid transport characteristics in secondary settling tanks began with the work of Camp (1946) and Larsen (1977) who identified the different processes in settling tanks by an intensive literature and field study. Furthermore, Larsen (1977) described an attempt to develop a 2-dimensional mathematical models on settling tank behaviour. A further experimental investigation of settling tank behaviour was made by Lumley (1985), Lumley and Horkeby (1988) and Lumley and Balmér (1990) who presented a description of the important processes in different parts of settling tanks. Also dynamic changes of suspended solids (SS) concentration in effluent and return flow and sludge accumulation in settling tanks were studied by Lumley and Balmér (1987) and Lumley et al. (1988).

In the area of numerical modelling of settling tanks Imam and McCorquadale (1983) and Imam et al. (1983) presented a 2-dimensional model with a constant eddy viscosity model to describe the turbulence and a transport/dispersion model to describe dissolved matter. It was found that a more precise prediction of the turbulence was needed to predict the dispersion of dissolved matter. The 2-dimensional models were improved by Celik et al. (1985), Stamou et al. (1989) and Adams and Rodi (1990) under professor W. Rodi at the University of Karlsruhe. These results showed that a K-ϵ model could predict the turbulence field in settling tanks much better than a constant eddy viscosity models.

The solid transport/dispersion was described in Stamou et al. (1989) as non-flocculable solids with constant settling velocities for different fractions of the solid. This description of settling of solids was valid for settling in e.g. primary settling tanks. To describe the settling of flocculable activated sludge, hindered settling and hereby variation in settling velocities depending on the suspended sludge concentration were introduced by Laroc et al. (1983) and Dahl et al. (1990).

Dahl et al. (1990) also introduced processes such as rheology of activated sludge suspension and the influence of density difference on the turbulence levels in the model. With these processes a steady sludge blanket could be simulated. In Krebs (1991) the flow field in settling tanks was described and several attempts to increase the efficiency of a settling tank by changing the flow field were discussed.

At present, none of the mentioned models are at a stage where they are used in the practical design of settling tanks.

2.2 Present design practice

The secondary settling tanks described in this section are the most commonly used horizontal flow settling tanks, either rectangular or circular, in activated sludge treatment plants, see Fig. 2.1. Other settling tanks like vertical flow settling tanks "Dortmund tanks" and lamella settling tanks are not described.

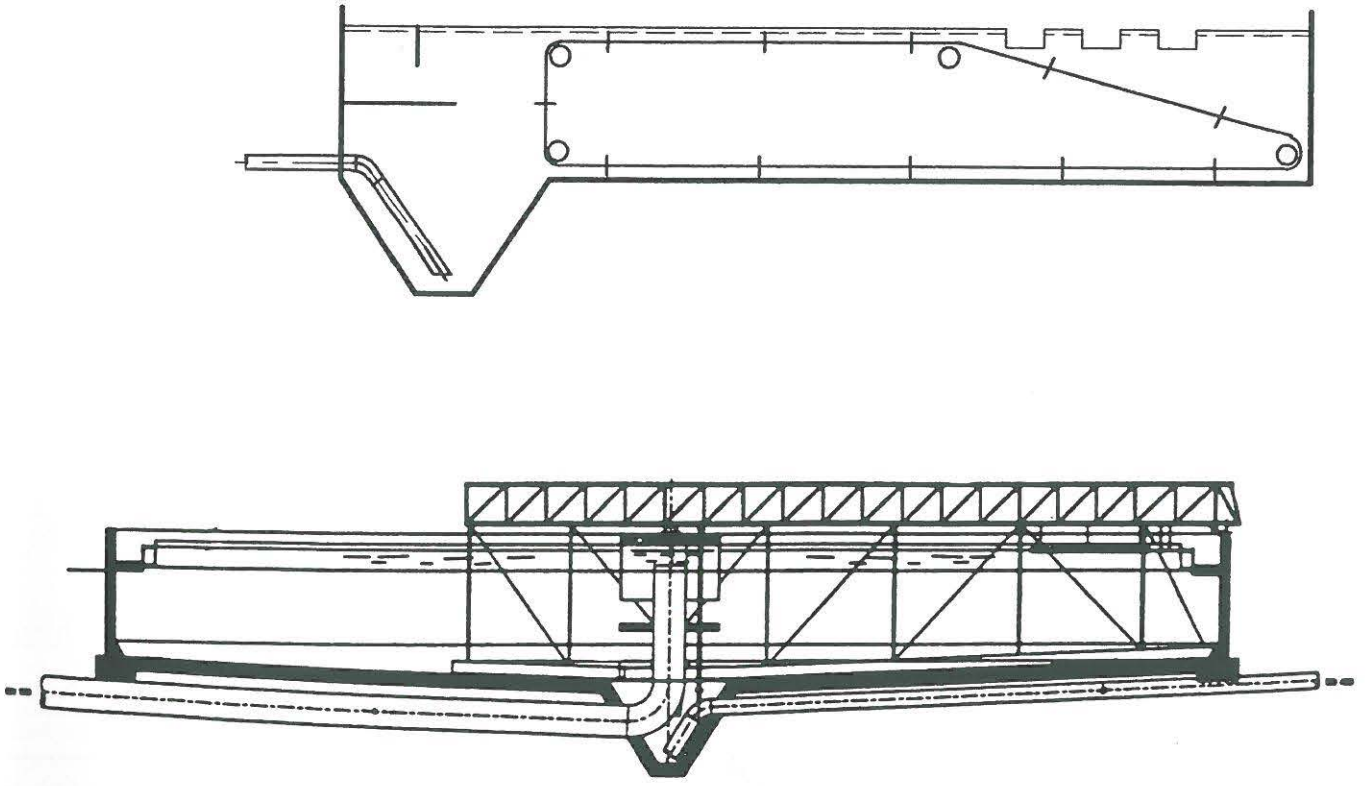

Fig. 2.1. Rectangular and circular, horizontal flow settling tanks.

2.2.1 Design practice

The following description gives an example of Danish design practice and is based on internal notes in Krüger (Krüger, 1993).
Today, wastewater treatment plants must comply with strict effluent requirements even during transient loads. Treatment in the secondary settling tanks is the last process in many treatment plants before discharge into the recipient. Therefore, requirements with respect to the functions and reliability of settling tanks are high, which must be considered in the design practice. The processes in the two tank types, rectangular and circular, are very similar. Thus the present design practices are similar for both tank types.

Process design parameters

As the first step, the design parameters surface area, depth and return sludge flow are found.

The external conditions affecting these parameters are

- Hydraulic conditions
- Sludge conditions
- Effluent quality requirements

Hydraulic conditions

Naturally, the hydraulic conditions must be considered when designing the settling tanks. The hydraulic loading over a given period on a treatment plant may differ considerably from plant to plant. A large number of variables can affect the hydraulic loading.

- Combined/separate sewer system
- Seasonal, weekly and daily load variations
- Wet weather load
- Infiltration in sewer system
- Storage capacity of the combined sewer network

In very few places, load measurements are available from hour to hour for a period of several years. If such measurements are available, the data can be treated statistically resulting in commulated fractile distribution and histograms of the load. In other cases, EDP models can be used to simulate the sewer system using rain events for several years. Furthermore, these model simulations are able to take new planned parts of the sewer system into account.

On the basis of the known hydraulic conditions, the maximum dry and wet weather load conditions are found for the commulated fractile to be used depending on the chosen reliability.

The maximum dry weather load is typically an 80% commulated fractile of the total load. The maximum wet weather load is typically 1.5 times but always below twice the maximum dry weather load. The effluent requirement for maximum wet weather load is up to 5 mgSS/l higher than for maximum dry weather load. Both loads are used in the design practice and the largest settling tank found with these loads are used.

Sludge conditions

The characteristics of the sludge separated in the settling tank must be considered. These characteristics are assumed to vary like the hydraulic load from one treatment plant to another depending on

- Wastewater characteristics
- Biological treatment

In order to include different types of sludge in the design practice, the following parameters are used to characterize the sludge

- Sludge volume index (SVI)
- Suspended sludge concentration (SS)

In the design practice, SVI and SS are some of the basic parameters for calculation of surface area, tank depth and return flow. Depending on the wastewater characteristics and the treatment processes, SVI is chosen in the order of 120 - 200 ml/g. On the basis of the SVI found, a SS concentration in the process tank is chosen. As a design rule, SVI*SS in the magnitude of 600 ml/l is chosen.

Effluent quality requirements

When designing secondary settling tanks, the SS concentration and the phosphorus concentration effluent demand, typically 20 mgSS/l and 1-1.5 mgP/l, respectively, must be considered. Depending on the dissolved phosphorus concentration and the phosphorus in the SS, the settling tanks must either be designed to meet the demand of 20 mgss/l or the phosphorus demand resulting in SS $<$ 20 mg/l.

An effluent concentration at 20 mgss/l is close to the practical limit of a settling tank performance, so if the effluent must contain less than 20 mgss/l, further treatment such as filtration is recommended. If filtration is used, settling tanks are designed for an effluent quality of 25 - 30 mgss/l.

Process design

Once the external conditions affecting on the process design parameters are described, the process design can be determined by means of the following calculations:

- Return sludge flow
- Surface area
- Sludge storage capacity, depth

where the sludge storage capacity needed gives the depth of the settling tank. In the process design, EDP models are used as a design tool. These models are developed as dynamic flux-theory models with empirical model descriptions based on experimental results especially from ATV (1988, 1991). Dynamic flux-theory models can be used to design settling tanks of a chosen length of wet weather loads, depending on the hydraulic conditions.

Return sludge flow

The return sludge flow is calculated from a mass balance, in which the SS concentration in the return flow depends on the following:

- SS concentration in influent
- Sludge volume index (SVI)
- Sludge blanket height
- Sludge concentration time (t_e)
- Short circuit Ω

The problem of calculating the SS concentration in the return flow is solved empirically as described in Bilmeier (1988). The SS concentration at the bottom of the tank SS_b is calculated by using t_e and SVI in the empirical equation.

$$SS_b = \frac{1000 \cdot 3\sqrt{t_e}}{SVI} \qquad (2.1)$$

The short circuit factor Ω is calculated from an estimated recirculation factor R_t by the empirical equation.

$$\Omega = 0.35 + 0.23 \ln(R_t) \qquad (2.2)$$

Eq. (2.2) is valid for settling tanks without inlet baffles to control the influent. For settling tanks with inlet baffles eq. (2.2) is changed to

$$\Omega = (0.35 + 0.23 \ln(R_t)) \cdot (100 - BF)/100 \qquad (2.3)$$

where BF is a factor typically at 80% for a good inlet design. Then the SS concentration in the return flow SS_r is calculated from equation (2.4) where SS_p is the SS concentration in the process tanks.

$$SS_r = \Omega \cdot SS_p + (1 - \Omega) \cdot SS_b \qquad (2.4)$$

A new R is found from the mass balance described as.

$$R = \frac{SS_p}{SS_r - SS_p} \qquad (2.5)$$

If R defers from R_t, a new calculation of SS_r is made using $R_t = R$. Then a new R is calculated. This procedure is continued until $R \approx R_t$.

Surface area

One of the best known process parameters is the hydraulic surface load defined as HOB = Q/A. For calculation of the necessary surface area A the following parameters are used:

- Q influent
- Q return flow
- SS influent (SS_p)
- SVI
- SS effluent (SS_e)

The surface area is calculated using the empirical theory from (Billmeier 1988) giving equation (2.6) and using a mass balance.

$$HOB = \frac{Q}{A} = \frac{100 \cdot H}{SS_p \cdot SVI \cdot (1+R)} \cdot \sqrt{\frac{SS_e}{3.15}} \qquad (2.6)$$

where H is the total tank depth and SS_e is the maximum effluent SS concentration. The equation is valid for SVI in the magnitude of 80 - 225 only.

Sludge storage capacity, depth

In order to design the settling tank depth, the necessary sludge storage capacity must be calculated. Sludge storage is necessary under wet weather loads in order to increase the SS concentrations in the return flow and to keep the sludge in the treatment plant. If the settling tank is designed correctly, a steady state will appear between the increased influent SS mass and the SS mass in the return flow without any sludge escape from the settling tank. The sludge storage capacity is calculated

by means of the mass balance including the calculation of the return sludge concentration in a dynamic algorithm with small time steps. When calculating the sludge storage, the mean SS concentration is assumed to be equal to the influent SS concentration. The SS concentration in the influent is equal to the SS-concentration in the process tanks.

Under wet weather loads, the SS concentration in the process tanks decreases due to the sludge storage capacity in the settling tanks. This storage can be up to 20% of the total SS mass in the process tanks, depending on the duration of the wet weather load. The sludge storing in the settling tanks affects the capacity of the biological treatment and must be considered when designing the entire treatment plant. The depth H is chosen in the magnitude of 3 - 5 m with 4 m as the recommended. H is the total depth combined by the depth of 4 zones seen on Fig. 2.2.

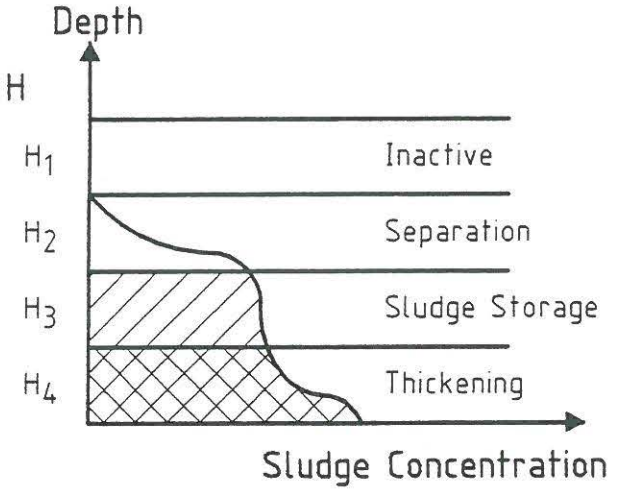

Fig. 2.2. Different zones in secondary settling tank.

The inactive zone depth H_1 is always 0.5 m. The separation zone depth H_2 is calculated from the empirical equation.

$$H_2 = \frac{0.3 \cdot Q \cdot (1+R)}{A \cdot \left(1 - \frac{SS_p \cdot SVI}{1000}\right)} \qquad (2.7)$$

The sludge storage zone depth H_3 is calculated by the following equations.

$$SS_{H_3} = \frac{H_2 + H_2/2}{H_2 + H_3 + H_4/2} \cdot SS_b \qquad (2.8)$$

$$H_3 = \frac{SLUDGE_{acc}}{SS_{H_3} \cdot A} \qquad (2.9)$$

where $SLUDGE_{acc}$ is the amount of sludge to be accumulated in the settling tanks under wet weather load. $SLUDGE_{acc}$ is calculated as the amount of sludge lost in the process tanks $SLUDGE_p$ and the amount of changed accumulation of sludge in H_4 $SLUDGE_{H4}$.

$$SLUDGE_{acc} = SLUDGE_p + SLUDGE_{H_4} \qquad (2.10)$$

The thickening zone depth H_4 is calculated from the equation.

$$H_4 = \frac{Q \cdot (1+R) \cdot (1-\Omega) \cdot SS_B \cdot t_e}{SS_B \cdot A} \qquad (2.11)$$

and

$$H = H_1 + H_2 + H_3 + H_4$$

On the basis of the found process design parameters of the return sludge flow, surface area and settling tank depth, the geometric configuration and machinery can be selected.

2.2.2 Geometric configuration and machinery

In connection with the process design of the settling tank the geometric configuration and machinery of the settling tank must be determined. The process design is based on the assumption that an optimum solution should be found.

The following areas of a settling tank are described.

- Inlet arrangement
- Outlet arrangement
- Scum removal
- Sludge collection system

These areas are different in rectangular compared to circular settling tanks and are described separately for the two tank types.

Rectangular settling tank

Based on the found surface area A in the process design, the tank length and width are decided within the following ranges.

$$5 < \frac{length}{width} < 7$$

assuming a max. length of 45 m for line scrapers and 50 m for chain scrapers. The length should not be less than 30 m and the width chosen between 4 and 8 m. The depth H of the settling tank was found in the process design.

Inlet arrangement

In the rectangular settling tank normally used, the influent is introduced directly above the return sludge pit. This might result in a high, short circuit flow if the influent arrangement is not designed correctly. The inlet arrangement, in which the influent is baffled away from the return sludge pit, is shown in Fig. 2.3.

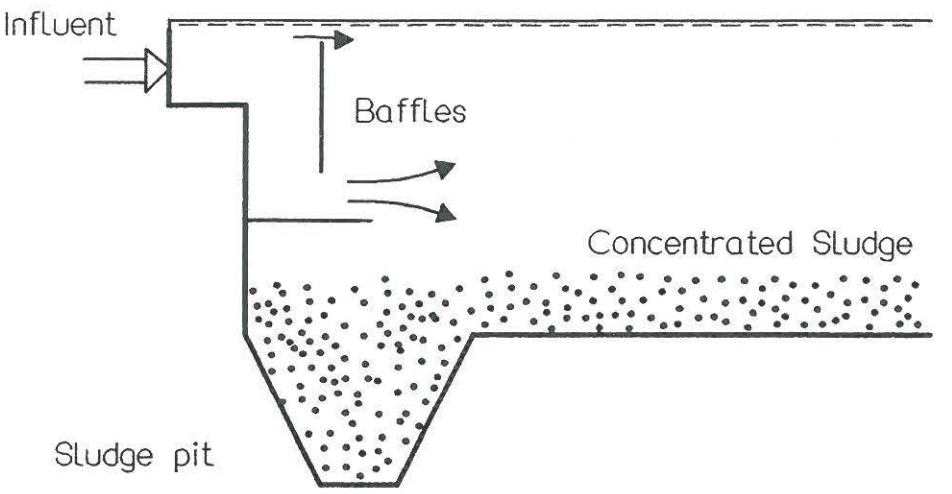

Fig. 2.3. Influent arrangement in rectangular settling tanks.

Baffling is important in rectangular settling tanks, in which the influent enters the settling tank over a board and falls down towards the sludge pit due to downward velocities and high density. This downward flow is changed with the baffling.

Effluent arrangement

In rectangular settling tanks, effluent weirs are placed at the most optimum spot without any extra cost because the maximum width is 8 m. Typically, the effluent weirs are placed in the outlet end of the settling tank, which explains the name used for this part of the settling tank. Nevertheless, the concentration of effluent weirs close to the end wall has proved to decrease the efficiency of the settling tank. The reason for this is rise of the sludge blanket caused by the high velocities over the effluent weirs affecting the pressure balance in the flow field known as the Bernoulli effect. Therefore, effluent weirs are spread over a larger surface area. See Fig. 2.4.

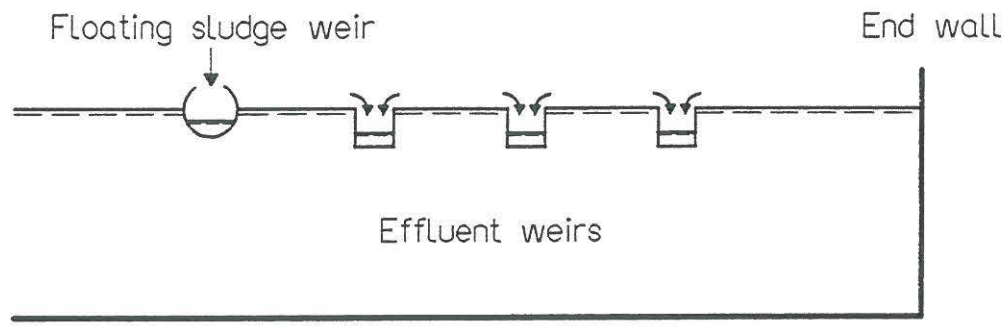

Fig. 2.4. Exampel of placement of effluent weirs.

Scum

In rectangular settling tanks, the scum on the water surface is removed by a special weir placed at the water surface in front of the effluent weirs, see Fig. 2.4. If chain sludge scrapers are used, the scum is transported towards the scum weir. If no system for collection of scum is present, the effluent quality will decrease due to increased SS concentration of typically 5 - 10 mgss/l and in some cases even more.

Sludge collection systems

The purpose of the sludge collection system is to transport the concentrated sludge on the tank bottom to the process tanks. This can be done in several ways either by scrapers transporting the sludge towards a return sludge pit or through suction direct from the tank bottom. In principle, the most commonly used scrapers can be designed in two ways, as chain scraper, see Fig. 2.5.a, or as line scraper, see Fig. 2.5.b.

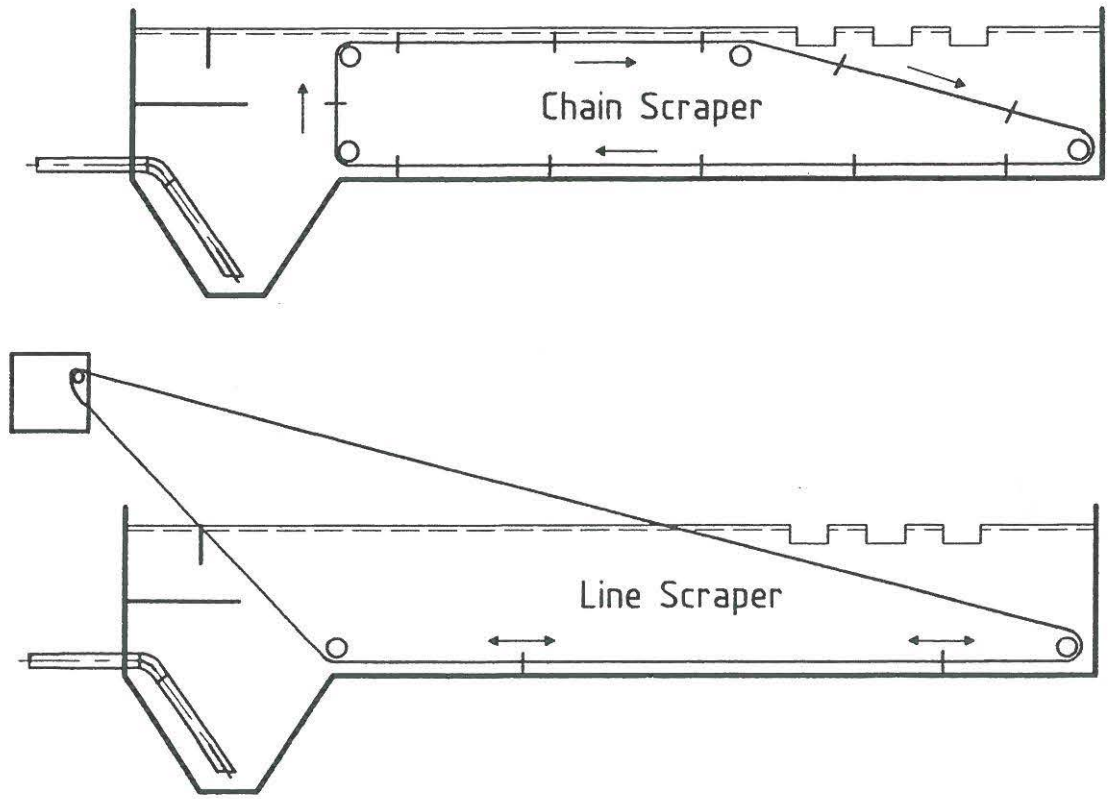

Fig. 2.5. Scraper for rectangular settling tanks.

Circular settling tanks

The calculation of the diameter D of a circular settling tank is based on the process design surface area. For practical reasons D $\geq$ 10 m. The tank depth found in the process design is defined at 2/3 of the radius.

Inlet arrangement

The influent enters the circular settling tank through a vertical inlet pipe and falls downwards due to density differences between the influent and the surrounding suspension. Baffles are installed to prevent the downward flow from reaching the return sludge pit. See Fig. 2.6.

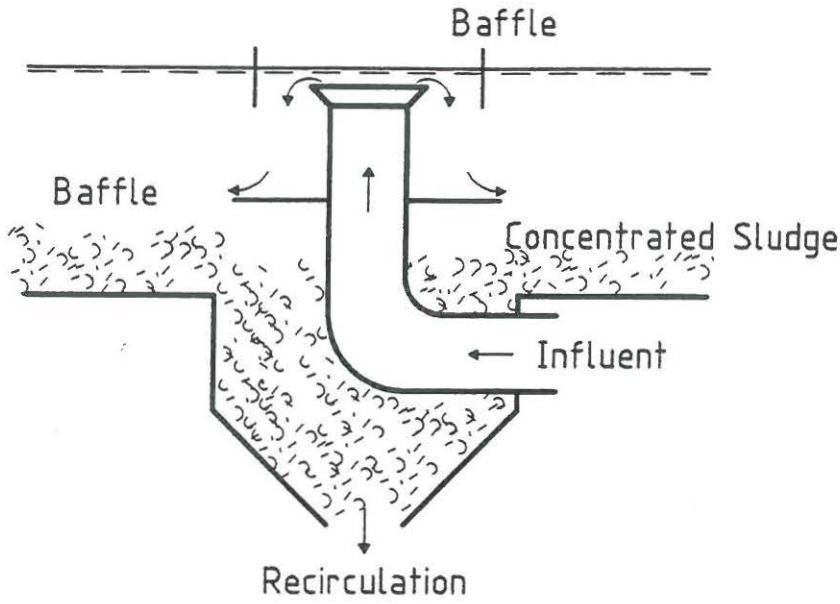

Fig. 2.6. Inlet arrangement for circular settling tanks.

Outlet arrangement

To reduce constructional costs, the effluent weir in circular tanks is normally placed near the outer wall. This means a risk of resuspended suspended solids in the effluent caused by that reason described previously. If the effluent weir is placed near the end wall, experience shows that effluent must pass from the centre side only, as shown in Fig. 2.7.

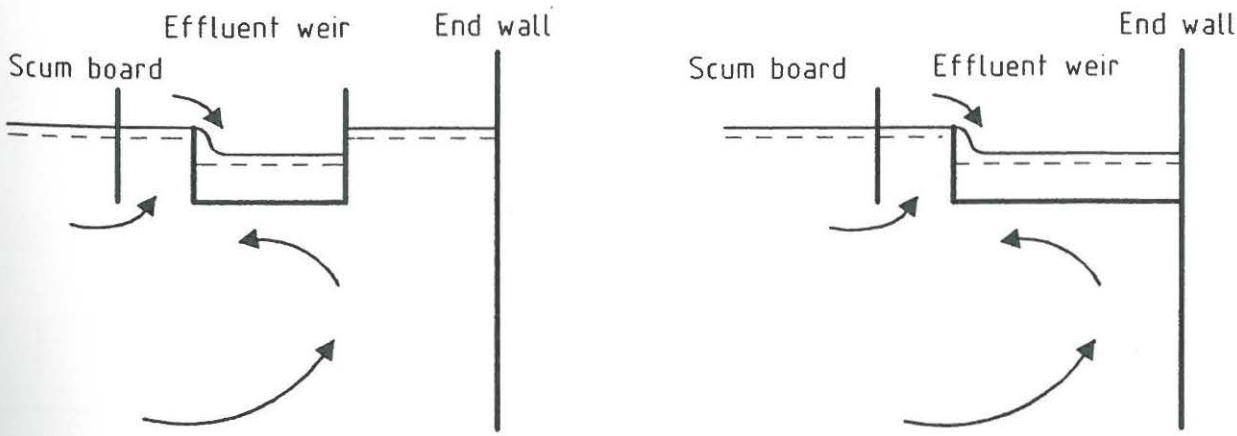

Fig. 2.7. Outlet arrangement for circular settling tanks.

Both solutions from Fig. 2.7 are used, and they have almost the same effect.

Scum

In addition, Fig. 2.7 shows the most simple solution to prevent scum in the effluent. Just in front of the effluent weirs a scum board is placed. A more efficient and expensive solution is to install a scum scraper and a sludge pit on the scraper bridge, and pump the scum away from the sludge pit. See Fig. 2.8.

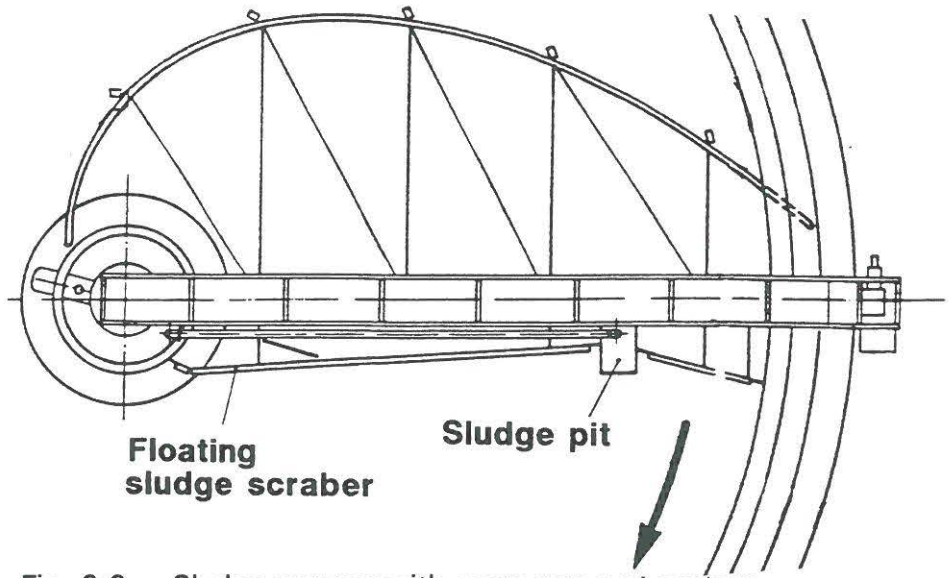

Fig. 2.8. Sludge scraper with scum removal system.

Sludge collection system

Sludge collection systems in circular settling tanks can also be designed either as scrapers or suction devices. Fig. 2.8 shows a single scraper. The scrapers can either be a single scraper as in Fig. 2.8, a one and a half or a double scraper depending on the sludge collection needed.

3. SYSTEM ANALYSIS

Secondary settling tanks are usually the final treatment of the wastewater, where activated sludge generated by activated sludge processes in the biological treatment of the wastewater are separated from the clean water. See Fig. 3.1.

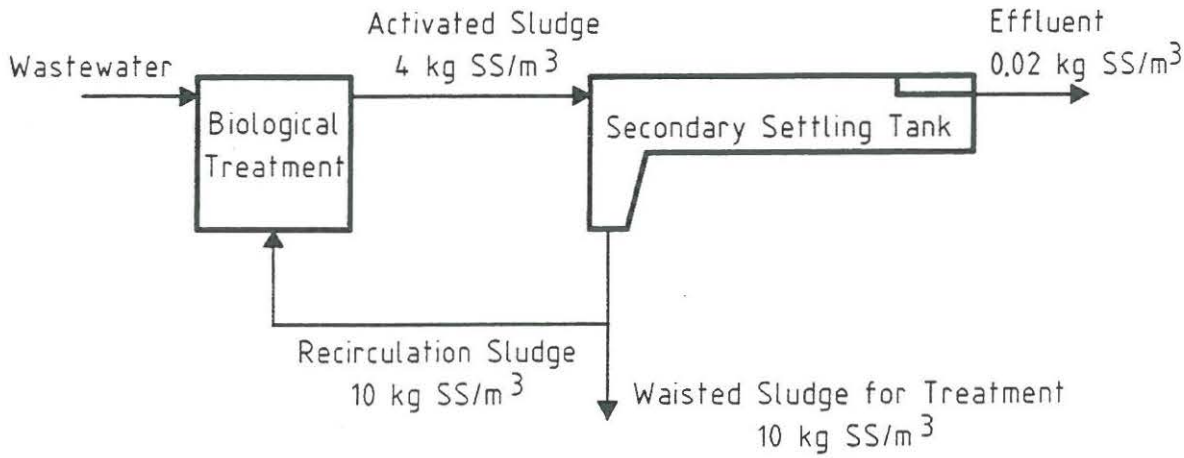

Fig. 3.1. Secondary settling tank in a wastewater treatment plant.

The settling tank receives the influent activated sludge suspension and must provide a effluent quality which meets official standards and a highly concentrated sludge to return to the activated sludge processes and to waste sludge for further treatment.

A more detailed analysis of the physical processes affecting the flow and sludge transport in a settling tank and the characteristics of activated sludge are described in the following.

3.1 Flow and sludge transport

To get a view of the secondary settling tank, Fig. 3.2 can be considered as a longitudinal cross section of a rectangular settling tank or a cross section of a circular settling tank where the inlet is in the centre.

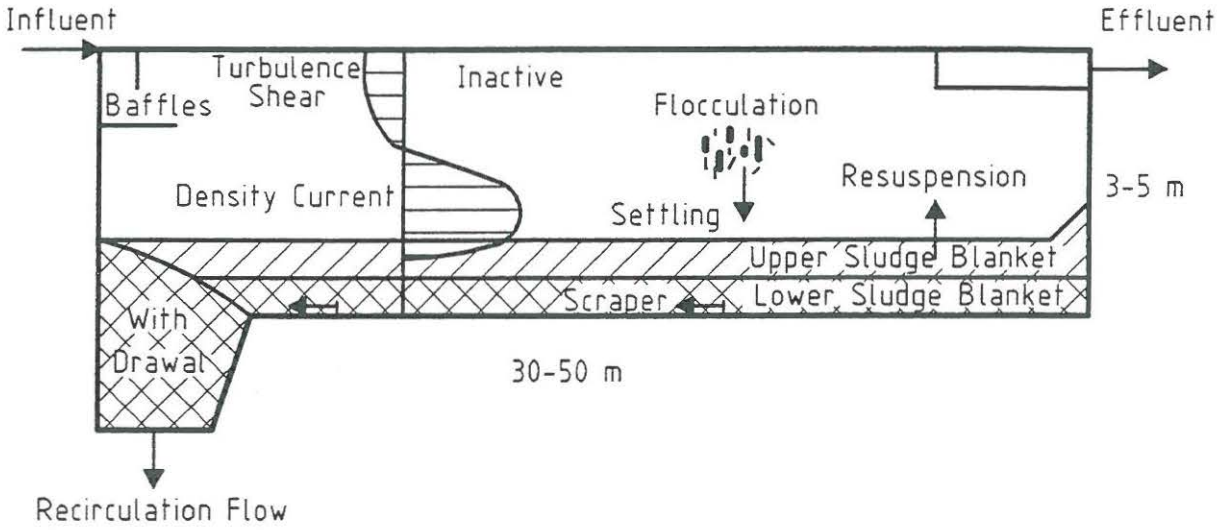

Fig. 3.2. Physical processes in a secondary settling tank.

Fig. 3.2 displays the physical processes which are significant to the function of the settling tank according to Larsen (1977), Lumley and Balmér (1990), Dahl et al. (1990) and Petersen (1992).

In the following, these physical processes are described in different zones of the settling tank. Lumley and Balmér (1990) suggested a division in 7 zones where the zones are chosen according to a difference in sludge concentration and zones where physical processes predominate.

Influent zone

The influent zone is characterized by a weakly 3-dimensional (3D) flow and a high level of turbulence and mixing due to the high energy in the influent. The energy in the influent consists of kinetic energy and potential energy caused by density differences between the influent and the surrounding suspension. Differences in sludge concentration induces the density differences. Kinetic energy starts to transform by dissipation into heat and by mixing into potential energy when turbulence as vertical mixing has to work against gravity (Larsen, 1977). The potential energy in the influent creates the density current and draws a portion of the influent directly into the recirculating flow causing short circuiting. The short circuiting is limited by inlet baffles to direct the influent away from the withdrawal zone.

Flocculation changes dynamically the size distribution of the dispersed particles and flocs. The flocculation responds to variations in turbulence levels and concentrations and forms dispersed particles and flocs in a wide size range, giving a range of settling velocities. The turbulence in this zone thus affect the flocculation.

Density current

The creation of a density current above the sludge blanket as a horizontal flow makes the flow in a secondary settling tank a stratified flow phenomenon (Larsen, 1977), (Cordoba-Molina et al., 1979) and (DeVantier and Laroc, 1987). The density current is characterised by a 2D flow and a relative constant velocity in the magnitude of 3-6 cm/s. An increase in hydraulic load does not increase the velocity but the height of the density current (Larsen, 1977).

A large part of the sludge transport and settling in a settling tank takes place in the density current. At the top of the density current with low sludge concentration, each dispersed particle and floc settle separately with a settling velocity depending on the density, size and shape. Flocculation also effect the size range here due to turbulence. The part of the sludge with high settling velocities will settle out in the first part of the settling tank, while the part settling more slowly is transported through the settling tank by the density current. Sufficient time must be provided for the sludge to traverse the density current and settle out, before the density current reaches the effluent end.

At the bottom of the density current where the sludge concentration is higher, the vertical differences in density interact with turbulence as vertical mixing has to work against gravity which increases the dissipation of turbulence. This may be one of the processes behind the formation of the sludge blanket. The vertical mixing nevertheless resuspend sludge from the sludge blanket into the density current and works against settling.

Effluent zone

In the effluent zone the effluent is drawn towards the effluent weirs with relatively high vertical velocities. To provide a high effluent quality the vertical velocities must not exceed the separate floc settling velocities and draw the sludge with the effluent. As mentioned previously, the sludge must settle out of the density current before the effluent end to prevent the withdrawal. But the dispersed particle and flocs with the lowest settling velocities often remain in the density current and can make the effluent quality critical.

Inactive zone

As a result of the stratification, the inactive zone is created. This zone may occupy a substantial volume of the settling tank depending on the sludge blanket height. The flow field is a slow 2D return flow toward the inlet end.

Upper sludge blanket zone

Activated sludge separated from the density current settles out on top of the accumulated sludge. The sludge accumulates until a concentration is reached where contact is made between the flocs. This concentration often defines the sludge blanket interface. The upper sludge blanket zone contains a sludge buffer, which means that the zone height rises and falls with the sludge blanket. The buffer zone is designed to allow accumulation of an amount of operating sludge, so that the effluent concentration is not affected by nominal sludge blanket levels. The compression of the sludge in the upper sludge blanket zone is affected by the sludge settling characteristics, the sludge blanket height and the retention time in this zone.

Changes in the rheology characteristics are one of the reasons for relatively low velocities under the sludge blanket interface and the flow is mainly laminar due to the increased dissipation of turbulence and the stable vertical density gradients.

Lower sludge blanket zone

The activated sludge thickens in the sludge blanket, so it accumulates at higher concentrations on the settling tank bottom. In experiments reported by Lumley (1985) it is observed that the iso-concentration line around 10 kgss/m3 was almost stationary in different tests, while the iso-concentration line at 3-5 kgss/m3 varies with the sludge blanket height. It is this stationary zone which is the lower sludge blanket zone. In this zone sludge collection systems are transporting the sludge either mechanically toward the sludge pit or by hydraulic suction devices out of the settling tank. Sludge transport in the sludge blanket can also be performed by a hydraulic flow induced by the overall flow field.

Withdrawal zone

The thickened sludge which is transported towards the sludge pit either mechanically or hydraulically, is mixed with the short circuited influent in the withdrawal zone. From sludge concentration measurement by Lumley (1985) it is seen that the sludge concentration in the recycle and the concentration on the edge of the sludge pit are approximately similar. This indicates that the mixing of the thickened sludge and the influent takes place outside the sludge pit. This mixing decreases the efficiency of the settling tank.

3.2 Transient load

With the understanding from the previous description of a secondary settling tank, the following will describe how critical conditions can occur in settling tanks under transient loads. Transient loads on wastewater treatment plants during wet weather affect the secondary settling tank after a short delay caused by the fact that the flow first has to run through the previous parts of the treatment plants.

At wet weather loads mass transfer of sludge to the settling tank increases to a level typically beyond the capacity of the settling tank. The sludge blanket height responds to such an increasing sludge load and starts to rise (Lumley and Balmér, 1987). Increased accumulated sludge and sludge blanket height can affect the effluent quality. With a higher sludge blanket the effective pressure in the sludge network matrix increases. The increased effective pressure increases the compaction rate near the tank bottom, resulting in a higher concentration in the return flow. This process depends on the retention time of the sludge in the sludge blanket part and the effective pressure during the retention time.

Increased sludge accumulation is not the only condition to be considered under wet weather loads. Increased hydraulic loads will increase the turbulence in the entire settling tank and affect the sludge floc size distribution and the settling characteristics of the sludge (see section 3.3.2) leading to less efficient settling of the sludge and higher sludge blanket height. An increased turbulence level will also increase the hydraulic dispersion of the sludge.

The density current height increases with increased hydraulic loads, which makes the distance the settling sludge has to traverse before reaching the sludge blanket longer. If sufficient time for traversing the density current is not available before the density current reaches the effluent end, the higher velocities near the effluent weirs will increase the size of selective withdrawal of highly concentrated suspension from the sludge blanket.

3.3 Activated sludge

Below a more detailed description of the highly cohesive organic material activated sludge is presented. This section is divided into two subsections, one describing characteristics of activated sludge flocs themselves and one the characteristics of activated sludge in suspension.

3.3.1 Activated sludge flocs

Activated sludge flocs consist of bacteria, dead organic and inorganic material formed by bioflocculation and a bacterial structural network (Andreasen et. al, 1990), (Li and Ganczarczyk, 1986) and (Parker et al., 1972). Bioflocculation is accomplished by exopolymer bridging, created from exopolymer secretion from the bacteria. The bacterial structural network is provided by filamentous microorganisms, acting as a backbone for attachment of bacteria, dispersed particles and for the structural integrity of the flocs. Besides the activated sludge flocs, a ciliate protozoa community is present in activated sludge, which feed upon bacteria and dispersed particles (Esteban et al., 1991).

Li and Ganczarczyk (1986) reported that 13 physical characteristics of activated sludge flocs have been studied. These characteristics and their interdependent relationship are listed in Table 3.1.

No.	Parameter	Directly measured	Derived	Can be derived from characteristics of	Can influence other characteristics of
1	Size	Yes	Yes	Surface area Settling velocity Volume	Surface area Volume Settling velocity Density Strength Water release Porosity
2	Surface area	Yes	Yes	Size Volume	Volume
3	Volume	No	Yes	Size Surface area	Surface area
4	Shape	No	No	—	Surface area Volume Strength Settling velocity
5	Filament number and length	Yes	No	—	Size Settling velocity Density Strength Surface area
6	Settling velocity	Yes	No	—	Density
7	Density	Yes	Yes	Size Settling velocity	Porosity Water content
8	Strength	No	Yes	Size	Size Water release
9	Porosity	No	Yes	Density	Water content Pore radius Tortuosity
10	Water content	No	Yes	Density	Porosity Water release
11	Water release	Yes	No	—	Water content
12	Pore radius	No	Yes	Surface area Porosity	—
13	Tortuosity	No	Yes	Porosity	—

Table 3.1. Physical characteristics of activated sludge flocs and their interdependence (Li and Ganczarczyk, 1986).

From table 3.1 it appears that the settling velocity is closely related to the density and the size of the sludge flocs, which according to table 3.1 can be deduced from the settling velocity. Therefore the following description of physical characteristics of activated sludge flocs will concentrate on the sludge floc size, flocculation and density. A description of the sludge flocs settling velocities is found in section 3.3.2.

Activated sludge flocs sizes

Owing to the way in which they are formed sludge flocs have irregular shapes. Therefore, they can be described in different ways, e.g. longest dimension, shortest dimension, perimeter and breadth and height. When

looking at measurements of activated sludge floc sizes, it is necessary to note the used definition (Li and Ganczarczyk, 1986).

From flocculation theory, flocculation and disintegration rates are affected by Brownian diffusion for interparticle collisions, laminar and turbulent fluid shear and different settling velocities of particles and flocs (O'Melia, 1985). In Li and Ganczarczyk (1986) and Parker et al. (1972) the effect of flocculation and disintegration rates on dispersed particle and floc sizes were described more practically, to depend on the processes turbulence level, sludge component (bacteria, dead organic and inorganic material) and sludge concentration. The effect of these processes on the dispersed particle and floc sizes are described in the following. Turbulent eddies induce surface erosion of dispersed particles on sludge flocs when the maximum surface shearing stress exceeds the shear strength of the exo-polymer bridge bonds attaching the dispersed particles to the floc surface (Parker et al., 1972). Turbulent eddies can also induce disintegration of activated sludge flocs. In Parker (1970) it was found that the rate of surface erosion was influenced by small eddies in the viscous dissipation subrange. Because of the nature of turbulence the large scale motion is passed on to smaller scale and finally down to the viscous dissipation sub-range (Rodi, 1984). The rate of erosion on activated sludge flocs is therefore affected indirectly by the large scale motion.

In the viscous dissipation subrange turbulence energy is lost into heat. Camp and Stein (1943) described all the energy lost as heat by the velocity gradient at one point G_P by

$$G_P = \sqrt{\frac{\Phi_p}{\mu}} \tag{3.1}$$

where Φ_p is the work of shear per unit of volume per unit of time at the point and μ is the dynamic viscosity. For flocculation a root mean-square (rms) velocity gradient G_m for a volume is found to be directly proportional to flocculation (Camp and Stein, 1943).

$$G_m = \sqrt{\frac{\Phi_m}{\mu}} \tag{3.2}$$

where Φ_m is the mean of Φ_p in the volume. A more conventionally used rms velocity gradient is presented in Parker et al. (1972).

$$G = \sqrt{\frac{\epsilon}{\nu}} \tag{3.3}$$

where ϵ is the energy dissipation per unit of mass per unit of time and $\nu = \mu/\rho$ the kinematic viscosity.

Parker et al. (1972) measured the dispersed particle and floc size distribution in a laboratory experiment at specific turbulence levels. See Fig. 3.3.

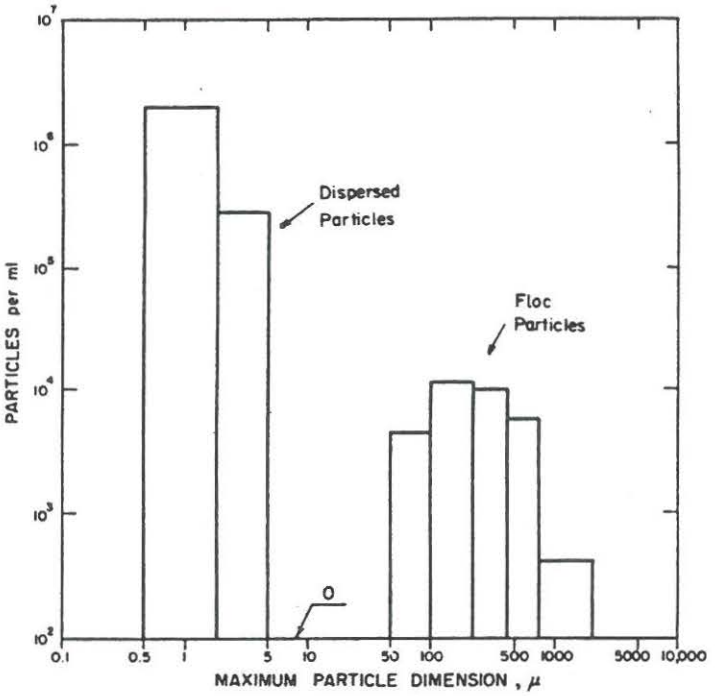

Fig. 3.3. Floc size distribution at $G = 79\ s^{-1}$ (Parker et al., 1972).

Fig. 3.3 shows a bimodal division, i.e. the sludge flocs with filament network and the dispersed particles. A large fraction of the sludge flocs is eroded because the size of the flocs is larger than the viscous dissipation subrange. There are two reasons why the flocs are maintained. Firstly, the flocculation rate is higher than the breakup rate and secondly, the presence of a filament network giving the flocs a stronger shear strength (Parker et al., 1972). The importance of filamentous bacteria for the activated sludge floc size is illustrated in Fig. 3.4.

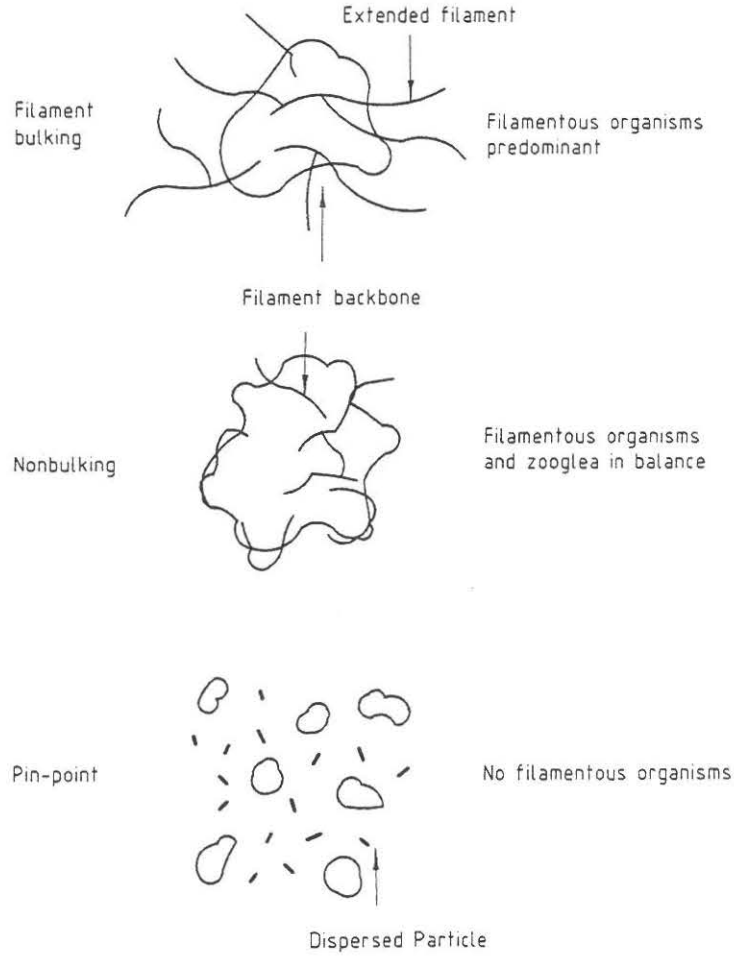

Fig. 3.4. Floc types for different filament levels (Palm and Jenkins, 1980).

Fig. 3.4 illustrates how these three types of sludge flocs, i.e. bulking sludge, 'ideal sludge' and pin-point sludge, can be viewed in terms of the relation between the filamentous and the zoogloeal (flocculating) organisms present. Ciliate protozoa's ability to feed on bacteria and dispersed particles is found to stimulate the flocculation (Esteban et al., 1991), and accordingly, the floc size is increased.

The activated sludge concentration can affect the sludge floc size in two ways. With an increased concentration, the average floc size increase due to increased opportunities for collision between particles. At a high concentration, two other phenomena, squeeze and split, occur, and the average floc size decreases (Li and Ganczarczyk, 1986) and (Javaheri and Dick, 1969). Li and Ganczarczyk (1991) have examined the distribution of sludge flocs sizes on different quantities for five conventional wastewater treatment plants. See table 3.2.

Size, μm	Distributions			
	By number	By area	By volume	By mass
<2	30–80%	<2%	Negligible	2–8%
2–16	17–70%	1–8%	Negligible	5–28%
16–128	1–4%	20–70%	10–80%	50–80%
128–256	<1%	5–50%	10–70%	5–25%
>256	Negligible	0–50%	0–60%	0–30%

Table 3.2 Distribution of activated sludge floc sizes on different quantities.

From Table 3.2 it is seen that the sludge flocs (< 2 μm) with small settling velocities amount to 2-8 % of the total mass. With an influent concentration in the magnitude of 3-5 kgss/m^3 and a demand for effluent concentration in the magnitude of 15-20 gSS/m^3, a sufficient part of these small flocs has to settle in the secondary settling tank in order to give a good effluent quality.

Density

The individual activated sludge floc settling velocity increases with an increased floc density (Li and Ganczarczyk, 1986). According to measurements carried out by Dammel and Schroeder (1991) floc density varies between 1.02-1.06 g/ml for seven activated sludge treatment plants and with little variation over time at each treatment plant. This indicates that the floc density depends on the wastewater characteristics and the treatment process.

The results from studies of the relationships between the floc size and the floc density show that the floc density decreases with increased floc size. This indicates an increased porosity of the floc with increased floc size (Li and Ganczarczyk, 1986).

3.3.2 Activated sludge in suspension

In this section, the characteristics of activated sludge in suspension will be described with respect to the settling and the rheology of the suspension. Normally, the settling is divided into three categories: free settling, hindered settling and compaction, depending upon the sludge concentration.

Free settling

Free settling occurs at low sludge concentrations, where each floc and dispersed particle settle with their individual settling velocity. The individual settling velocity is mainly related to characteristics such as floc size and floc density which is described in section 3.3.1. The relationship between individual floc settling velocity and the floc size was measured by a multi-exposure photographic method by Li and Ganczarczyk (1987) with the results as shown in Fig. 3.5.

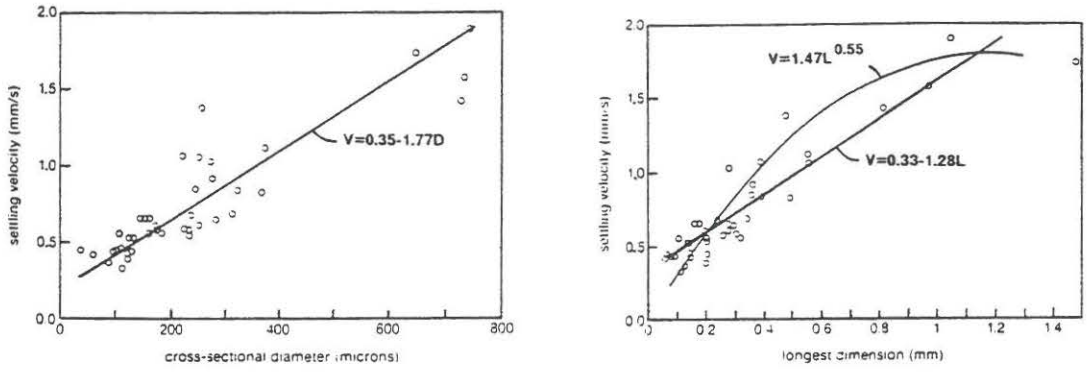

Fig. 3.5. Relationship between individual floc settling velocity and floc size (Li and Ganczarczyk, 1987). a. cross-sectional diameter, b. longest dimention.

The correlation coefficient is calculated to be 0.75 for the cross-sectional diameter and 0.90 and 0.88 for the longest dimension size scale for linear and power function, respectively. One of the uncertainties of the photographic sizing method is that the irregular flocs are seen from one side only. From Fig. 3.5 it appears how important floc size is for the settling of activated sludge and thus for the capacity of a secondary settling tank.

Hindered settling

At an increasing concentration, free settling gradually changes to hindered settling. According to Mandersloatet al. (1986), who examined solid-liquid separation, this will happen when the volumetric concentration of the solid is ($\Phi > 0.15$). The volumetric concentration Φ is defined to have a value between 0 and 1 with $\Phi = 0$ for clean water and $\Phi = 1$ for the highest suspended solid concentration which can be obtained under settling and compaction.

As the sludge concentration increases, settling velocities are influenced by both direct and indirect (i.e. hydrodynamic) interaction among the sludge flocs. The effect of hydrodynamic interaction can be taken into account by using Φ of the sludge (Buscall and White, 1987).

The effect of direct interaction is working in two ways. Direct interaction affects the size distribution of flocs and thus the volume concentration of the sludge and it allows energy to be stored in a particle network matrix by means of potential energy and to create a particular pressure. More correctly it is an effective pressure. The particular pressure affects the force balance of the whole suspension (Buscall and White, 1987). Calibrated relationships for the hindered settling velocity and the volumetric sludge concentration according to the Ritchardson and Zaki expression are reported for specific activated sludge by Lavelle (1978) and Laroc et al. (1983) with power coefficients α at 4.65 - 4.7.

$$v_s = v_0 \cdot (1 - \Phi)^{\alpha} \tag{3.4}$$

where v_s is the hindered settling velocity, v_o is the free settling velocity and α is a constant.

Other investigators, Pitman (1984), Daigger and Roper (1985), Koopman and Gadee (1983), Wahlberg and Keinoth (1988) and Rachwal et. al (1982) have found good relationships between settling velocities in hindered zone and sludge concentration with the following expression first presented by Vesilind (1968).

$$v_s = v_0 \cdot a^{(\alpha \cdot C)} \tag{3.5}$$

where a and α are constants and α=f(SVI) in some cases and C is the sludge concentration. a and α have to be measured for each type of sludge. These relationships are compared with settling velocity measurements at different SVI's and are in most cases found to give a good prediction of the hindered settling velocity. Wahlberg and Keinoth (1988) tried to set up an expression for all SVI's (e.g. stirred, deluded and not stirred), but only succeeded in setting up one expression for each kind of SVI.

In case of a high filament level in the activated sludge where extended filaments reach out of the flocs 'bulking sludge' see Fig. 3.4, a network matrix is created at low concentrations in which the distance between the flocs is larger than for 'ideal sludge', Fig. 3.4. This results in a lower settling velocity at a specific sludge concentration. The network matrix between sludge flocs in the hindered settling zone creates a situation where flocs and particles are captured in the network matrix. As shown in Table 3.2, 2 - 8% of the total mass have sizes below 2 μm and have therefore low settling velocities. A large part of these, 2 - 8% of the total mass, will be captured in the network matrix and filtrated out of the suspensions. This filtration is important for a good effluent quality.

Compaction

At high sludge concentrations where $\Phi \rightarrow 1$, the thickening of sludge is no longer referred to as settling but as compaction of sludge as there are no flow velocities. The compaction is induced by the effective pressure from the upper layers of sludge, separating water from the suspension (Mandersloat et al., 1986).

In the compaction regime, a high filament level will reduce the effective pressure due to lower concentrations in the upper layers of sludge, and the compaction will be less efficient.

Rheology of activated sludge suspension

At high sludge concentrations in the sludge blanket the rheology of the suspension changes and is found to be Bingham plastic or pseudoplastic with yield strength as well as thixotropic (Dick and Ewing, 1967), (Wood and Dick, 1975) and (Campbell and Crescuolo, 1982). See Fig. 3.6.

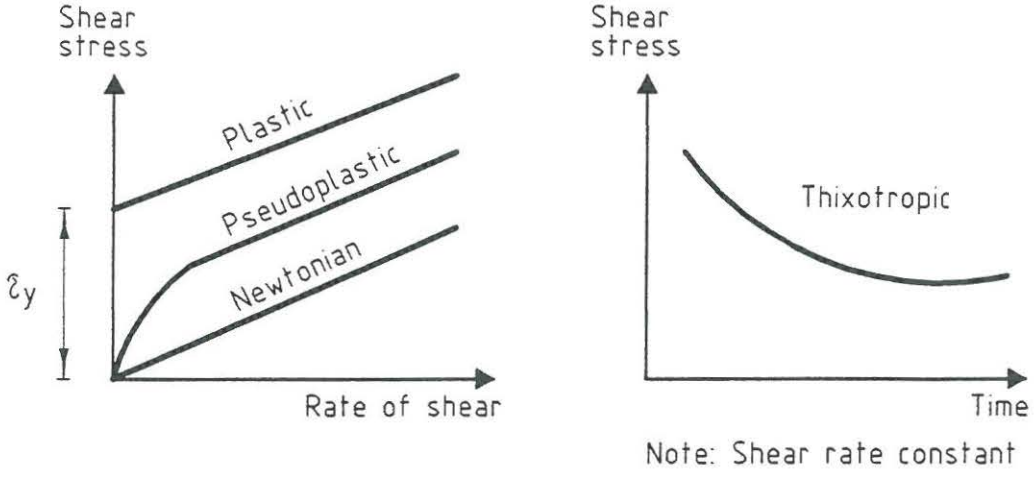

Fig. 3.6. Definition of rheology characteristics of activated sludge.

The reported pseudoplastic characteristic is caused by measurement errors in the commercial viscometer (Dick and Buck, 1985). Furthermore, Dick and Buck (1985) demonstrated that settling occurs during thixotropic measurements by means of commercial viscometer. Previous reports of pronounced thixotropic changes in activated sludge may therefore, at least partly, be due to settling (Dick and Buck, 1985). In equation 3.6. the mathematic description of Bingham plastic is seen.

$$\tau = \tau_y + \eta \frac{dU_i}{dx_j} \qquad (3.6)$$

where τ_y is the yield strength or critical shear stress and η is the plastic viscosity. Measurement of activated sludge rheology in Dick and Buck (1985) is shown in Fig. 3.7.

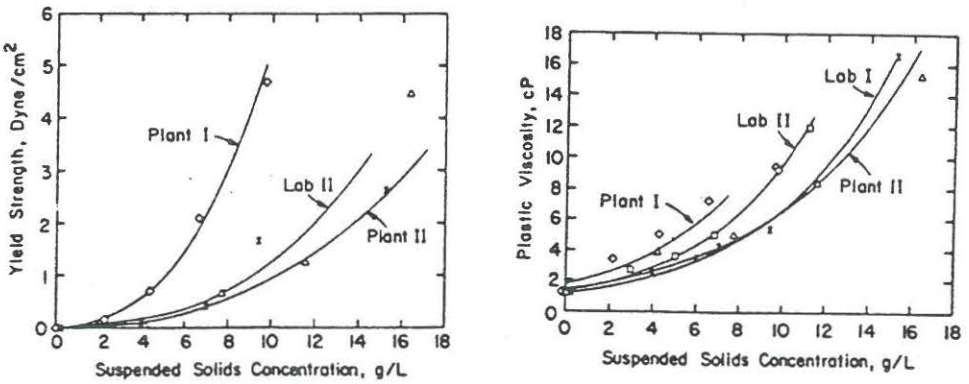

Fig. 3.7. Rheology data of Bingham plastic activated sludge (Dick and Buck, 1985).

Wood and Dick (1975) measured rheology characteristics of various types of activated sludge with different characteristics ranging from Zoogloeal (flocculating) sludge to stiff branched filament sludge. These measurements show large differences in sludge yield strength and plastics viscosity of the various types of sludge dependent upon sludge concentrations. According to Campbell and Crescuolo (1982), the use of reported rheology data is extremely risky unless complete details of the test procedure are available as well. The reason for this is the strong dependence of the rheology data on the viscometer operation.

Another approach for describing the rheology of an activated sludge suspension is to describe the kinematic viscosity ν as a function of only the sludge concentration. An equation is presented in Bokil and Bewta (1972).

$$\nu = \frac{3{,}273 \cdot 10^{0{,}132C}}{\rho} \qquad (3.7)$$

where C is the concentration in kgSS/m^3 and ρ is the density of the suspension in kg/m^3.

3.4 Synthesis

From sections 3.1-3.3 it appears that the secondary settling tanks form a complex system with a number of processes to be considered. This section describes what must be included in a numerical model which can simulate a secondary settling tank.

In section 3.1 secondary settling tanks are described as a mainly 2 dimensional flow system with weakly 3 dimensional flows typically near the inlet. A geometric configuration of the numerical model as 2 dimensional is expected to give satisfactory simulation due to the mainly 2 dimensional flow. The hydraulic and sludge load on a settling tank can accordingly to the description in section 3.2. change widely. The numerical model should therefore be a non-steady model which could simulate these transient loads.

A settling tank can be approached as either a two-phase system with the water and the suspended sludge as the two phases or as a one-phase system with transport/dispersion of the suspended sludge. From section 3.1 settling tanks are known to be a stratified flow phenomenon. According to Svensson (1985) it is extremely difficult to develop numerical models for two phase systems of stratified flow with settling. Therefore, the secondary settling tanks is approached as an one-phase system.

To describe the physical processes in the settling tank, a set of variables is necessary. These variables are described by either transport equations or equations of state linking the variables to each other. The following main variables are included in the numerical model.

U, V	Velocity components
P	Pressure
ν_t	Turbulent eddy viscosity
C_f, C_p	Concentration variables
G	rms velocity gradient
ρ	Density
ν	Kinematic viscosity

For simulation of 2 dimensional mean flows the two velocity components U and V, one for each cartesian direction, and the pressure P are used as variables. The mean flow can be induced both hydraulic and by the sludge collection system.

The turbulent flow in part of the settling tank is simulated by a turbulent eddy viscosity ν_t. ν_t can be modelled by different models either a constant ν_t model, a one parameter k-l model and a two parameter k-ϵ model (Rodi, 1984). k is the kinetic energy, l is the length scale of the turbulent motion and ϵ is the dissipation rate of k. In section 2.1 it is argued that the k-ϵ model is the best model to predict ν_t in settling tanks and the k-ϵ model is therefore used.

From Fig. 3.3 it is seen that there is a wide range of floc sizes and a bimodal distribution in dispersed particles and flocs. This phenomenon

depends on the suspended sludge concentration and the fluctuating velocity gradient described by the parameter G. To describe this kind of system a multi fraction model can be used as described in von Smolockowski (1916, 1918), where the dispersed particles and flocs are divided into several fractions according to their sizes and a description of the interactions between these fractions is made. This approach require a detailed knowledge of the flocculation and disintegration processes, which is not available with the present knowledge of the sludge characteristics, thus a more simple approach is used here. A two fraction model is used by Parker et al. (1972) on activated sludge and by Ødegaard (1979) and Caillaux et al. (1992) on other materials. With this simplification, turbulence level and dispersed particle and floc concentration is assumed to affect the system as shown in Fig. 3.8.

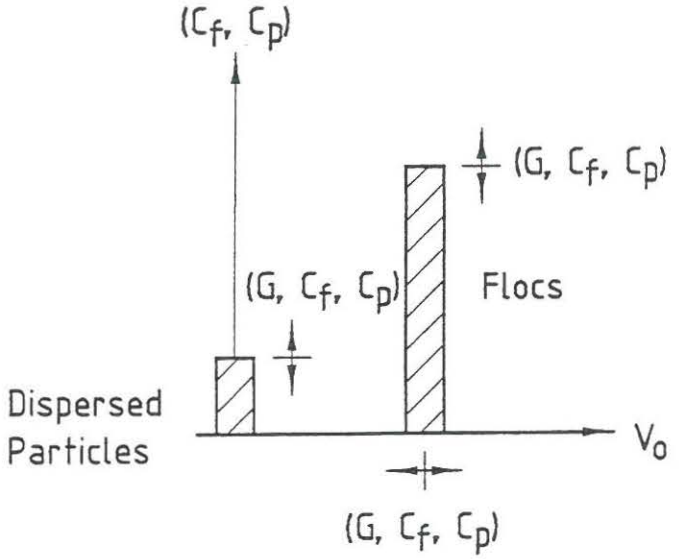

Fig. 3.8. The two fraction simplification of the flocculation, disintegration and settling of dispersed particles and flocs.

The arrows in Fig. 3.8 indicate that the concentrations and the free settling velocity changes for different values of the variables. In this system the variables are the concentrations for the dispersed particles C_p and flocs C_f and the rms velocity gradient G. G describes the effect of the turbulence on flocculation and disintegration. The dispersed particles are described as non-settleable and the flocs to have only one free settling velocity. The description of sludge floc settling in hindered and compaction regimes are included in the transport/dispersion description of C_f.

The stratified flow in settling tanks due to different sludge concentrations is included in the numerical model by the density variable ρ which is a function of the sludge concentration.

The rheology of activated sludge suspension is in section 3.3.2 described as Bingham plastic. In the numerical model the Bingham plastic characteristic is implemented by the kinematic viscosity ν which is affected by the sludge concentration and the velocity gradient. With the variables described, the physical processes described in sections 3.1 - 3.3 are included in the numerical model.

4. THE NUMERICAL MODEL AND CALIBRATION STRATEGY

The development of the numerical model to simulate secondary settling tanks is based on the results of the system analysis described in section 3.4. With the description of the necessary variables in the numerical model to describe all the physical processes in settling tanks this chapter describes the necessary assumptions for development of the numerical model and the mathematical formulation of the model. Furthermore, the used calibration strategy for the model is described. For a more detailed description of the formulation of the mathematical model, see appendix 1.

4.1 Mathematical model

The following sections present in short the governing differential equations on which the numerical model is based. The numerical model contains 4 separate models i.e. a hydrodynamic model, a transport model, a turbulence model and a flocculation model which are described separately.

4.1.1 Hydrodynamic

For the governing hydrodynamical equations the basic assumptions and the used physical law's can be listed as: isotropic and incompressible fluid, Newtons 2nd law, Boussinesq's approximation that assume that the variation in density are small compared to the absolute value and finally the eddy viscosity concept. The governing hydrodynamical equations for a turbulent, stratified and Newtonian fluid are shown in tensor notation.

Continuity equation:

$$\frac{\partial U_i}{\partial x_i}=0 \tag{4.1}$$

Momentum equation:

$$\frac{\partial U_i}{\partial t}+U_j\frac{\partial U_i}{\partial x_j}=-\frac{1}{\rho_r}\frac{\partial P}{\partial x_i}+\frac{\partial}{\partial x_j}\left((\nu_t+\nu)\frac{\partial U_i}{\partial x_j}\right)+g\frac{\rho-\rho_r}{\rho_r} \tag{4.2}$$

Here U denotes a velocity component, P is the pressure, ν is the kinematic viscosity, ν_t is the turbulent eddy viscosity, ρ is the density, ρ_r is the reference density, g is the gravitational acceleration, x is the cartesian spatial coordinate, t is time and i and j are tensor indices. In (4.2) the parameters ν, ρ and ν_t have to be quantified.

The Bingham plastic stress relation is included in the equation for a Newtonian fluid (4.2) with a description of ν as a function of the velocity gradient and suspended sludge concentration. The mathematical description of shear stress for Bingham plastic fluid is shown in equation (4.3) and for a Newtonian fluid in equation (4.4).

$$\tau = \tau_y + \eta \frac{dU_i}{dx_j} \tag{4.3}$$

where τ is the shear stress, τ_y is the critical shear stress and η is the plastic viscosity.

$$\tau = \mu \frac{dU_i}{dx_j} \tag{4.4}$$

where μ is the dynamic viscosity.

In equation (4.3) τ_y and η are functions of the suspended sludge concentration. Fig. 3.9 showed some measured relationships for different activated sludge which showed specific relation for each sludge. The equations of state for ϵ_y and η are therefore only presented in general here.

$$\tau_y = f(C) \tag{4.5}$$

$$\eta = f(C) \tag{4.6}$$

where C is the sludge concentration. From equation (4.3) and (4.4) an equation for μ was found to include the Bingham plastic expression in the Newtonian expression. See equation (4.7).

$$\mu = \left(\frac{\tau_y}{\dot{\gamma}}\right) + \eta \tag{4.7}$$

where $\dot{\gamma}$ is the velocity gradient from the k-ϵ model, see equation (4.16).

With $\nu = \mu/\rho$ the expression for Bingham plastic is included in the model formulation.

The density of the suspension ρ depends on the actual mixing of water and sludge each with their own density, where the mixing is described by the concentration of sludge C in the suspension. The equation of state linking ρ and C is therefore assumed to be a linear relation as shown in general in (4.8).

$$\rho = \rho_r + \alpha \cdot C \tag{4.8}$$

where $\propto$ is a constant depending on the actual density of the sludge which changes for different sludge as described in section 3.3.1.

The eddy viscosity ν_t is described by a turbulence model, which is discussed in section 4.2.3.

Initial and boundary conditions

As initial conditions the model variables U_i and P was zero. For wall boundaries the U_i component perpendicular to the wall is zero and the parallel component is found by using logarithmic velocity law for the viscose sublayer at the wall. At free water surface symmetry conditions is assumed and only the perpendicular U_i component is zero.

For the influent and recirculation flow boundaries the perpendicular U_i component is equal to the influent and recirculation flow velocities and P is calculated from the velocities. In the effluent boundary P is zero and the perpendicular U_i component is calculated by the continuity equation.

4.1.2 Transport

For the transport/dispersion Fick's 1st law combined with the conservation of mass yield the transport/dispersion equation. The transport/dispersion of the suspended sludge is described by the transport/dispersion equation where it is assumed that the sludge follows the flow except for transport processes described in the source terms.

$$\frac{\partial C}{\partial t}+U_i\frac{\partial C}{\partial x_i}=\frac{\partial}{\partial x_i}\left(\frac{\nu_t}{\sigma_t}\frac{\partial C}{\partial x_i}\right)+S+S_{p,f} \qquad (4.9)$$

The source term S is used to describe the transport by settling of the suspended sludge. An equation is used for each of the two variables the non-settleable dispersed particles C_p and the settleable flocs C_f. For C_p the source term S is equal to zero and for C_f the source term S is included as

$$S=v\frac{\partial C_f}{\partial x_i} \qquad (4.10)$$

where v is the settling velocity equal to the hindered settling velocity v_s in the hindered and compaction regimes and equal to the free settling velocity v_o in the free settling regime. Also for v_s and v_o is shown general equations due to their dependence of the actual activated sludge. From sections 3.3 and 3.4 it is seen that

$$v_s = f(C) \tag{4.11}$$

$$v_o = f(C,G) \tag{4.12}$$

where G is the rms velocity gradient. The source term $S_{p,f}$ describes the change in concentration for the actual variable either dispersed particles or flocs due to flocculation and disintegration. For dispersed particles $S_{p,f} = S_p$ and for flocs $S_{p,f} = S_f$. S_p and S_f are described for the flocculation in section 4.2.4.

Initial and boundary conditions

The initial condition for the variable C is equal to the influent sludge concentration. For wall and free surface boundaries the transport/dispersion is zero and for recirculation flow and effluent boundary the transport follows the flow. The influent concentration is used as influent boundary.

4.1.3 Turbulence

In section 3.4 the k-ϵ model is chosen as the turbulence model. The assumption for the k-ϵ model is that the eddy viscosity concept can be used. The equations for a complete k-ϵ model are:

$$\nu_t = c_\mu \frac{k^2}{\epsilon} \tag{4.13}$$

$$\frac{\partial k}{\partial t} + U_i \frac{\partial k}{\partial x_i} = \frac{\partial}{\partial x_i}\left(\frac{\nu_t}{\sigma_k}\frac{\partial k}{\partial x_i}\right) + P_k + G_k \tag{4.14}$$

$$\frac{\partial \epsilon}{\partial t} + U_i \frac{\partial \epsilon}{\partial x_i} = \frac{\partial}{\partial x_i}\left(\frac{\nu_t}{\sigma_\epsilon}\frac{\partial \epsilon}{\partial x_i}\right) + c_{1\epsilon}\frac{\epsilon}{k}\cdot P_k + c_{1\epsilon}\frac{\epsilon}{k}(1 - c_{3\epsilon})\cdot G_k - c_{2\epsilon}\frac{\epsilon^2}{k} \tag{4.15}$$

$$P_k = \nu_t \left(\frac{\partial U_i}{\partial x_j} + \frac{\partial U_j}{\partial x_i}\right)\frac{\partial U_i}{\partial x_j} \tag{4.16}$$

$$G_k = \frac{g_i}{\rho_r}\frac{\nu_t}{\sigma_t}\frac{\partial \rho}{\partial x_i} \tag{4.17}$$

where k is the kinetic energy, P_k is the production of k, G_k is the buoyancy production/destruction of k, ϵ is the dissipation rate of k and c_μ, σ_k, σ_ϵ, $c_{1\epsilon}$,

$c_{2\epsilon}$, $c_{3\epsilon}$ are constants. From extensive experiments, values of the constants in the k-ϵ model have been found. The values are shown in Table 3.1.

c_μ	$c_{1\epsilon}$	$c_{2\epsilon}$	σ_k	σ_ϵ	σ_t	$c_{3\epsilon}$
0.09	1.44	1.92	1.0	1.3	1.0	0.8

Table 3.1. k-ϵ model constants (Rodi, 1984).

Initial and boundary conditions

The initial condition for k and ϵ is equal to the influent condition where k and ϵ are calculated from the influent velocity. For wall boundary the equations for k and ϵ presented in appendix 1 is used. K and ϵ is calculated from the local resulting friction velocity U_f. At the free surface the boundary conditions for k is a symmetry condition and for ϵ the wall boundary condition.

4.1.4 Flocculation

The basic assumption for flocculation is to consider the sludge as a two fraction system. The two fraction systems for flocculation and disintegration of dispersed particles and flocs are described by the rate of flocculation R_f and the rate of disintegration R_p as shown in equation (4.18) and (4.19) (Parker at al., 1972).

$$R_f = K_A \cdot C_p \cdot C_f \cdot G \tag{4.18}$$

$$R_P = K_B \cdot C_f \cdot G^2 \tag{4.19}$$

where

$$G = \sqrt{\frac{\epsilon}{\nu}} \tag{4.20}$$

is the rms velocity gradient, K_A, K_B are constants and C_f, C_P are concentrations of flocs and dispersed particles, respectively.

From equation (4.18) it is seen that R_f is dependent of C_p, C_f and G. This shows that the value of each of these variable affect flocculation equally. From equation (4.19) is seen that R_p is dependent of only C_f and G with a exponent rate at 2 for G. Therefore, C_p did not affect the disintegration of flocs while G have a higher effect on disintegration than flocculation.

The flocculation and disintegration balance between dispersed particles and flocs is found in all points and the source terms S_p and S_f for the dispersed particles and flocs, respectively is found as shown in equation (4.21) and (4.22) and included in the transport/dispersion equations as shown in section 4.2.2.

$$S_P = R_P - R_f \tag{4.21}$$

$$S_f = R_f - R_P \tag{4.22}$$

4.1.5 Solution method

The numerical models is made as an extension to the PHOENICS program. PHOENICS stands for Parabolic, Hyperbolic Or Elliptic Numerical Integration Code Series and is a code which simulates fluid flow, heat transfer, chemical reactions and related phenomena (Spalding, 1989). The use of PHOENICS gives a well documented computer code with several specialised features for development of a numerical model of settling tanks. Furthermore, PHOENICS gives the flexibility of extending the code as requested. The numerical solution used is described in detail in appendix 2.

The numerical grid sizes shall be set to a size where the numerical model can simulate all the different hydraulic and sludge processes. This means that the grid sizes are chosen as large as possible, to limit the computation time, but without effecting the solution. Due to the mainly horizontal flow, the grid sizes can be larger in the horizontal direction than in the vertical direction. In horizontal direction the grid size is between 0.2-2.0 m and for the vertical direction between 0.05-0.1 m.

The accuracy of the numerical model depended on the accuracy of the model description of each physical process. All the model descriptions of physical processes shall therefore have the same accuracy to obtain the best possible numerical model.

4.2 Calibration Strategy

The purpose of this section is to describe how the numerical model is verified, calibrated and validated by different steps as described in the next chapters. By verification of the numerical model is meant a control of the different model descriptions of physical processes by comparing with analytical and known solutions. Calibration of the numerical model

means changing the value of parameters to obtain the best possible likeness between model simulations and measurements. Finally, validation means comparing model simulations with new measurements with new initial and boundary conditions. First, the parameters in the model formulation which are measured directly and the parameters which are found by calibration of the model are described.

From section 4.2 several general equations for the Bingham plastic characteristic, the density differences, the settling velocities and the flocculation and disintegration rates are seen. For these equations the relationship between variables is found either by measurements or calibration. In chapter 5 the different measurement procedures are described which are developed in order to measure these relationships. For the relationship between the sludge concentration and parameters in the Bingham plastic description of the suspension, a measurement procedure is not developed for direct measurements. Therefore, it is necessary to calibrate these parameters.

4.2.1 Verification

The numerical model described in this chapter is a further development of a model presented in Dahl et al. (1990) and is to some extent developed in parallel with a model presented in Petersen (1992). The verification of the numerical models, formulation of the mean flow, buoyancy and turbulence are presented in Dahl et al. (1990) and Petersen (1992). By comparing measurements and simulations of a channel flow, the model predicted a logarithmic velocity profile well. Also the profiles for the turbulence model parameters k, ϵ and ν_t is predicted well by the model. In different stratified flows the simulation of turbulence mixing is found to be in agreement with measurements. For the model simulation of buoyancy a front driven by buoyancy case is simulated an the model predicted the buoyancy well. The verification of the model formulation of the transport by settling is shown here. A 1-dimensional case with a constant settling velocity for all sludge concentrations and non-turbulence is used. A uniform sludge concentration is the initial condition, and as the settling starts, the height of the sludge blanket shall fall linearly due to the constant settling velocity. In Fig. 4.1 the settling system and the simulation results are presented and compared with the expected height of the sludge blanket.

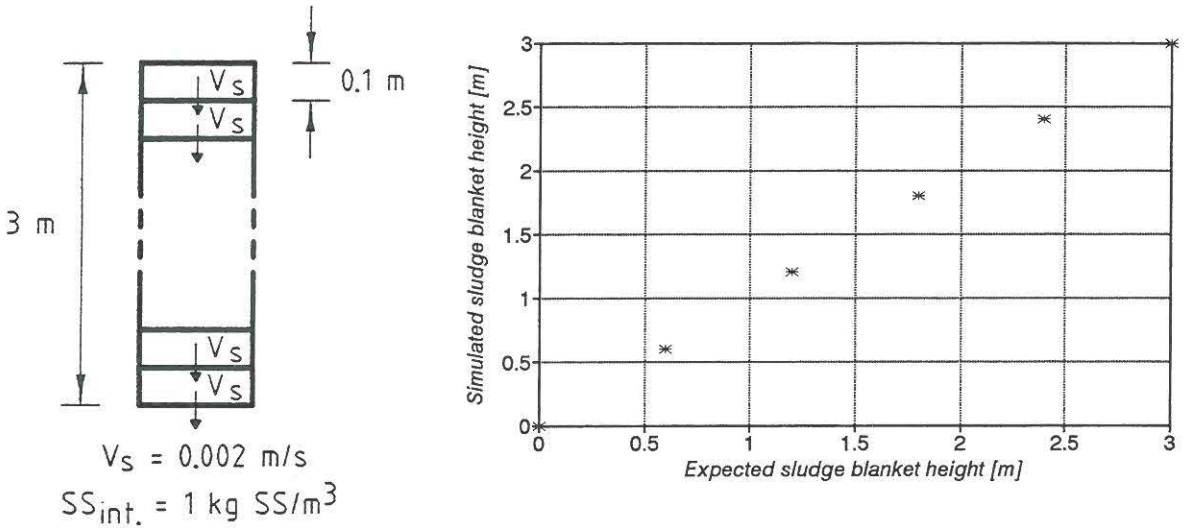

Fig. 4.1. Result of verification of transport by settling.

As seen on Fig. 4.1 the sludge blanket height is predicted well by the numerical model. For the flocculation model the verification concerned the conservation of sludge mass despite of the changing between the two sludge fractions. A conservation of sludge mass is found.

4.2.2 Calibration

In chapter 6 a model tank experiment is presented. The model tank was developed for providing measurements of the physical processes present in settling tanks under controlled conditions. The used instrumentation is presented in chapter 5. The idea is to calibrate the numerical model with these measurements. For the model simulation, relationships between model variables was measured according to the measurement procedures described in chapter 5 and then included in the model formulation. With the calibration the last parameters in the model formulation is found.

4.2.3 Validation

The numerical model is first validated by comparing new model tank measurements with model simulations. Second chapter 7 presents the validation of the numerical model on full-scale measurements at two wastewater treatment plants. The two treatment plants differed in characteristic of activated sludge and settling tank geometry. For model simulation, relationship between model variables was measured at each treatment plant by the measurement procedures presented in chapter 5. The instrumentation of the full-scale measurements is also seen in chapter 5. Finally, chapter 8 describes the improvement of a secondary settling tank by using the numerical model.

5. BASIC MEASUREMENTS

In this chapter, the basic instrumentation used for both measuring of relationships between model variables, model tank measurement and full scale measurements are described. Furthermore, a descriptions of the measurement procedures for measuring relationships between model variables are presented.

5.1 Instrumentation

This section describe the instrumentation used for measuring the sludge concentration, the mean horizontal flow velocity and retention time for a tracer.

5.1.1 Measurement of sludge concentration

To measure the sludge concentration, an optical turbidity meter, type OSLIM was used. See Fig. 5.1.

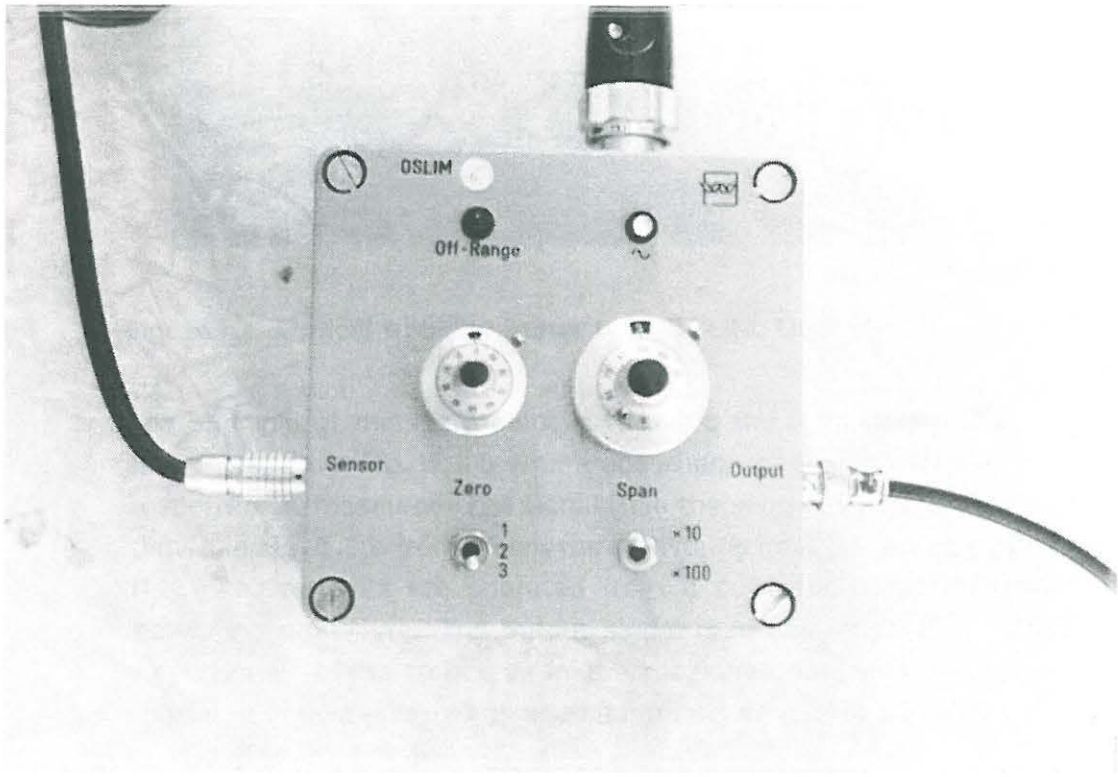

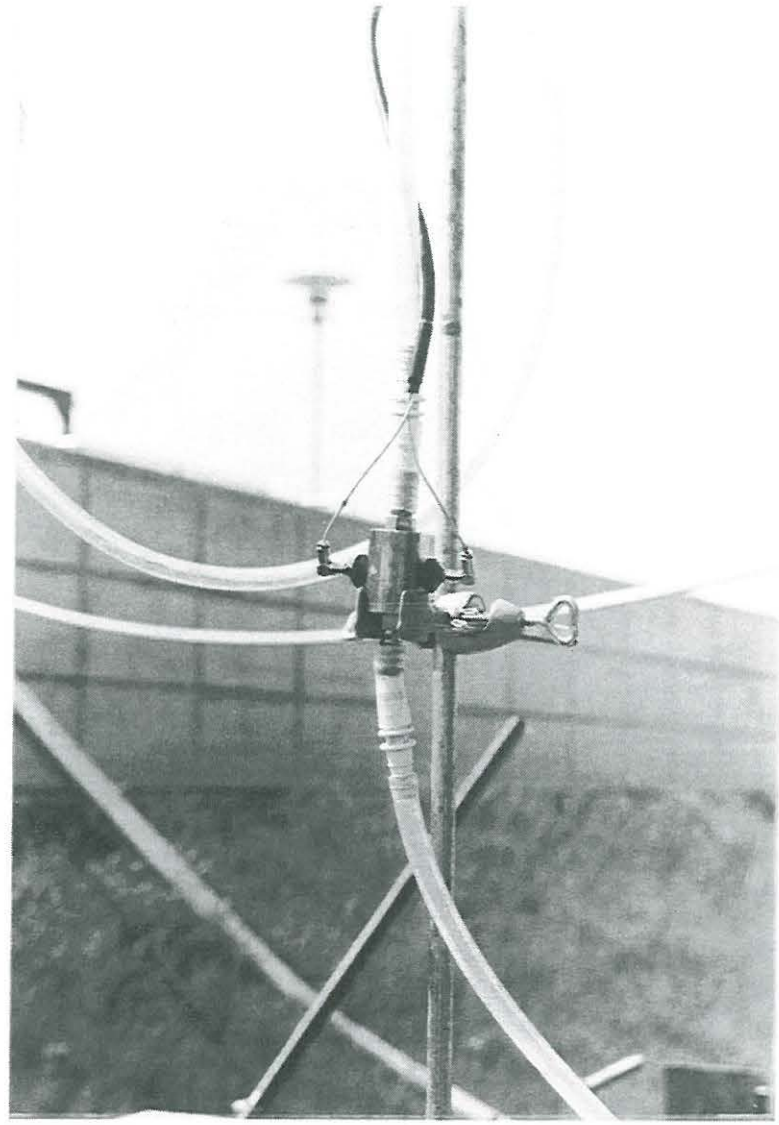

Fig. 5.1. Optical turbidity meter type OSLIM, Delft Hydraulics.

The principle of this instrument is to pump the suspension through the sensor shown in Fig. 5.1 b where absorbtion of the light caused by the suspension is measured. The signal from the sensor is sent to an amplifier shown in Fig. 5.1 a from which the measuring interval can be controlled. The measurements are operated from a pc, which also controls the measuring procedure. The output signal is in the range of 1 - 10 volt proportional to the turbidity. In the measurements one measurement consisted of averaging 10 measurements per second in 10 seconds equal to 100 measurements.

A calibration curve between volt and sludge concentration was made each day. Suspensions with different concentrations were pumped through the sensor giving a voltage. The suspended sludge concentrations in these samples were then measured in a laboratory by filtration. To check the

calibration measurements were performed occasionally on one of the known samples during a day.

In the model tank and the measurements of free settling velocity and flocculation each sample was pumped directly from the measuring point through the sensor. In the full scale studies batch samples were drawn with the sampler shown in Fig. 5.2 with 0.25 m between each sample. The samples were afterwards circulated through the sensor and a sludge concentration profile determined.

Fig. 5.2. Sampler for taking batch samples in full scale settling tanks.

5.1.2 Measurement of mean horizontal flow velocity

An OTT Velocity Sensor NAUTILUS C2000 was used for measuring the horizontal mean velocities. The sensor is a electromagnetic induction sensor measuring one velocity component. The velocity is measured each second and can be averaged immediately for a period of 5 - 60 seconds in order to measure a mean velocity. Fig. 5.3 shows the sensor and the electronic box in which the velocity and the average are calculated. In the measurements an average period at 30 seconds was used .

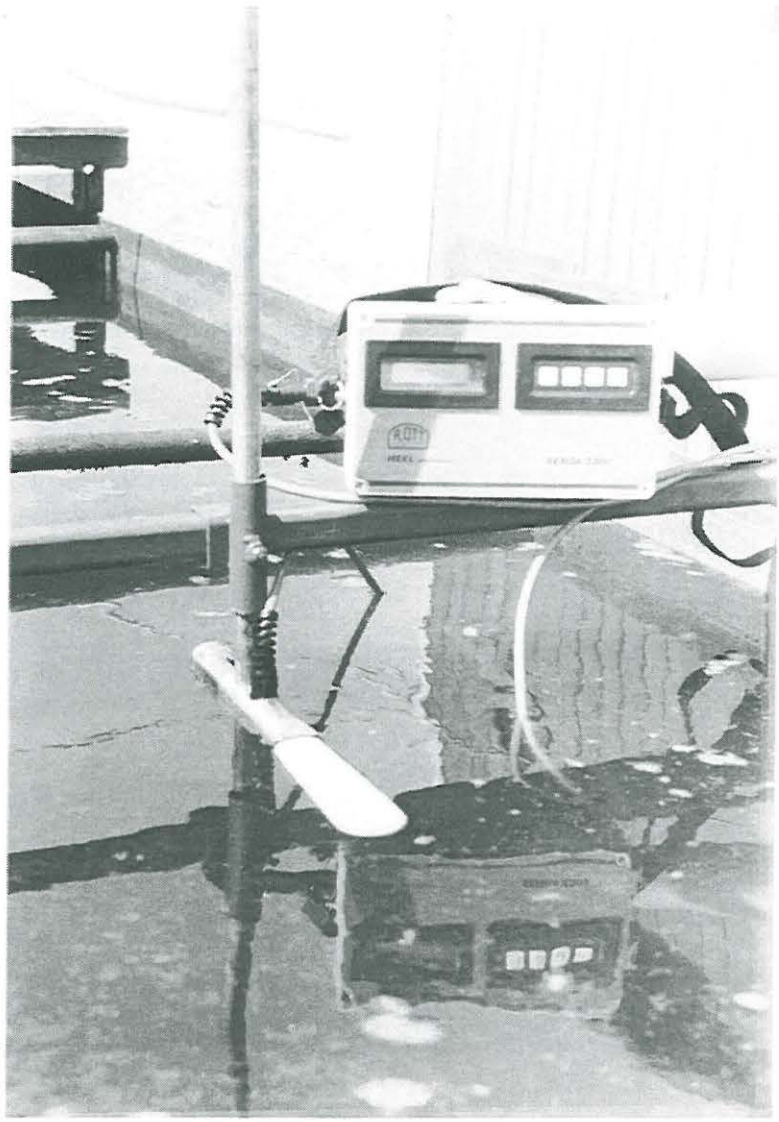

Fig. 5.3. OTT Velocity Sensor NAUTILUS C2000.

5.1.3 Measurement of retention time

To measure the retention time was used a fluorometer which was placed between the effluent weirs. As tracer was used rodamin WT which is known not to be absorbed to sludge flocs (Stamou and Adams, 1988). In Fig. 5.4 the fluorometer is shown. The measurements were controlled from a pc where all the measurement results were stored.

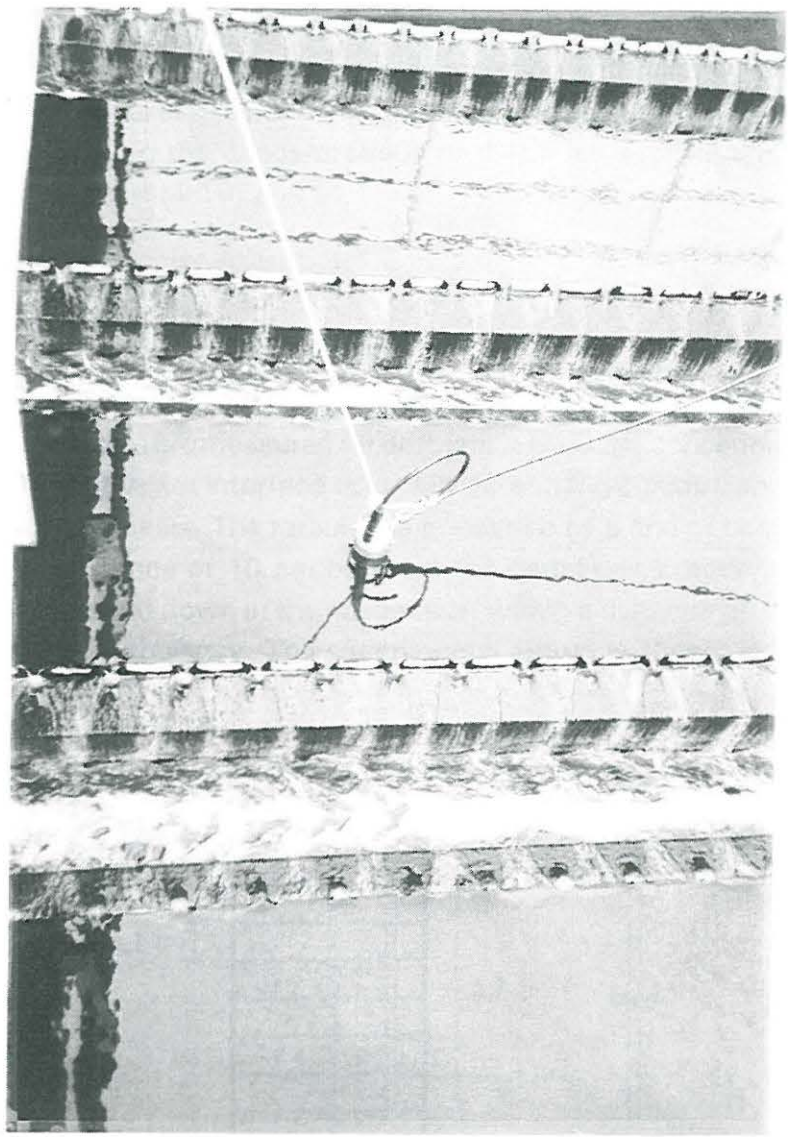

Fig. 5.4. Flourometer.

5.2 Settling and flocculation measurements

In this section the procedures for measuring the settling and flocculation of sludge are described. The settling and flocculation was measured using settling columns.

The purpose of the measurements was to estimate settling velocities in the regimes, free and hindered settling. In the settling columns the sludge concentration and G are the variables in the free settling regime and only the sludge concentration in the hindered settling regime (see equations (4.11) and (4.12)). By measuring the settling velocities directly, the effect of other independent parameters known to affect the settling velocities, e.g. filament level, sludge floc size and floc density discussed in section 3.3 are taken into account. Different settling columns were used for each regime.

In the free settling regime the flocculation and disintegration between dispersed particle and flocs were also examined. The relationship is dependent on the concentrations of dispersed particle and flocs and G (see equation (4.16) and (4.17)).

5.2.1 Free settling regime

In this measurement procedure, settling velocities, flocculation and disintegration are measured for different low sludge concentrations, where no sludge blanket interface occurs in the settling column, and for different turbulence levels. The turbulence is induced by a grid of bars constructed with a distance of 10 cm between the bars in all directions. The grid is moved up and down in the suspension within a distance of 10 cm in order to induce turbulence. The experimental set-up is shown in Fig. 5.5.

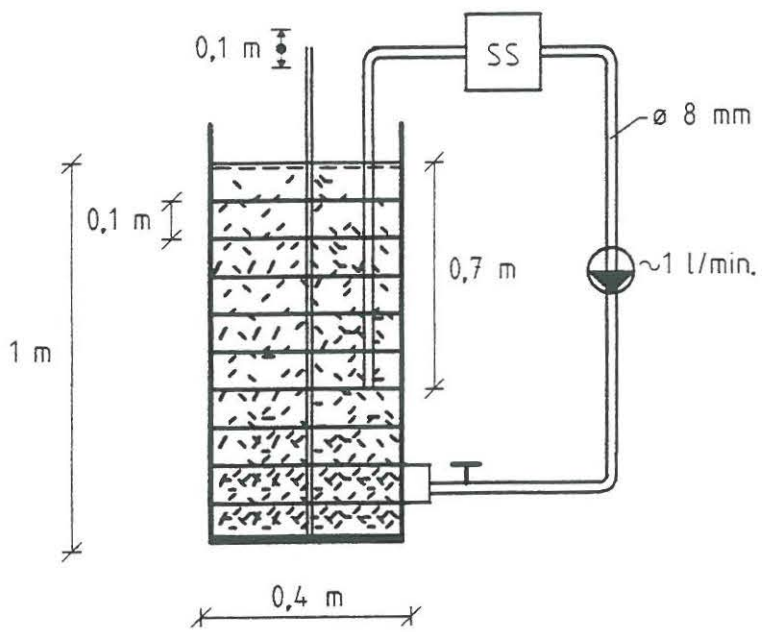

Fig. 5.5. Settling column for measuring free settling velocities, flocculation and disintegration.

To describe the turbulence in the settling column for different frequencies of the stirring, measurements were made to describe the turbulence parameters G and ν_t as functions of the mean velocities of the grid. The parameter G is known from section 3.3.1 to be the scale which describes the turbulence effect on flocculation and disintegration of dispersed particles and flocs. With the definition of

$$G = \sqrt{\epsilon/\nu} \tag{5.1}$$

where ϵ is the dissipation of turbulent kinetic energy and ν is the kinetic viscosity an experiment was made to find the energy lost from a uniform flow passing one grid plane with a known velocity. The energy lost can be set equal to ϵ which describes the dissipation of turbulent kinetic energy into heat. With known values of ϵ for different flow velocities the relationship between G and the flow velocities is found. In Fig. 5.6 the experimental set-up is seen in a flow channel.

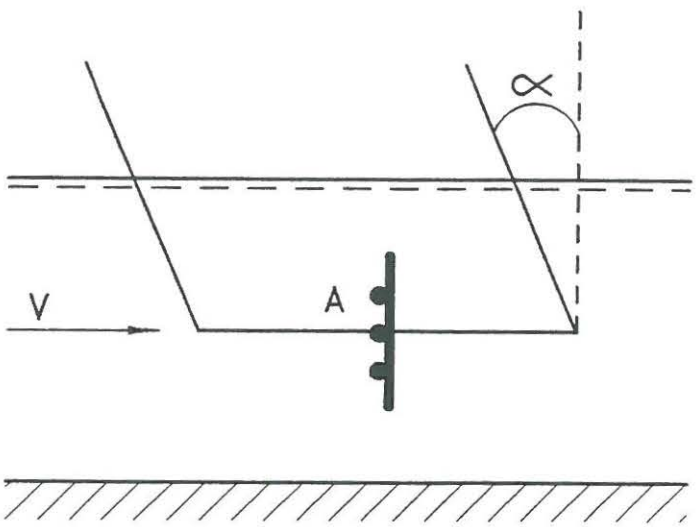

Fig. 5.6. One grid plane placed in a uniform flow field.

By measuring the angle α for different flow velocities and knowing the mass of the whole system ϵ can be calculated. The force balance for the grid is seen in Fig. 5.7 with m as the mass of the grid, g as the gravitational acceleration and A the area of the grid.

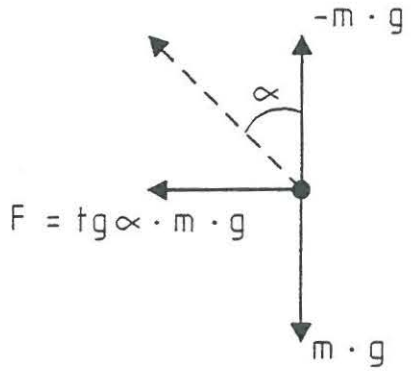

Fig. 5.7. Force balance for the grid.

Knowing the force used for lifting the grid system to the measured height, the dissipation of energy per unit time to provide this force is F · V. With ϵ as the dissipation of energy per unit time per unit mass.

$$\epsilon = \frac{F \cdot \overline{V}}{M} \tag{5.2}$$

where M is the mass of the volume flowing through A per time. G is then calculated from equation (5.1) with ν at 20°C as presented in Fig. 5.8.

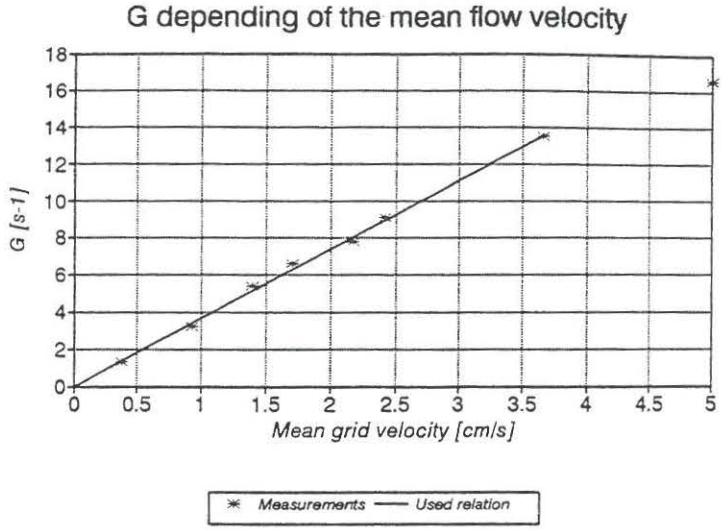

Fig. 5.8. Measured G depending on the mean flow velocity.

In Fig. 5.8 it is seen that the relationship is approximately linear within the interval of G from 0 - 13 s^{-1} with the expression in equation (5.3), although theoretically $G = K \cdot \overline{V}^{3/2}$.

$$G = 3.71 \cdot \overline{V} \tag{5.3}$$

A tracer experiment was carried out in order to find the relationship between the diffusion coefficient ν_t and the mean velocity of the grid. As tracer a weak salt solution was used which was poured into the bottom of the column initially filled with clean water. The salt concentration was measured at the water surface in the column. The experiment is modelled in a one-dimensional numerical transport/dispersion model. By changing ν_t in the model simulation until the simulations are equal to the measured results, ν_t is found. The relationship between the ν_t and the mean velocities of the grid is found to be

$$\nu_t = -1.0 \cdot 10^{-5} + 3.989 \cdot 10^{-5} \cdot \bar{V} \qquad (5.4)$$

with $\bar{V}$ in cm/s and in the range of 0.6 - 3.6 cm/s and ν_t in the range of $1.35 \cdot 10^{-5}$ - $1.16 \cdot 10^{-4}$ m^2/s.

For each measurement in the column, an initial sludge concentration and a turbulence level is chosen. Due to the grid, a special device is used to ensure a uniform suspension as initial condition. See Fig. 5.9.

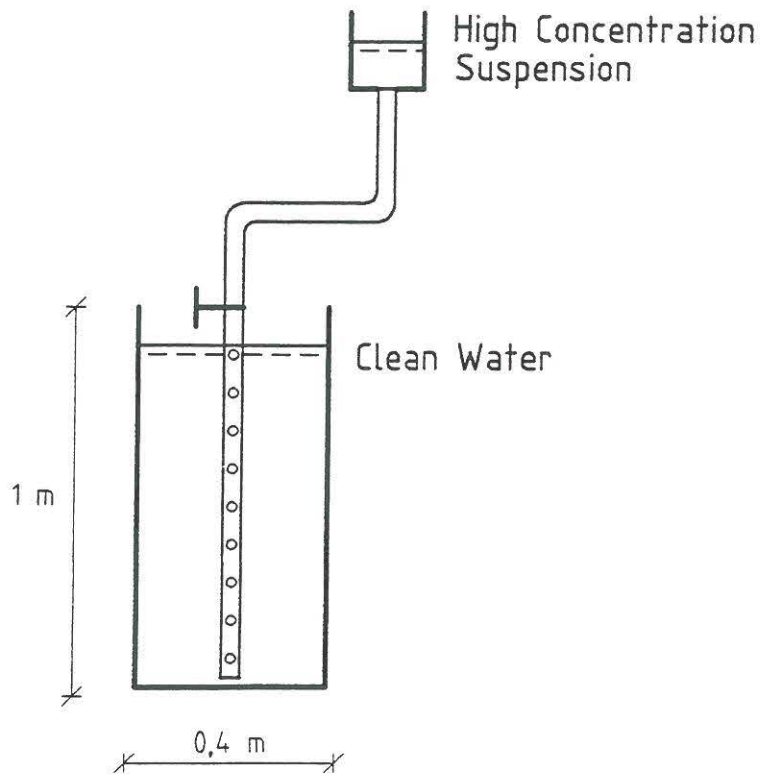

Fig. 5.9. Device for creation of a uniform concentration as initial condition in the column.

To obtain a uniform concentration a small amount of a suspension with high concentration is distributed vertically through holes in the pipe in "clean" water and thus mixing a suspension with the chosen initial concentration. This procedure can be used with the grid in the column. After the mixing the grid movement is started and the sludge concentration is measured continuously at a fixed point e.g. 70 cm from the water surface. The sludge concentration is measured with the instrument presented in section 5.1.1. When the measured concentration changed, it indicated that

$$v_i \cdot t \approx H \tag{5.5}$$

where v_i is the settling velocity for a fraction of the sludge, t is the time from the measuring start and H is the height from the measuring point to the water surface. Knowing t and H, v_i is found. This means that the distribution in free settling velocities for the sludge can be found from the changes in the measured concentrations at the measuring point.

After the settling, the fraction of the sludge which is non-settleable is defined as the dispersed particles and the settleable sludge as the flocs in the two fraction flocculation and disintegration model. The distribution between the two fractions depends on the initial sludge concentration and the turbulence level.

In these measurements, the measured settling velocities is a result of two processes, the settling and the dispersion due to turbulence. To separate these processes a 1-dimensional numerical model of the settling column is used. With the known turbulent eddy viscosity the settling velocity is calibrated so that the simulated sludge concentration in the measuring point have the best possible agreement with the measured concentrations. Furthermore, the flocculation and disintegration model is included in this numerical model and the constants K_A and K_B from equation (4.16) and (4.17) is calibrated by comparing simulations with the measurements of the distribution between the two fractions.

The relatively big volume used in the settling column is chosen to reduce the influence of sampling on the settling. Due to the low sludge concentrations, settling velocities are relatively large during these measurements and the column have to be high to give time for measuring the velocities.

5.2.2 Hindered settling

Settling velocity in the hindered settling regime was measured by following the depth of the sludge blanket interface in a stirred settling column for different sludge concentrations (White, 1976). See Fig. 5.10.

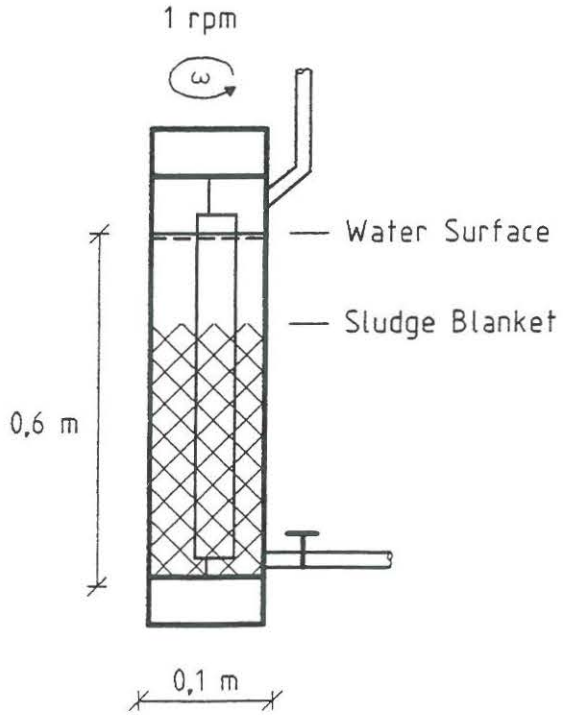

Fig. 5.10. Settling column for measurement of hindered settling velocities.

A suspension with the desired sludge concentration is mixed and the suspension is poured in the settling column. The depth of the sludge blanket interface is measured and the time registered. From these measurements the maximum settling velocity of the sludge blanket interface is calculated. This settling velocity is defined as the settling velocity for the initial concentration. Based on several experiments with different initial concentrations, the relationship is found between the concentration and the hindered settling velocity.

5.3 Density of suspension

The density of the suspension was measured with pycnometer glasses and the sludge concentration was measured by filtration. The measurements were carried out with sludge concentrations covering the concentration field in secondary settling tanks (i.e. 0 - 15 kgss/m^3)

5.4 Microscopic examination

From a microscopic examination of the activated sludge, different qualitative characteristics of the specific activated sludge can be determined. An examination shows the presence of characteristics like filament organ-

isms, ciliate protozoal communities and finally floc firmness and shapes. These data were a support for the validation of the other measurement data from the specific activated sludge.

6. MODEL TANK MEASUREMENTS AND SIMULATIONS

The purpose of the model tank measurements is to provide measurements of the physical processes present in settling tanks for comparison with numerical model simulations in order to calibrate the numerical model. With the calibrated numerical model a validation of the model is presented by comparing model simulations with model tank measurements with new initial and boundary conditions.

The model tank was set-up at Aalborg Øst wastewater treatment plant to ensure an influent suspension of activated sludge direct from an aeration tank at a full scale wastewater treatment plant. Aalborg Øst is a 177.000 PE wastewater treatment plant with mechanical, biological organic and nutrient, and chemical treatment.

6.1 Measurement configurations

The configuration of the model tank measurements consists of the model tank, a pipe system to provide the influent and a pump system to remove the effluent. A schematic drawing of the system together with a photograph is seen in Fig. 6.1.

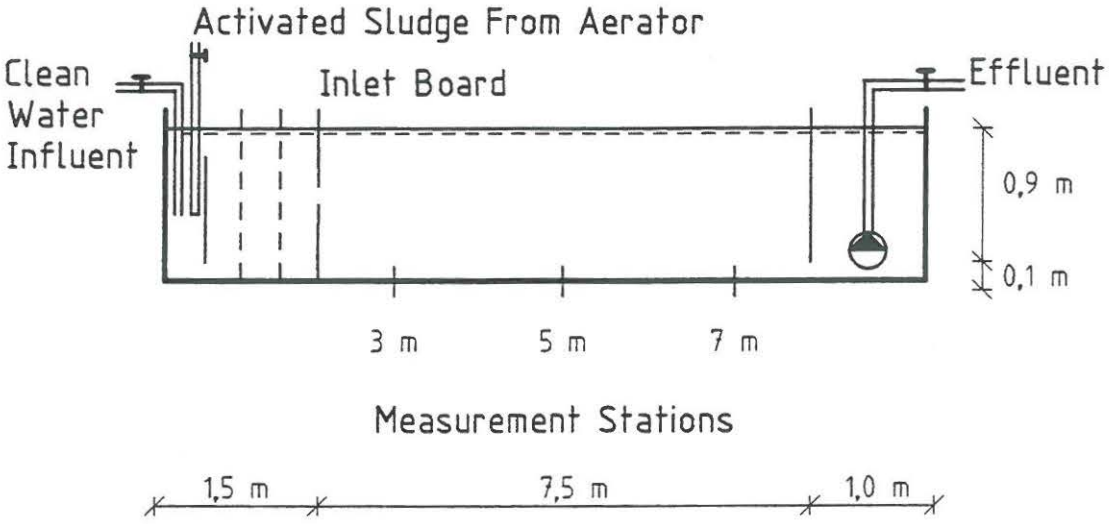

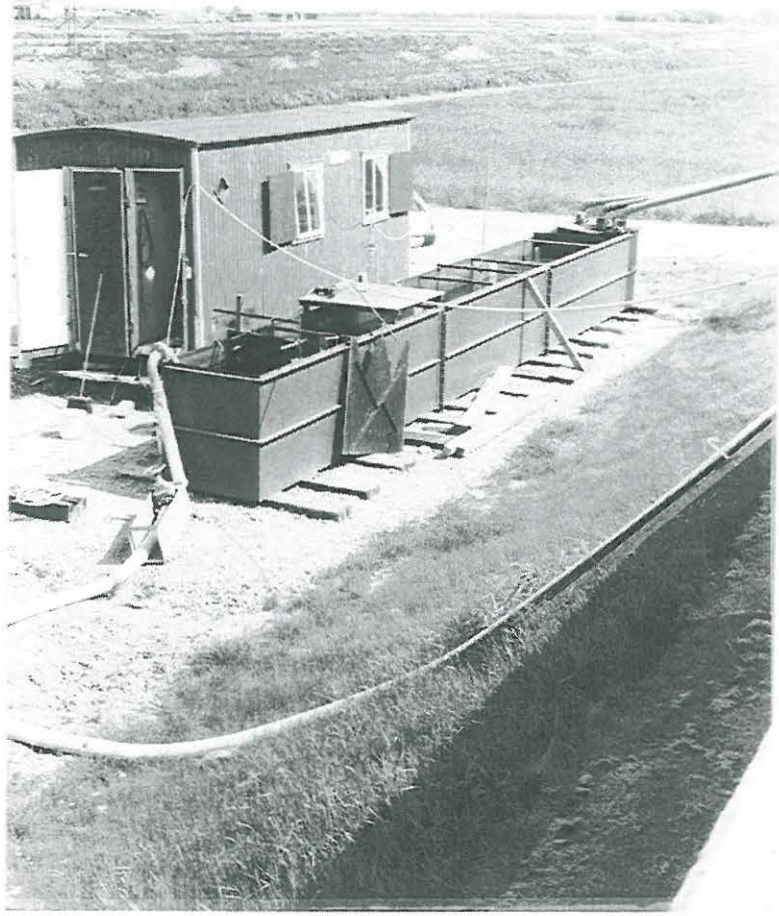

Fig. 6.1. Configuration of model tank.

The influent from the aeration tank is provided by three siphon conduit systems which is possible due to the water surface of the model tank being built 1 m below the water surface in the aeration tank. Once the siphon conduit systems is filled, the influent is controlled by valves placed at the model tank. The influent can be varied at the interval of 0 - 40 l/s. A picture of the siphon conduit system is shown in Fig. 6.2.

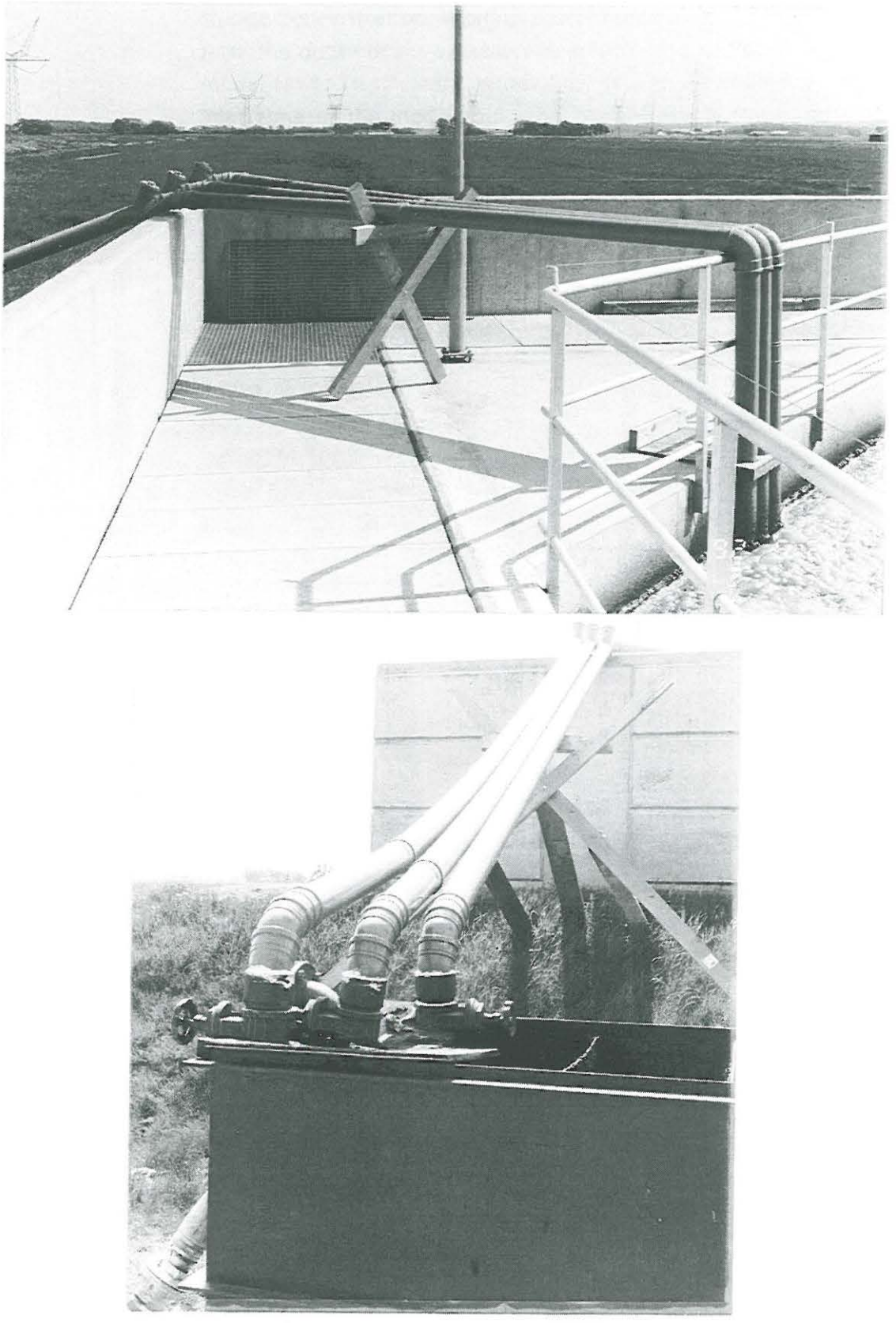

Fig. 6.2. Siphon conduit systems.

A siphon conduit systems was used to avoid destructions of the sludge flocs before settling in the model tank. In order to change the influent sludge concentration, a pump system was made to pump "clean" water from the outlet of the wastewater treatment plant back to the inlet of the model tank. The "clean" water flow is also controlled by a valve. In an inlet zone of the model tank, the "clean" water flow and the activated sludge flow are mixed to the desired flow with the desired sludge concentration. In Fig. 6.3 the inlet of clean water can be seen between the valves from the siphon conduit systems.

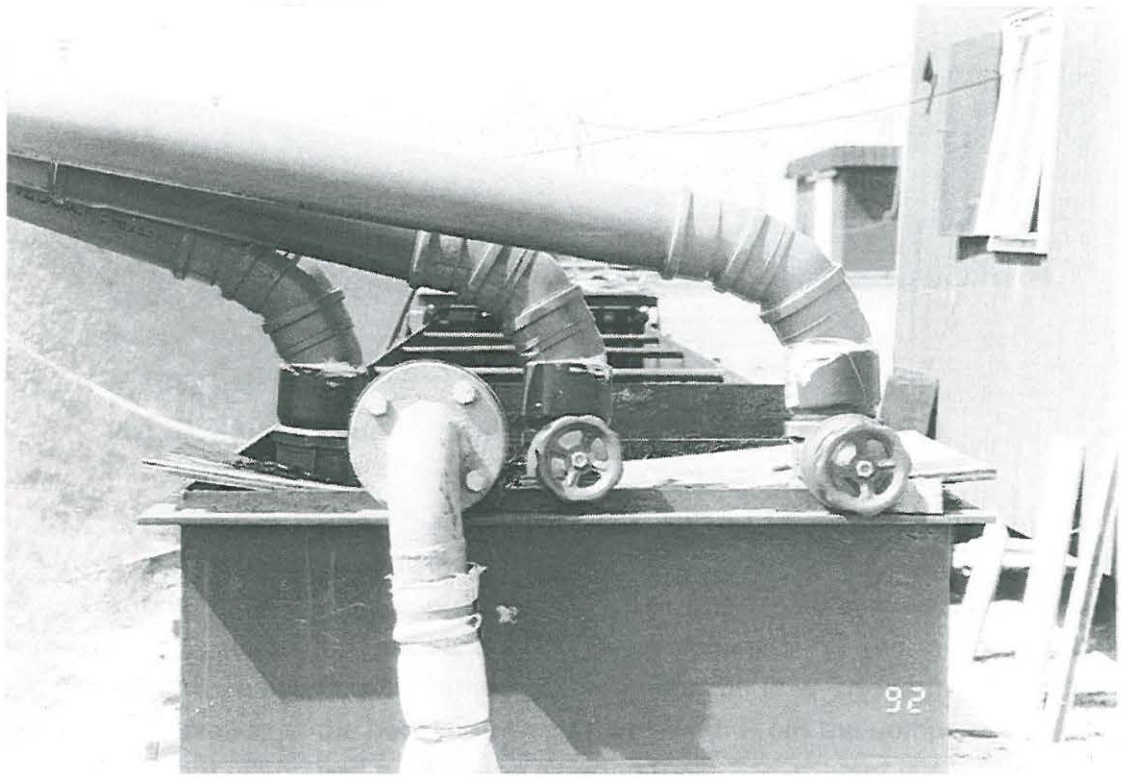

Fig. 6.3. Inlet of clean water.

Fig. 6.4 shows an inlet zone in which the influent is mixed and made into a uniformed flow owing to porous walls.

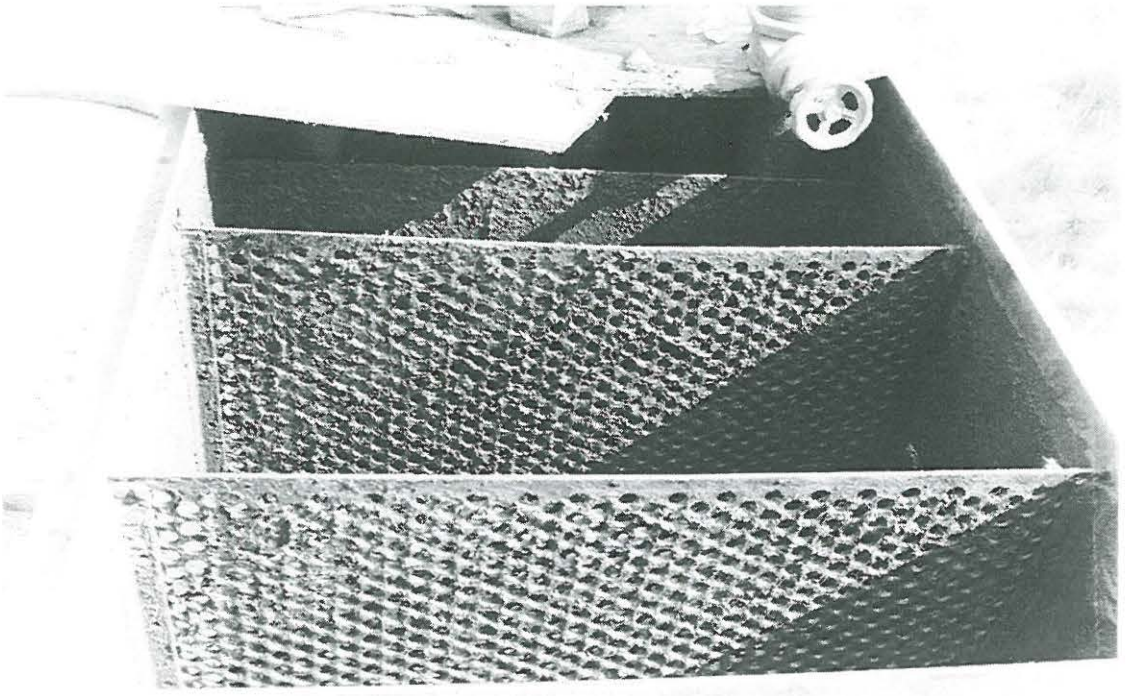

Fig. 6.4. Inlet zone with porous walls.

Downstream, after the porous walls, inlet boards can optionally be installed to control the influent. Between the inlet and outlet zones in the model tank, there is approximately 7.5 or 7.9 m as measuring area depending on the use of inlet boards. Downstream, after the measurement area there is an outlet compartment where the flow enters through a 10 cm opening at the bottom of the outlet board. From the compartment the effluent is pumped back to the aeration tank. The effluent is controlled by a valve as shown in Fig 6.5 and adjusted to match the desired influent to keep the same water depth during each measurement.

Fig. 6.5. Outlet flow pump system.

As a special arrangement, a wagon was placed on top of the model tank on which the measurement instruments can be placed and transported along the model tank, see Fig. 6.6 in the following subsection. From the picture in Fig. 6.1 three windows can be seen at the side of the model tank. These windows were placed close to the measurement stations described in following subsection.

6.2 Measurement procedures

With the described model tank measurement configuration in section 6.1, it is possible to control the flow through the model tank, the sludge concentration of the influent and the geometry of the inlet with boards. 12 different measurements were made with a combination of the control

parameter as shown in the matrix in Table 6.1. MLSS is the sludge concentration in the process tanks and the numbers in the table are the measurement numbers combined by the date of the measurement and a number.

SS influent = ½ MLSS

	Q_1	Q_2	Q_3
with inlet boards	15069201	12069201	11069201
without inlet boards	09069201	05069202	05069201

SS influent = MLSS

	Q_1	Q_2	Q_3
with inlet boards	16069203	16069202	16069201
without inlet boards	19069201	18069202	18069201

Table 6.1. Matrix of model tank measurements.

As influent sludge concentration two different concentrations were chosen. The two concentrations were MLSS and half of MLSS. With MLSS at approximately 4.3 kgss/m^3 the typical concentration levels in wastewater treatment plants were covered. Three different influent were used to cover the transient hydraulic loads in settling tanks. Typically, the maximum velocity in settling tanks is in the magnitude of 3-6 cm/s (Larsen, 1977). With the used influent the maximum velocity was about 10 cm/s which shows that the velocity in settling tanks is covered and in some cases exposed in the model tank measurements.

By dividing the measurements into two series, one with and one without inlet boards, different flow fields were investigated. In the measurements without inlet boards, the influent was spread over the entire cross section of the model tank, due to the porous walls. These measurements were made especially to calibrate the numerical model description of the Bingham plastic suspension characteristics. In the measurements with inlet boards, the boards created a 15 cm high influent jet placed just above the middle of the total model tank height.

Each measurement began with setting the desired influent and influent sludge concentration by the valves on the inlet pipes. The flow was calculated from the elapsed time for rising the water surface 10 cm. With the chosen influent and sludge concentration, the measurement began with an empty tank and was filled up by the influent. When the water depth

reached 1 m, the effluent equal to the influent was started. From this point, profiles of mean horizontal velocities and sludge concentrations were measured in station 3, 5 and 7 m (see Fig. 6.1.) according to a specific measuring procedure. The aim was to measure as many profiles as possible within the duration of the measurements. The porous walls were the critical point to the duration of the measurements because they were filled with screenings and needed cleaning.

The instruments used for measuring profiles of the sludge concentration and the mean horizontal velocity is described in sections 5.1.1 and 5.1.2, respectively. For each profile measurement, the concentration and velocity profiles were measured as close in time as possible.

6.3 Results

Results from the measurements described in section 6.1 are presented and discussed in this section. In section 6.3.1 the results from the measurement of relationship between model variables are presented and in section 6.3.2 the results from the model tank measurements.

6.3.1 Results of basic measurements

Free settling

The measurement set-up for measuring free settling velocities and flocculation in a settling column is presented in section 5.2.1. In the model tank measurements the flocculation and disintegration between non settleable dispersed particles and settleable flocs were not examined. This was due to the effluent at the bottom of the model tank which gave no natural effluent sludge concentration for settling tanks. In Fig. 3.8 in section 3.4 the free settling velocity is described as depending on both, the sludge concentration and the turbulence level. The influence from the turbulence level was excluded because of the minor interest in flocculation and the low concentration zones. In Fig. 6.6 the calculated settling velocities are seen for fractions of the initial sludge mass for one of the measurements.

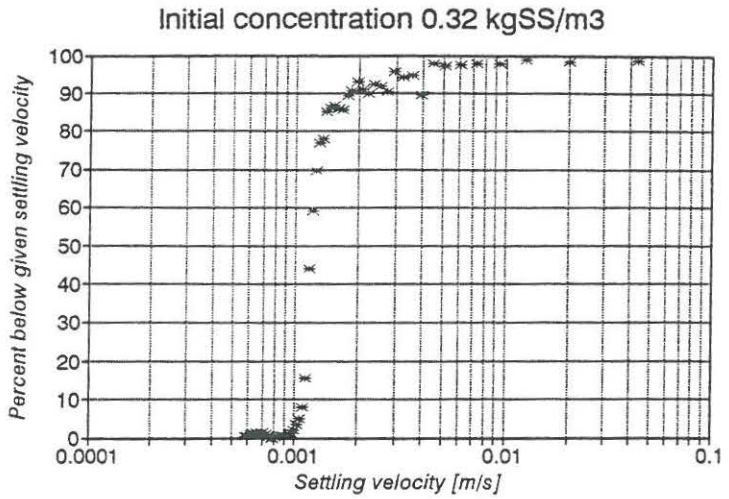

Fig. 6.6. Results from one settling column measurement in free settling regime.

The result in Fig. 6.6 showed a variation in free settling velocity for the sludge flocs. Nearly 15% of the total initial sludge mass settles faster than the approximate 80% of the sludge which settles with nearly the same velocity. Finally, 5% is found to have lower settling velocities and is defined as the non-settleable dispersed particles. Fig. 6.7 shows the measured mean free settling velocities for the different initial sludge concentrations.

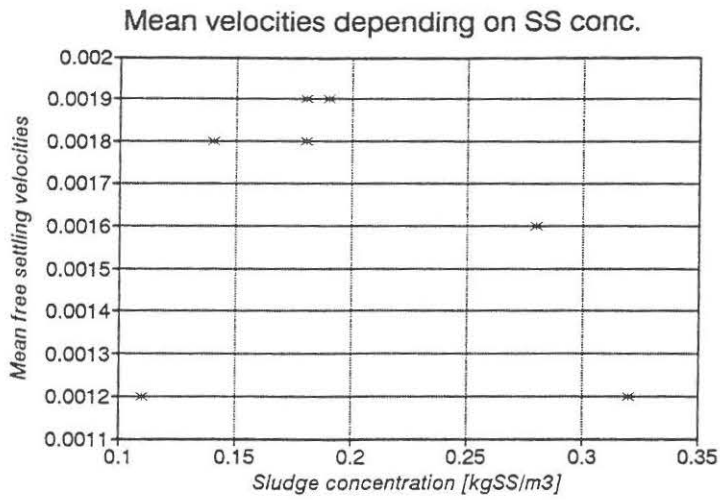

Fig. 6.7. Mean settling velocities of different initial sludge concentrations.

The variation in initial concentration shows that the highest settling velocities is found for a concentration in the range of 0.15 - 0.2 kgss/m^3. For the low concentration a lower settling velocity is found. This is expected to be a result of decreased flocculation rate due to decreased opportunity for collision between the sludge flocs, as described in chapter 3. In a measurement with initial concentration at 0.34 kgSS/m^3 hindered

settling occurred at the measurement point. The decreased settling velocities for the highest initial concentrations are therefore expected to be effected by a gradually change to hindered settling.

Hindered settling

In order to find the settling velocity in the hindered settling regime as a function of the sludge concentration, settling column measurements were made with the measurement procedure described in section 5.2.2. In Fig. 6.8 results of one column measurements are presented.

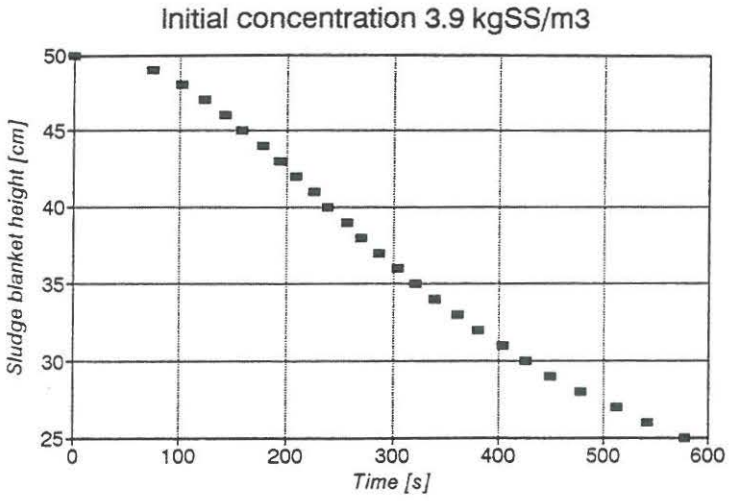

Fig. 6.8. Hindered settling column measurement for SS = 3.9 kg SS/m^3.

Fig. 6.8 shows how the settling velocity increases until a maximum settling velocity is reached and then continues to decrease. It is this maximum settling velocity which is defined as the settling velocity of the initial sludge concentration. The result of the measurement of the settling velocity in the hindered settling regime is presented in Fig. 6.9.

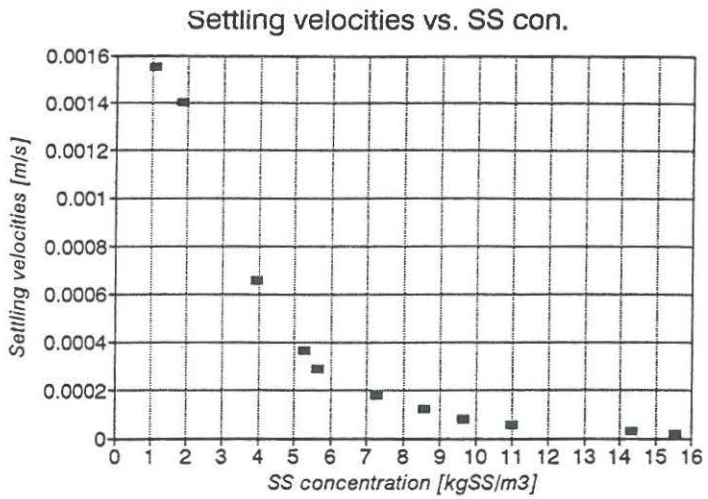

Fig. 6.9. Settling velocity depending on the sludge concentration in the hindered settling regime.

The concentrations shown in Fig. 6.9 reached up to 15.5 kgSS/m^3. For higher concentrations the measurement procedure could no longer be used owing to the sludge blanket interface was no longer a uniform horizontal interface but was effected by the walls and the stirring bars in the column.

With the results for settling velocities in free and hindered regimes a model description for the numerical model is found. A free settling velocity at 0.00185 m/s for a concentration at 0.15 kgSS/m^3 is used. Fig. 6.10 presents the measured settling velocities for different concentrations compared with the model description from equation (6.1).

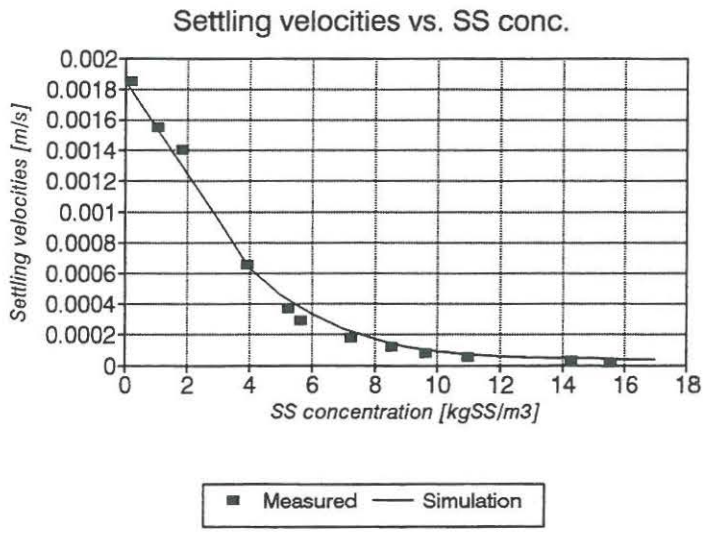

Fig. 6.10. Numerical model description of settling velocities compared with measured settling velocities.

$$v = 1.85 \cdot 10^{-5} + 2.0 \cdot 10^{-3} \cdot (1 - 4.17 \cdot 10^{-2} \cdot SS)^{6.7} \quad 0\text{-}3.5 \ kg\ SS/m^3$$

$$v = 1.63 \cdot 10^{-3} - 7.0 \cdot 10^{-5} \cdot SS^2 \quad 3.5\text{-}16.0 \ kg\ SS/m^3$$

$$v = 1.63 \cdot 10^{-3} + (16.0 - SS) \cdot 2.66 \cdot 10^{-6} \quad 16.0\text{-}29.0 \ kgSS/m^3 \qquad (6.1)$$

Density of the suspension

The density of the suspension as a function of the sludge concentration was measured several times before and during the model tank measurement period. Fig. 6.11 shows the result of one measurement and the line for an assumed linear dependency between the density and the concentration. For measuring density of suspensions with high sludge concentrations difficulties occurred with air bubbles in the suspension. Therefore, the measurement for the highest concentration in Fig. 6.11 is not included in the linear approximation to the measurements.

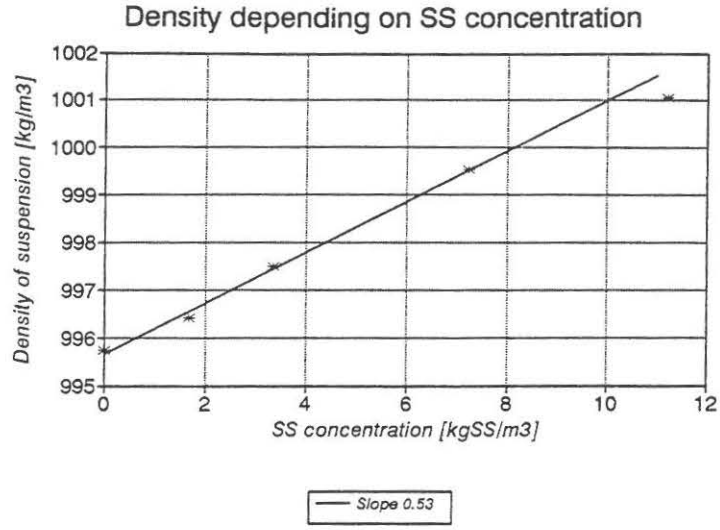

Fig. 6.11. Density as a function of sludge concentration 19.6.92.

Table 6.2 shows the slopes for the linear approximations to the results of the different measurements. It can be seen that there are no significant changes in the results over a period of nearly a month so that the relationship is expected to be constant for the model tank measurement period.

Date	Slope
11.5.92	0.55
20.5.92	0.55
19.6.92	0.53

Table 6.2. Measured slopes for the linear dependence between the density and sludge concentration.

With the measurement results in Table 6.2 the following equation of state is used as the model description in the numerical model.

$$\rho = \rho_r + 0.54 \cdot SS \qquad (6.2)$$

where ρ is the density of the suspension ρ_r is the reference density and SS is the sludge concentration.

Microscopical examination

Under the microscopical examinations of the activated sludge, several different filamentous microorganisms are found in a number, characterised as 3-4 in the Eikelboom index. The Eikelboom index is between 0 - 4 where 0 is for activated sludge without filamentous microorganisms and 4 is for a very high number of filamentous microorganisms (Eikelboom and van Buijsen, 1981). Furthermore, the sludge flocs are found to be weak, rounded and agglomerated in structure and medium and large in size. The sludge volume index SVI is found to be about 160. The characterisation of the activated sludge described above shows a somewhat poor sludge for settling due to a high filamentous index, but looking on the SVI a high value but still normal. In the future discussion of the measurement results, the high level of filamentous microorganisms shall be remembered due to its effect on the settling and rheological characteristics of the activated sludge.

6.3.2 Result of model tank measurements

From the measurement program which includes 12 different measurements, 4 measurements are chosen for presentation here. Different configurations of the measurement variation parameters, inlet geometry, sludge concentration and influent were used in the 4 measurements. The measurement conditions and results are presented in Fig. 6.12 - 6.15. In enclosure 1 the rest of the measurement results are presented. In Fig. 6.12 - 6.15 the mean horizontal velocity and sludge concentration profiles are seen in three different measurement stations at two different times in the measurements.

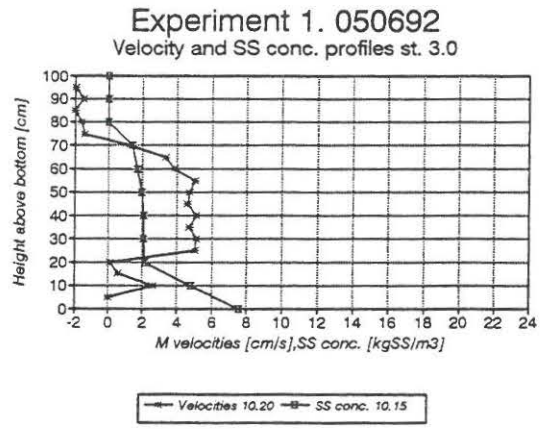

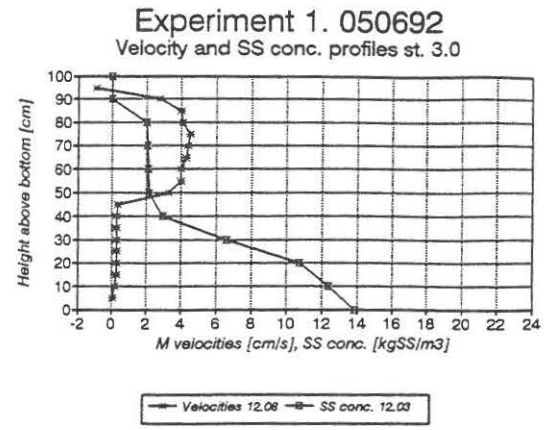

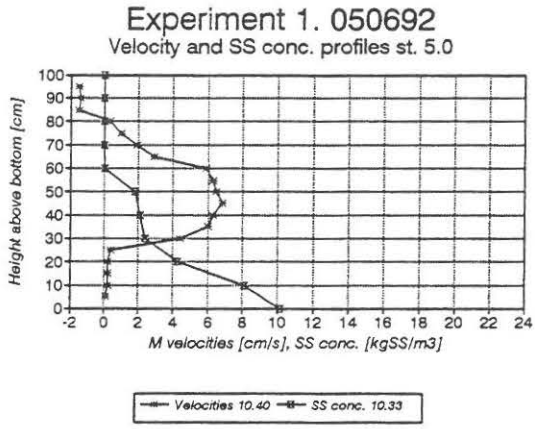

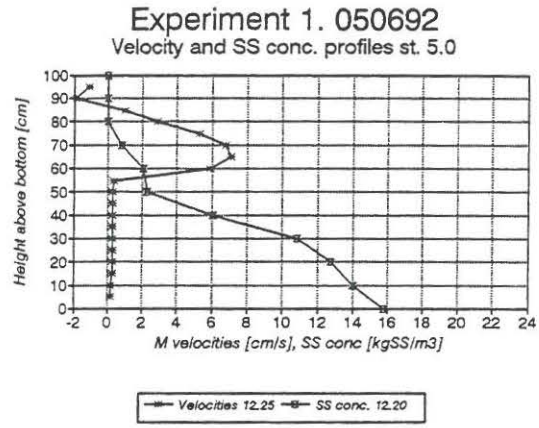

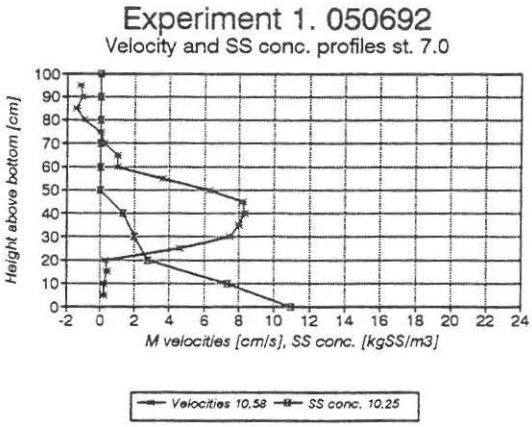

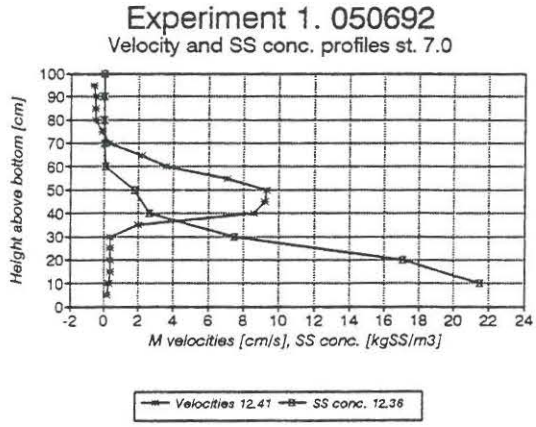

Fig. 6.12. Model tank measurement without inlet boards. Flow = 19.1 l/s and influent SS = 2.0 kgSS/m^3. Starting time: 10.05

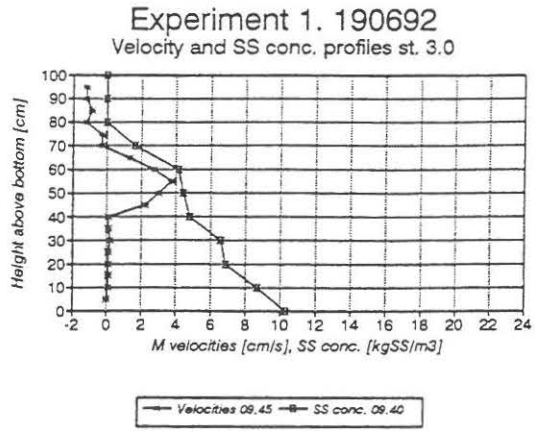

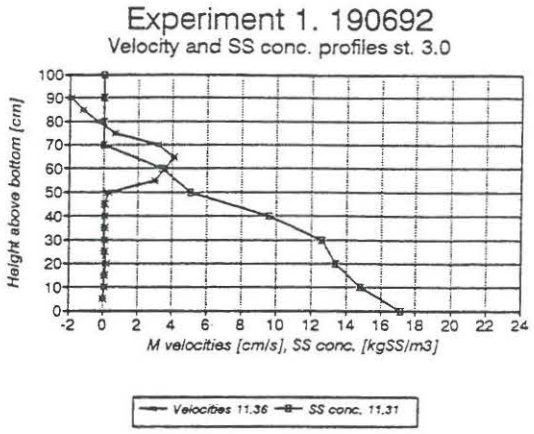

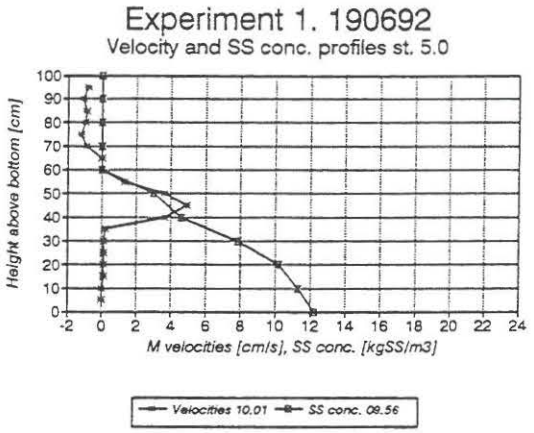

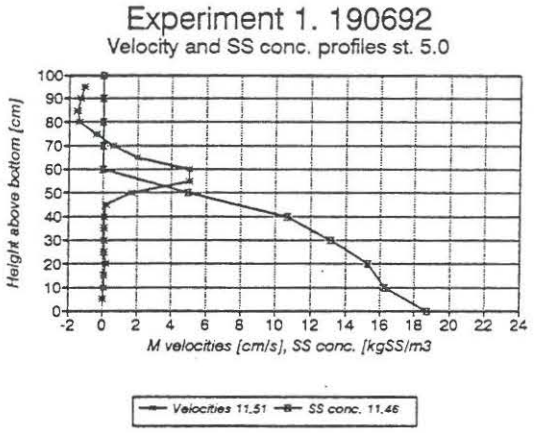

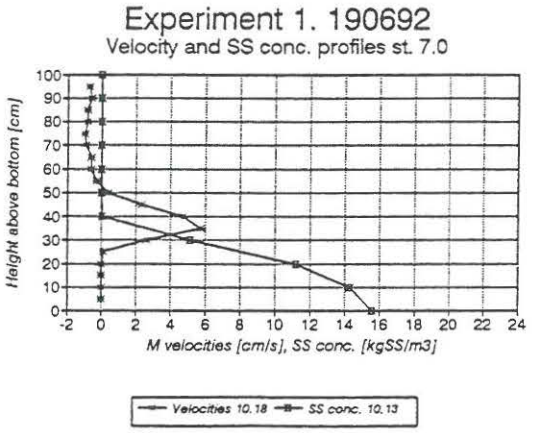

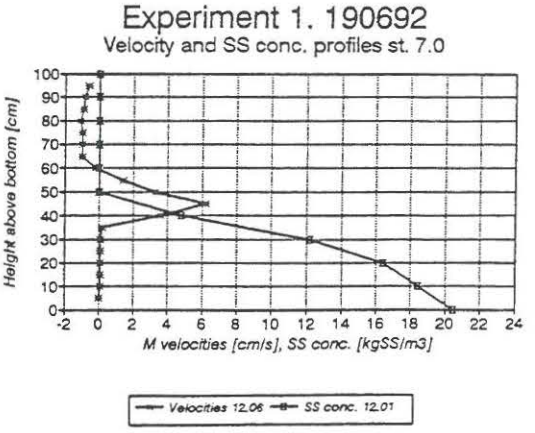

Fig. 6.13. Model tank measurement without inlet boards. Flow 5.4 l/s and influent SS = 4.3 kgSS/m^3. Starting time: 9.30

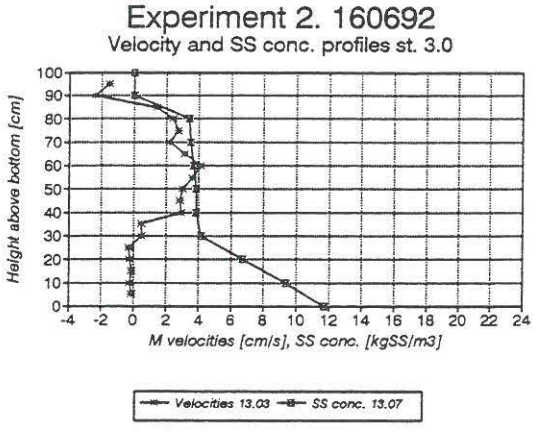

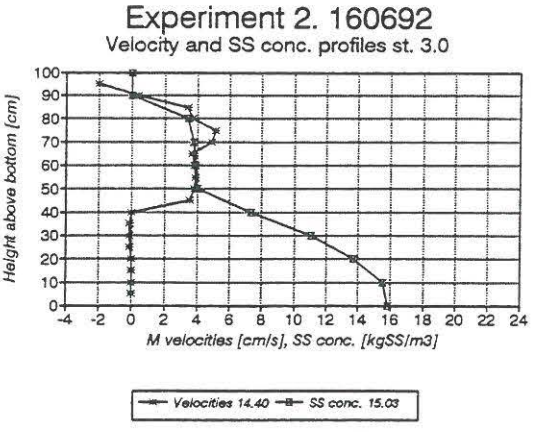

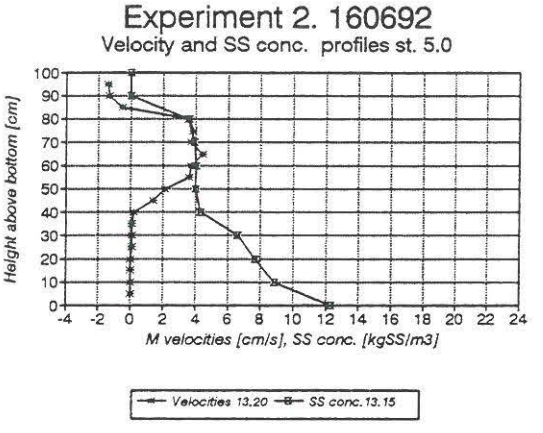

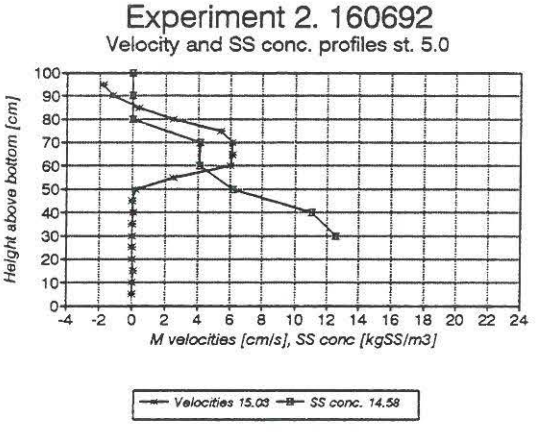

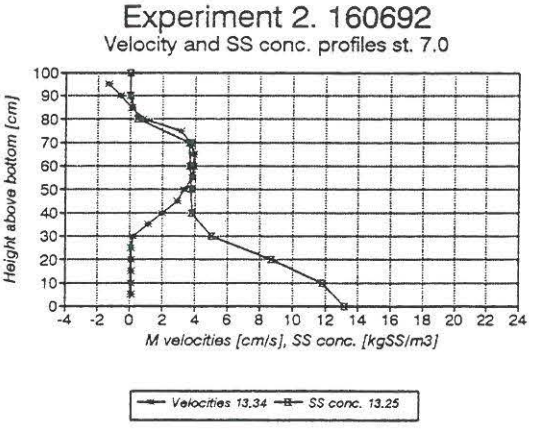

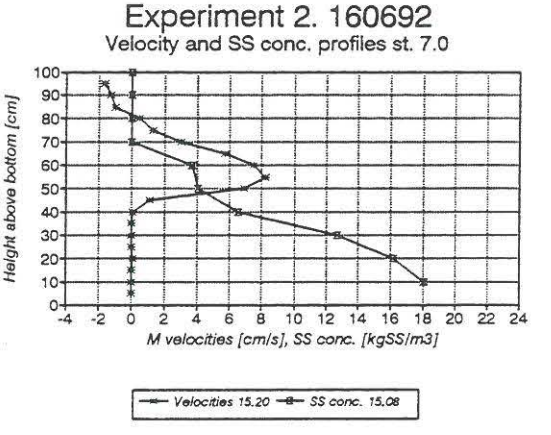

Fig. 6.14. Model tank measurement with inlet boards. Flow = 5.2 l/s and influent SS = 2.0 kgSS/m^3. Starting time: 12.57.

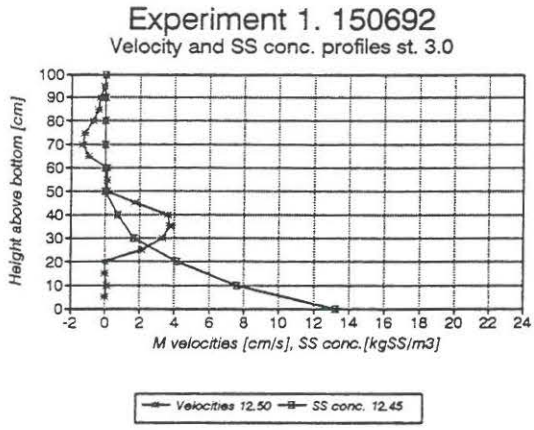

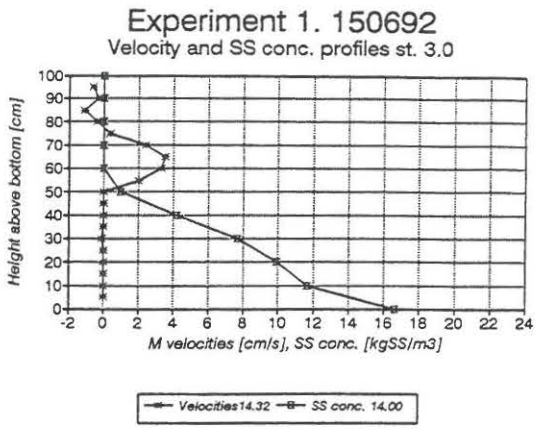

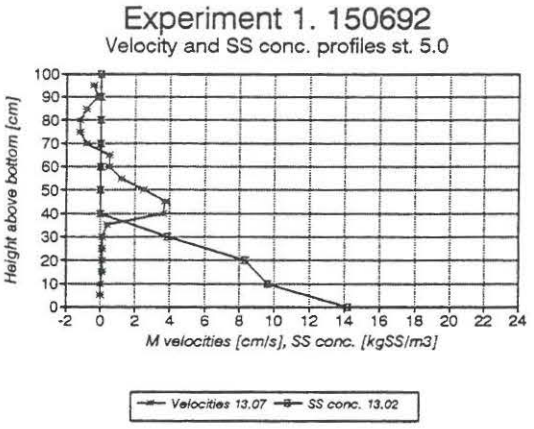

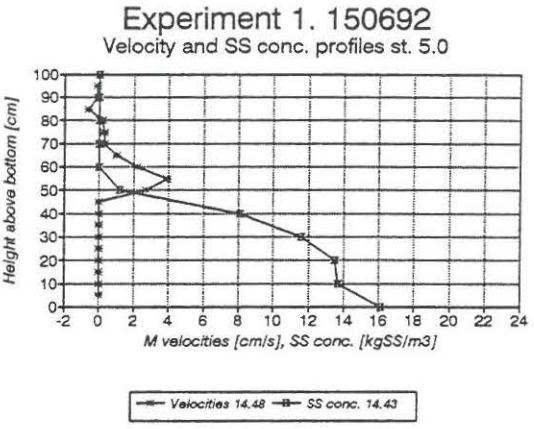

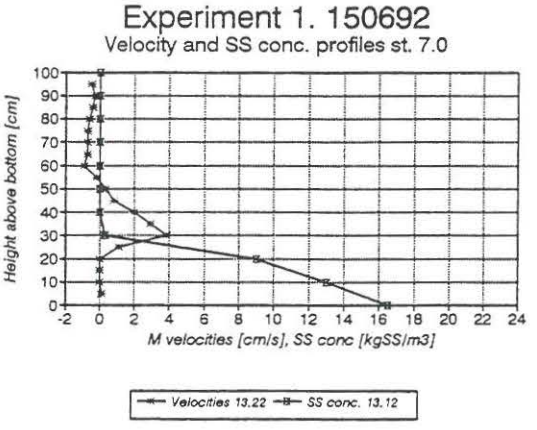

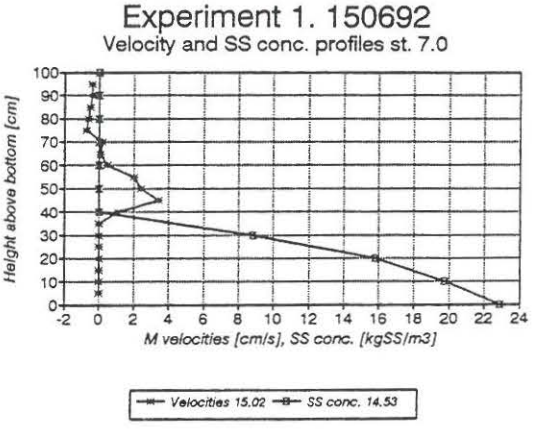

Fig. 6.15. Model tank measurement with inlet boards. Flow = 12.0 l/s and influent SS = 4.4 kgSS/m^3. Starting time: 12.57.

From the results in Fig. 6.12 - 6.15 it appears that the sludge concentrations in the density current decreases from station 3 to station 7 due to settling. Furthermore, the height of the density current decreases, and the maximum velocity increases. Approximately two hours later, the height of the accumulated sludge have increased, but the changes of the density current are the same. Another characteristic phenomenon is the high velocity gradient at the bottom of the density current and the very low velocities below. The physical explanation of this is the Bingham plastic characteristics of the activated sludge.

From the system analysis in section 3.1 it is known that the density current height depends on the flow, and that the maximum velocity is almost the same for different flows. Comparing the measurements shown in Fig. 6.12 and Fig. 6.13 it is seen that the density current height from Fig. 6.12 is almost double the density current height from Fig. 6.13. Furthermore, the maximum velocity increased from station 3 to station 7 in both measurements, and the maximum velocity is almost the same. This shows an agreement between the measurement results and the system analyses.

Owing to the higher influent sludge concentration in Fig. 6.12, the rise of the density current due to accumulation of sludge is small. This means that the initial mass of sludge in the model tank give a sludge profile, where the concentration equal to the influent concentration is close to the height of the final steady state solution. Nevertheless, the sludge accumulates at higher and higher concentrations under the density current.

The measurements in Fig. 6.14 and 6.15 included inlet boards, which especially have an effect on the measurement in Fig. 6.14 with low influent concentration. The inlet was between 50 - 65 cm above the bottom of the model tank, and looking at the profiles in the first plot from station 3 it is seen that the bottom of the density curve have gone down to 20 cm above the bottom. At station 5 the density current raises to 35 cm and in station 7 fall again to 20 cm. This dynamic movement of the density current can be explained as a construction of the buoyancy forces and the Bingham plastic characteristic of the suspension. After accumulation of more sludge, the height of the density current become more steady. In Fig. 6.15 there is no special effect of the inlet boards and size of the density current owing to the initial condition for accumulated sludge like in Fig. 6.13. The measurement results presented here show the reaction when changing the initial and influent conditions and represent most of the effects found in the total measurement program.

6.4 Calibration

With the measured relationships between model variables included in the model formulation, the numerical model is calibrated by comparing model simulations with model tank measurements. In section 3.4 is described that the model formulation of the Bingham plastic characteristic is necessary to calibrate. The model formulation is as follows

$$\tau = \left(\frac{\tau_y}{\dot{\gamma}*} + \eta \right) \dot{\gamma} \qquad (6.3)$$

where τ is the shear stress, τ_y is the critical shear stress, η is the plastic viscosity, $\dot{\gamma}$ is the velocity gradient and $\dot{\gamma}*$ is the velocity gradient of the previous time step. τ_y and η are functions of the sludge concentration. The calibration curves used in the model simulation for comparing with the measurement 19069201 are shown in Fig. 6.16. The curve for η is reported by Dick and Buck (1985) while the curve for τ_y is changed in the calibration.

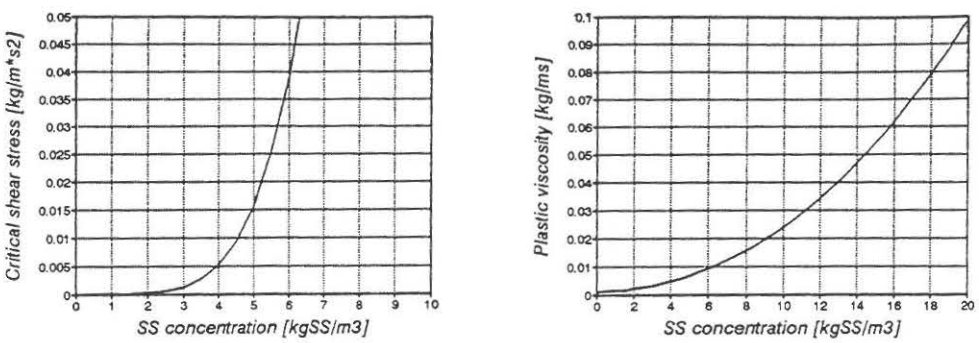

Fig. 6.16. Calibration curves for τ_y and η.

The steep slope for the curve of τ_y for high concentration is necessary to establish a steady sludge blanket and a high velocity gradient at the bottom of the density current as is shown in the measurements. Fig. 6.17 shows the simulation results compared with measurement 19069201.

Experiment 1. 190692
Velocity profiles st. 3.0

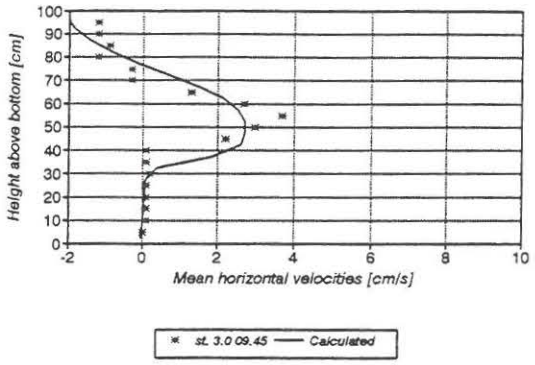

Experiment 1. 190692
Velocity profiles st. 3.0

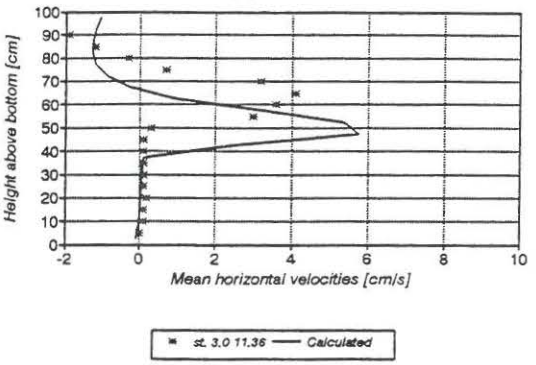

Experiment 1. 190692
SS concentration profiles st. 3.0

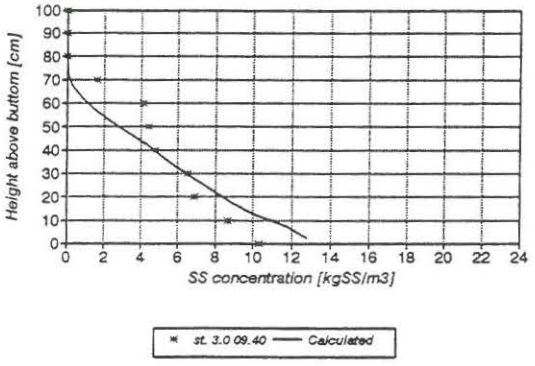

Experiment 1. 190692
SS concentration profiles st. 3.0

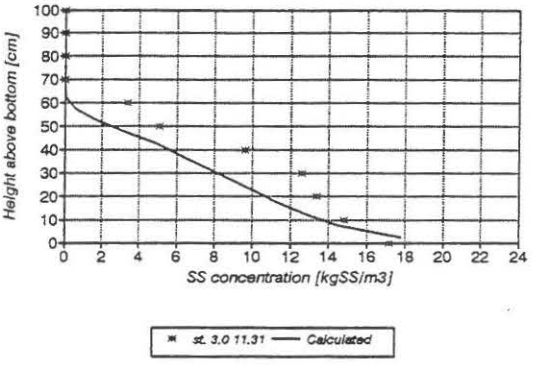

Experiment 1. 190692
Velocity profiles st. 5.0

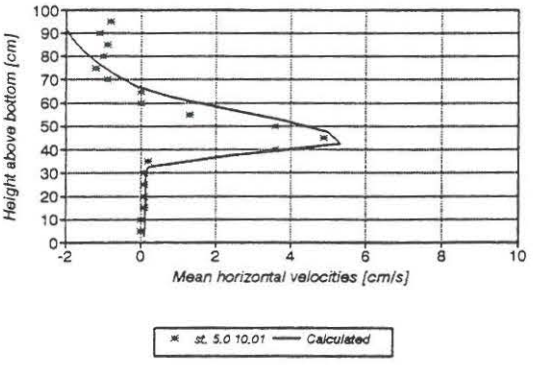

Experiment 1. 190692
Velocity profiles st. 5.0

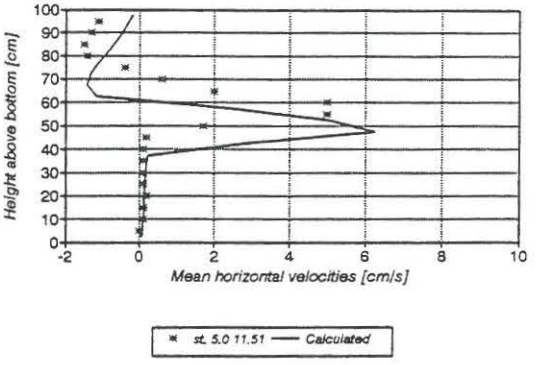

Experiment 1. 190692
SS concentration profiles st. 5.0

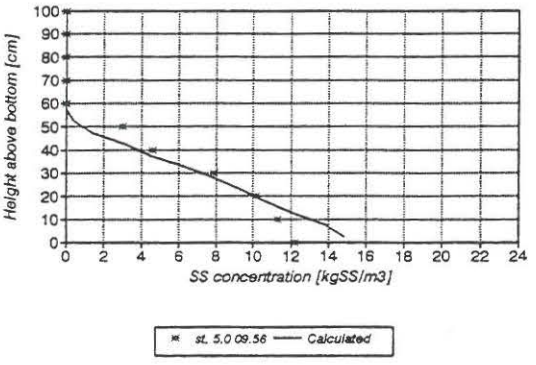

Experiment 1. 190692
SS concentrationsprofil st. 5.0

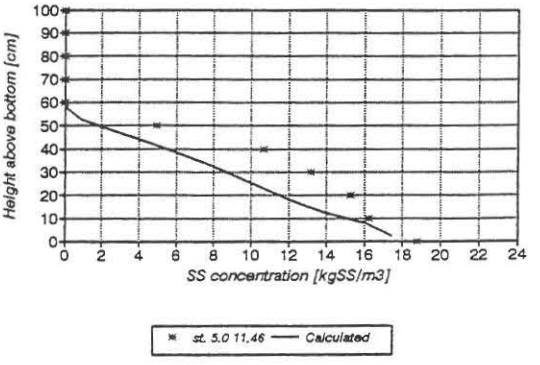

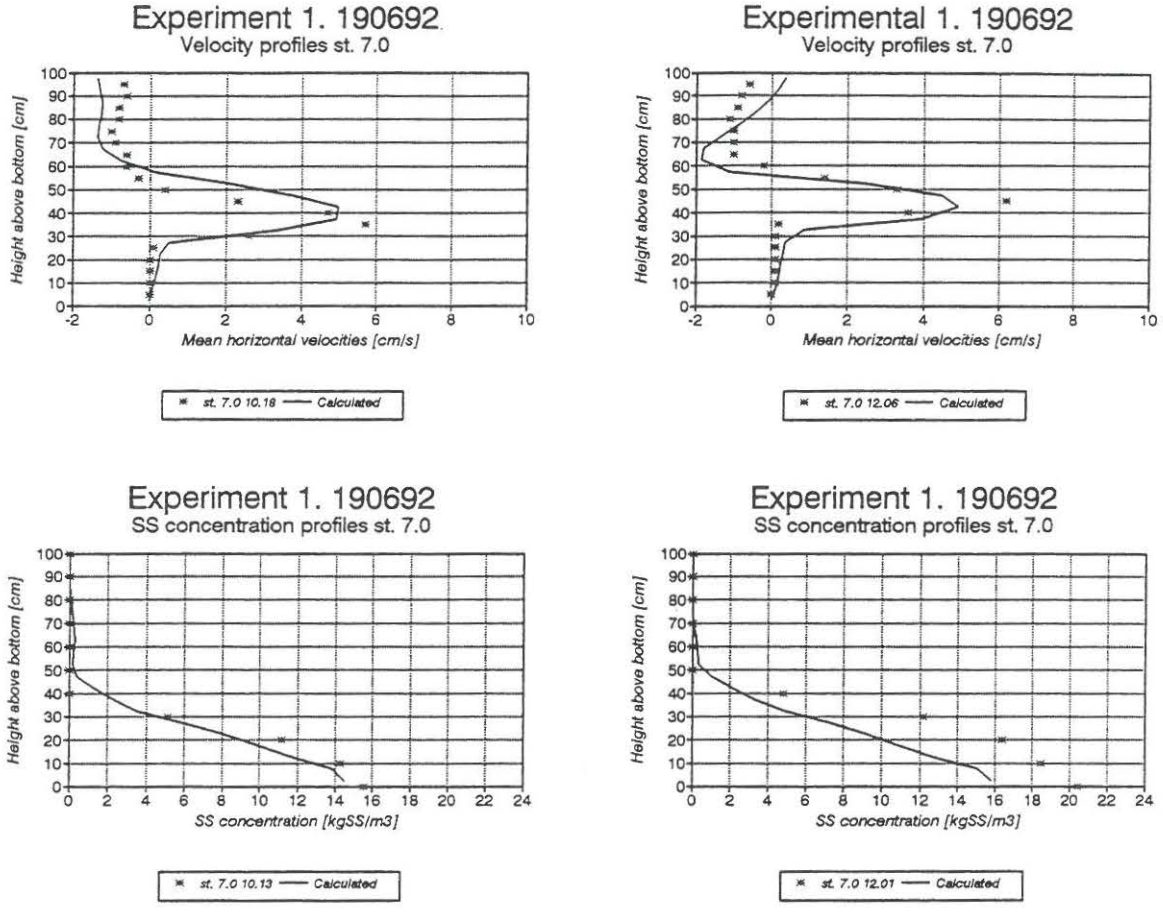

Fig. 6.17. Simulation results compared with measurement 19069201.

Fig. 6.17 shows that the model simulates well the steady sludge blanket and the high velocity gradient at the bottom of the density current in the three different measurement stations. In Fig. 6.1 the location of the measurement stations is seen. In station 7 the simulated velocities in the sludge blanket are higher than the measured velocities, and the simulated sludge concentration in the sludge blanket get too small. Both the simulated and measured profiles displays that the sludge concentrations at the bottom of the density current is slightly higher than the influent concentration. The vertical location of the density current is well predicted in all stations and the numerical model is found to simulate the model tank measurement 19069201 well.

Measurement 19069201 had an influent concentration of 4.0 kgSS/m^3. To fit the simulation to the measured results for measurement 05069201 with an influent concentration of 2.0 kgSS/m^3 a new calibration curve for τ_y is needed. The two different calibration curves for τ_y are shown in Fig. 6.18.

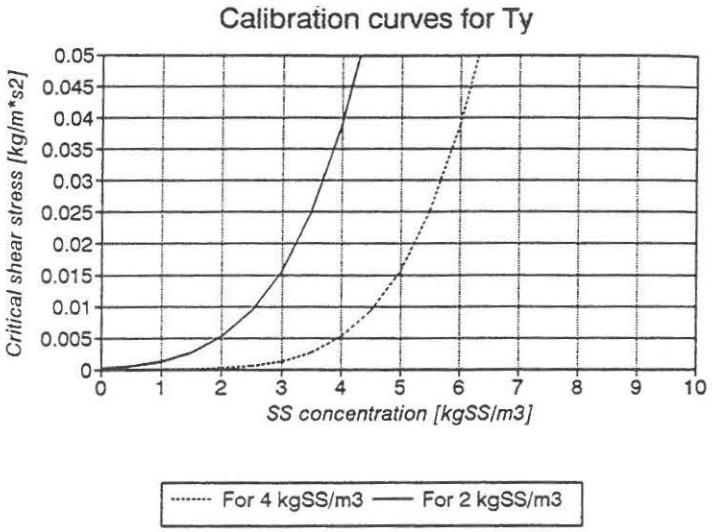

Fig. 6.18. Calibration curves for τ_y for the different measurements.

As seen from Fig. 6.18, the slope of the curves increases rapidly near the influent concentration for the two measurements, respectively. An explanation to this needed change in calibration for different influent concentration can be the thixotropic characteristic of sludge suspension. For a thixotropic suspension the critical shear stress τ_y changes when the suspension is exposed to different shearing rates. As mentioned previously, the sludge concentration in the bottom of the density current with high shear stress is near the influent concentration. The shear stress in the density current therefore affected suspensions with different sludge concentrations in measurement 19069201 and 05069201. This can be a reason for the needed change in calibration, but it is not necessarily the only one. The exact explanation is not found, but the calibration from Fig. 6.18 is used in the further numerical model simulation. Fig. 6.19 shows the simulation results compared with measurement 05069201.

Experiment 1. 050692
Velocity profiles st. 3.0

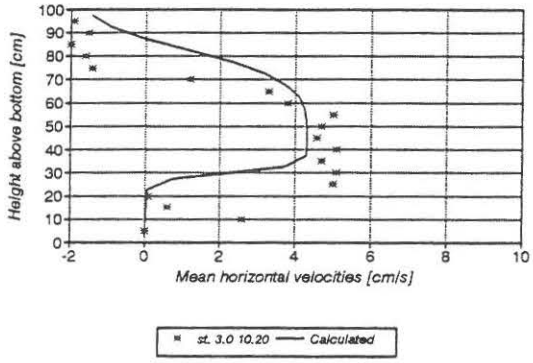

Experiment 1. 050692
Velocity profiles st. 3.0

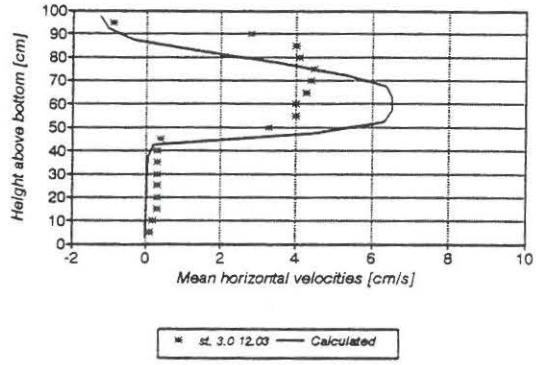

Experiment 1. 050692
SS concentration profiles st. 3.0

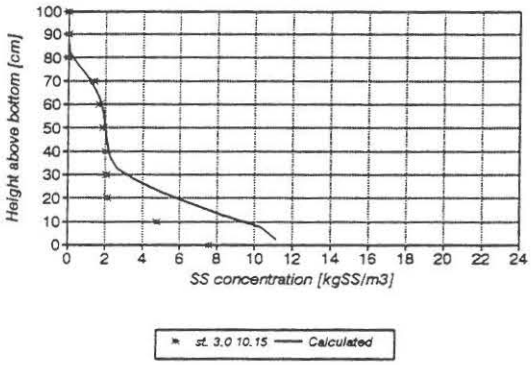

Experiment 1. 050692
SS concentration profiles st. 3.0

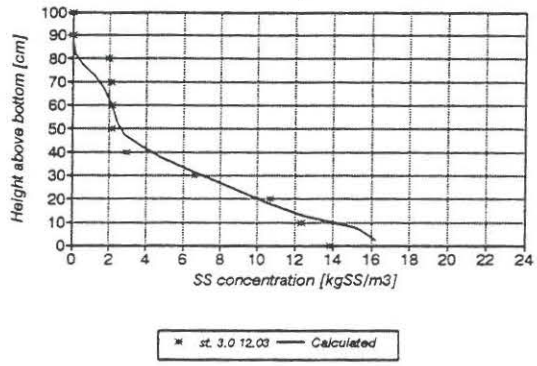

Experiment 1. 050692
Velocity profiles st. 5.0

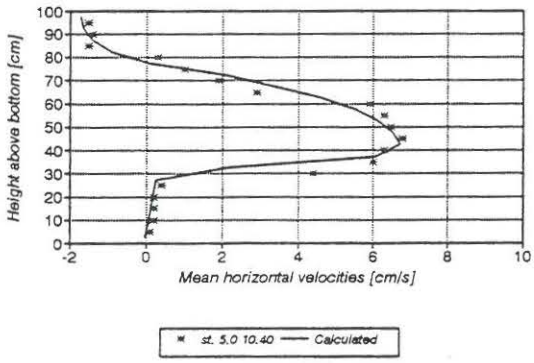

Experiment 1. 050692
Velocity profiles st. 5.0

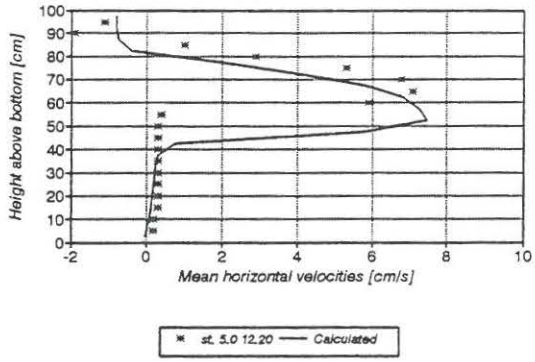

Experiment 1. 050692
SS concentration profiles st. 5.0

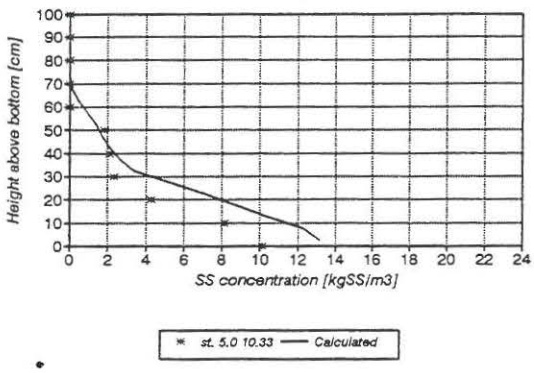

Experiment 1. 050692
SS concentration profiles st. 5.0

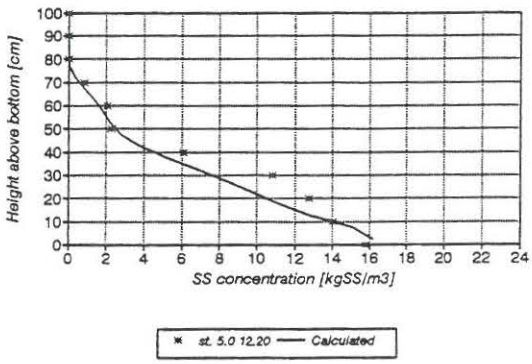

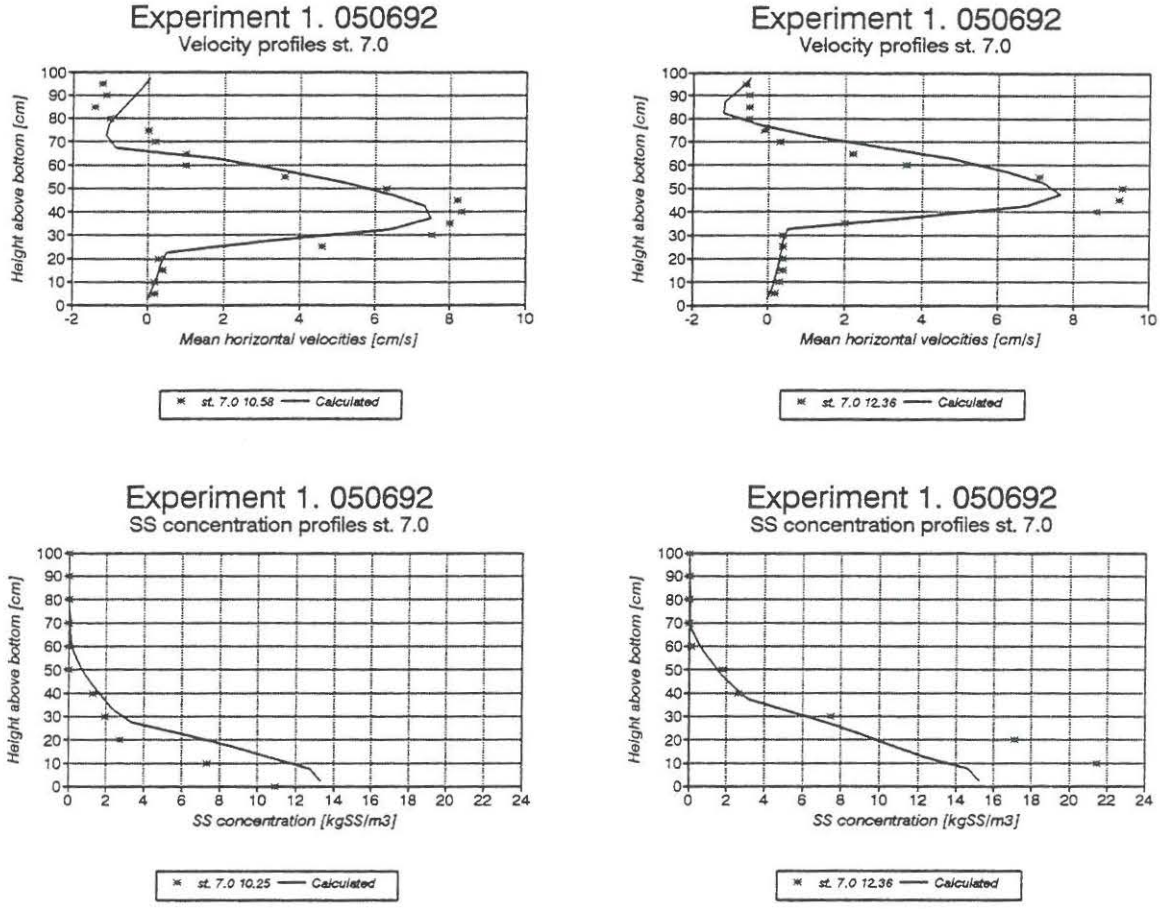

Fig. 6.19. Simulation results compared with measurement 05069201.

The overall picture of the flow in measurement 05069201 is similar to that described for measurement 19069201. In station 3 the simulated velocity profile have either a higher placed density current or a more narrow density current with higher velocities when compared with the measured profiles. These differences can be due to problems with the initial conditions and inlet boundary in the simulation. For stations 5 and 7, the simulations fit the measurements well, but for station 7 it appears that the maximum velocity is highest in the measured profile which can be due to three-dimensional effects near the outlet for this high flow measurement.

6.5 Validation

This section describes the validation of the numerical model by comparing model simulations with new model tank measurements. The only change in the model formulation is a new inlet geometry and a new influent and influent sludge concentration. Fig. 6.20 shows the measured results compared with simulated results for measurement 15069201. The inlet

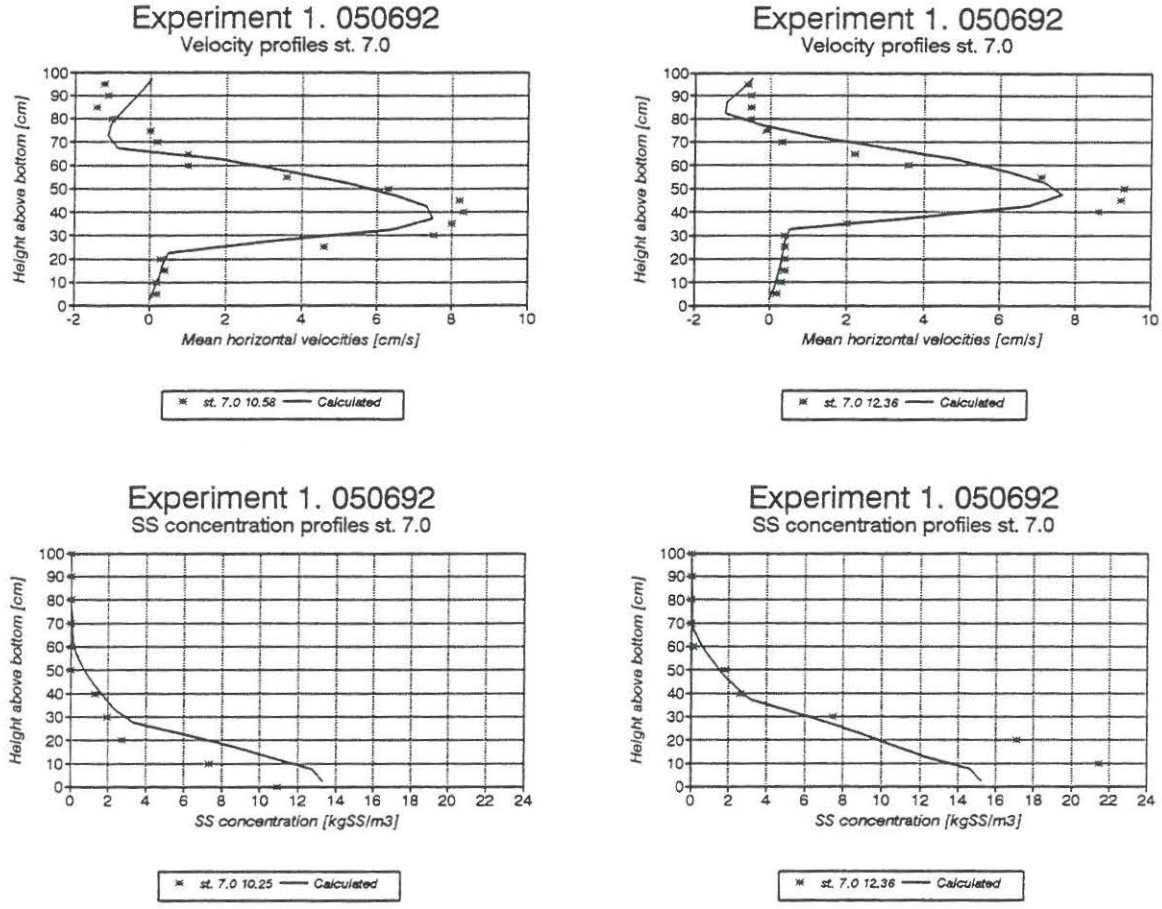

Fig. 6.19. Simulation results compared with measurement 05069201.

The overall picture of the flow in measurement 05069201 is similar to that described for measurement 19069201. In station 3 the simulated velocity profile have either a higher placed density current or a more narrow density current with higher velocities when compared with the measured profiles. These differences can be due to problems with the initial conditions and inlet boundary in the simulation. For stations 5 and 7, the simulations fit the measurements well, but for station 7 it appears that the maximum velocity is highest in the measured profile which can be due to three-dimensional effects near the outlet for this high flow measurement.

6.5 Validation

This section describes the validation of the numerical model by comparing model simulations with new model tank measurements. The only change in the model formulation is a new inlet geometry and a new influent and influent sludge concentration. Fig. 6.20 shows the measured results compared with simulated results for measurement 15069201. The inlet

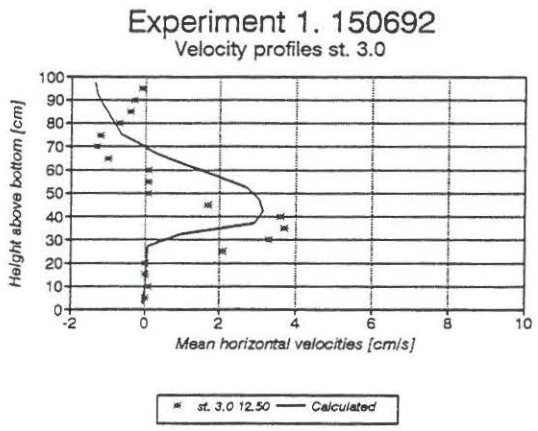
Experiment 1. 150692
Velocity profiles st. 3.0
Height above bottom [cm]
Mean horizontal velocities [cm/s]
st. 3.0 12.50 Calculated

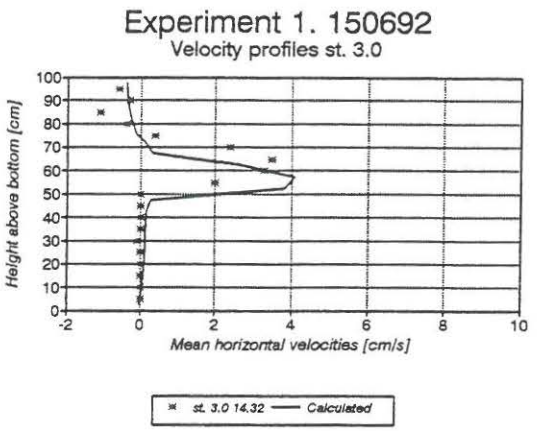
Experiment 1. 150692
Velocity profiles st. 3.0
Height above bottom [cm]
Mean horizontal velocities [cm/s]
st. 3.0 14.32 Calculated

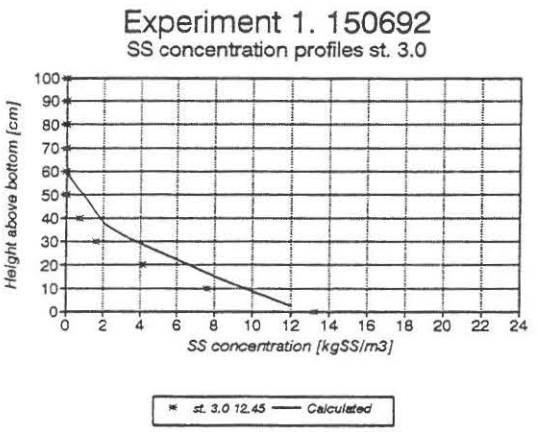
Experiment 1. 150692
SS concentration profiles st. 3.0
Height above bottom [cm]
SS concentration [kgSS/m3]
st. 3.0 12.45 Calculated

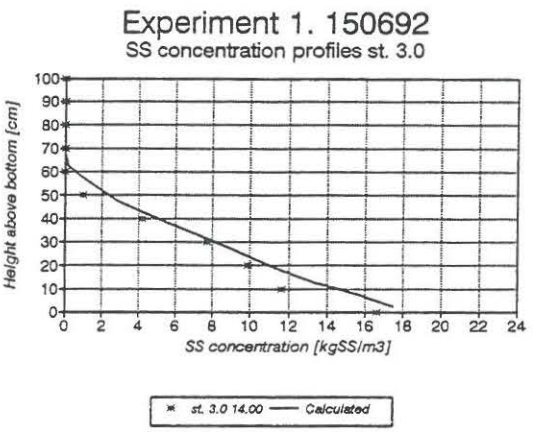
Experiment 1. 150692
SS concentration profiles st. 3.0
Height above bottom [cm]
SS concentration [kgSS/m3]
st. 3.0 14.00 Calculated

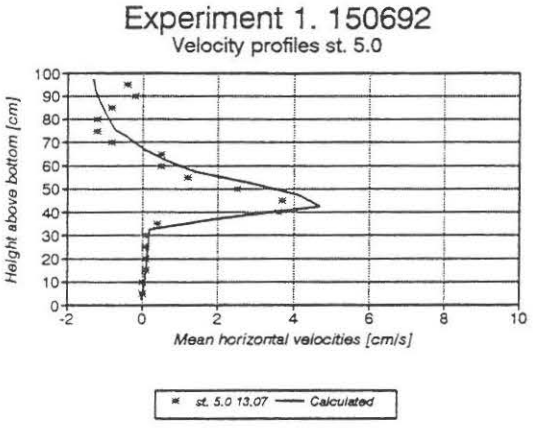
Experiment 1. 150692
Velocity profiles st. 5.0
Height above bottom [cm]
Mean horizontal velocities [cm/s]
st. 5.0 13.07 Calculated

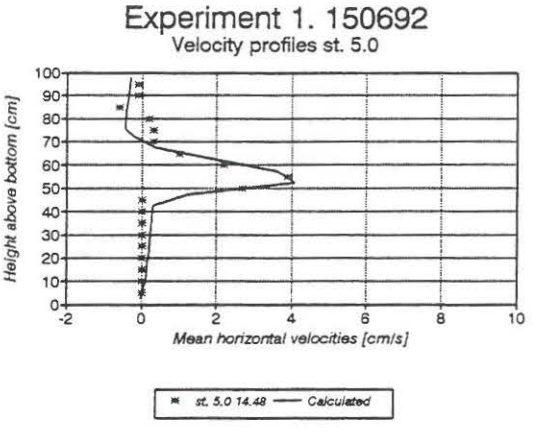
Experiment 1. 150692
Velocity profiles st. 5.0
Height above bottom [cm]
Mean horizontal velocities [cm/s]
st. 5.0 14.48 Calculated

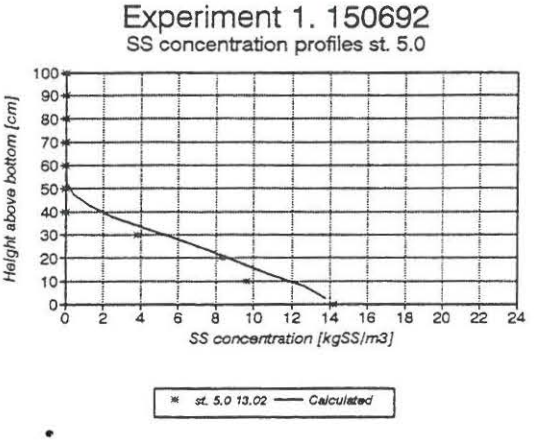
Experiment 1. 150692
SS concentration profiles st. 5.0
Height above bottom [cm]
SS concentration [kgSS/m3]
st. 5.0 13.02 Calculated

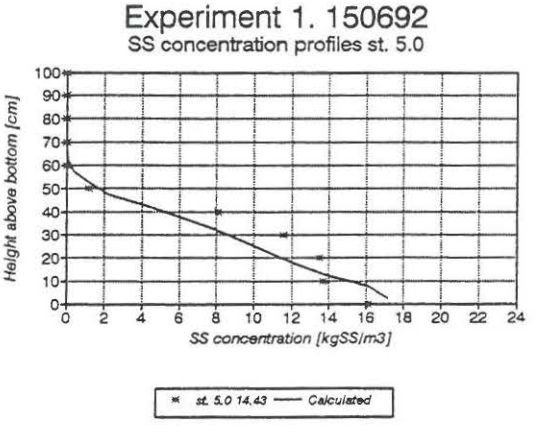
Experiment 1. 150692
SS concentration profiles st. 5.0
Height above bottom [cm]
SS concentration [kgSS/m3]
st. 5.0 14.43 Calculated

was here a slot between 50 and 65 cm above the bottom of the model tank.

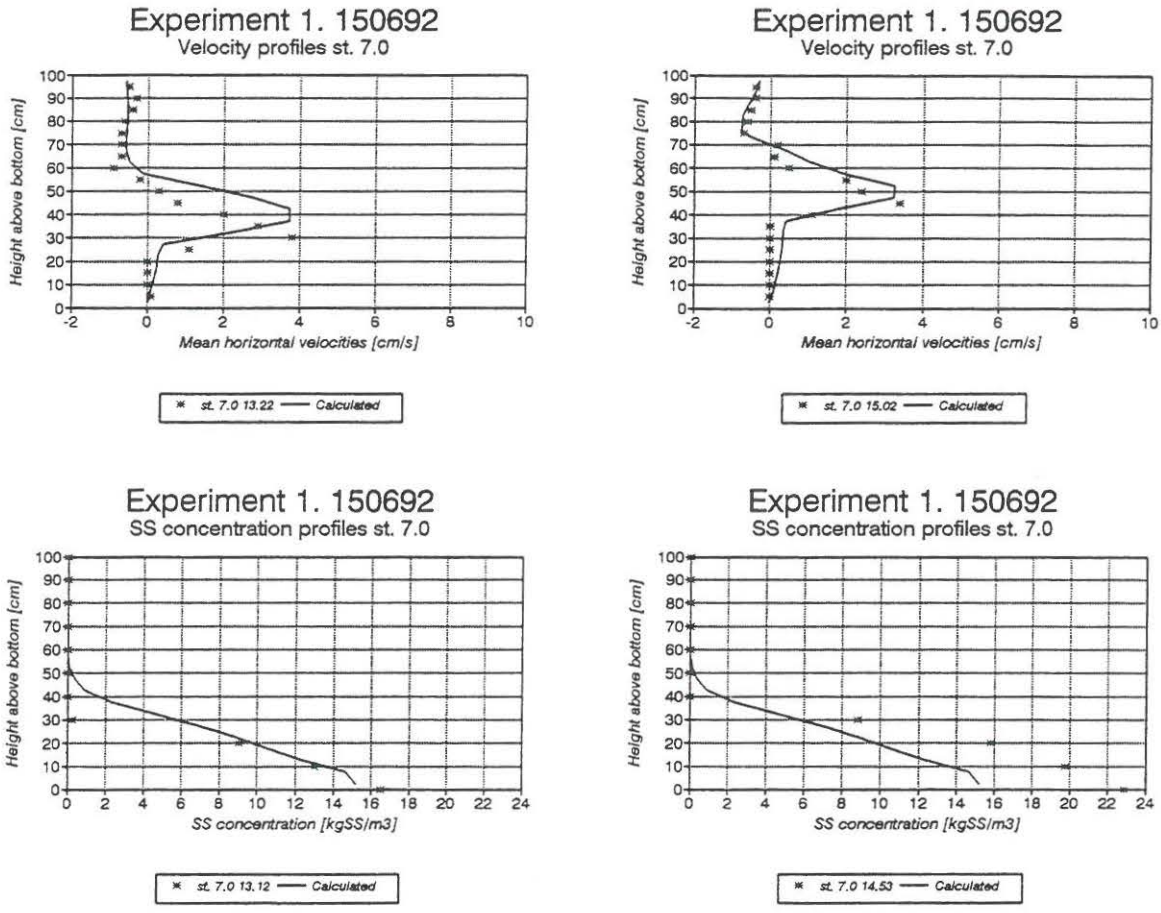

Fig. 6.20. Simulation results compared with measurement 15069201.

From the first measurement series it is seen that the density current in station 3 had decreased in height compared to the inlet due to the negative buoyancy. The density current then rising approximately 15 cm to station 5 and finally decreasing in station 7 due to the effluent at the bottom of the model tank. It appeared that the simulation results did not have the same change between the measurement station as the measured results. For the second series, the model tank have a higher content of sludge, and the comparison between measurement and simulation have a better agreement. The reason for the missing changes in the simulation result can be due to the Bingham plastic model description. The simulated results compared with measurement 16069202 is seen in Fig. 6.21.

Experiment 2. 160692
Velocity profiles st. 3.0

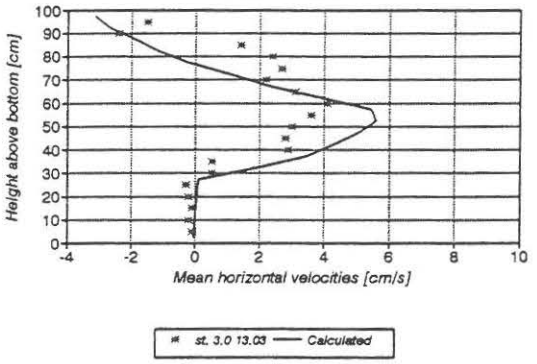

Experiment 2. 160692
Velocity profiles st. 3.0

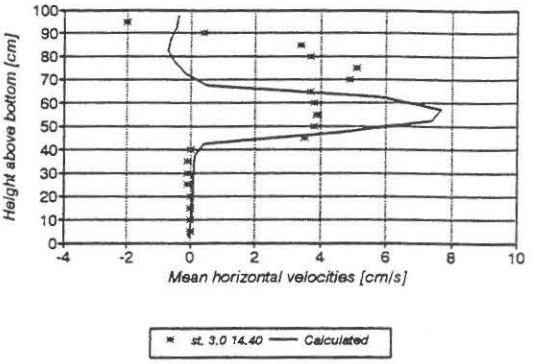

Experiment 2. 160692
SS concentration profiles st. 3.0

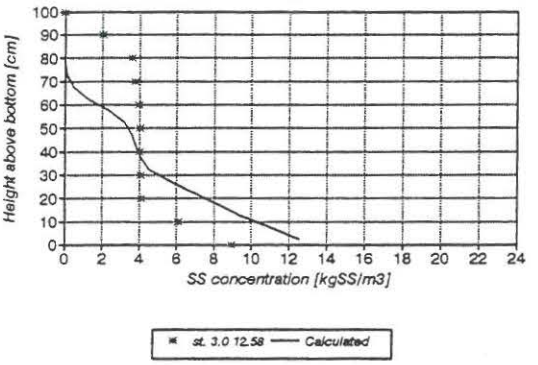

Experiment 2. 160692
SS concentration profiles st. 3.0

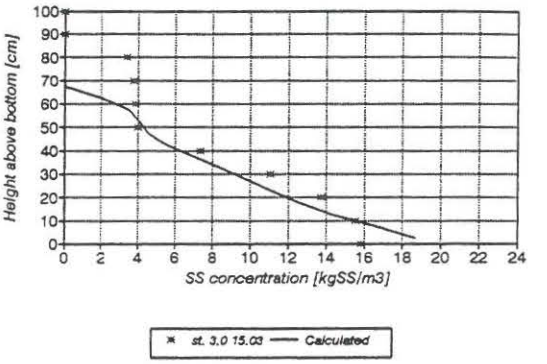

Experiment 2. 160692
Velocity profiles st. 5.0

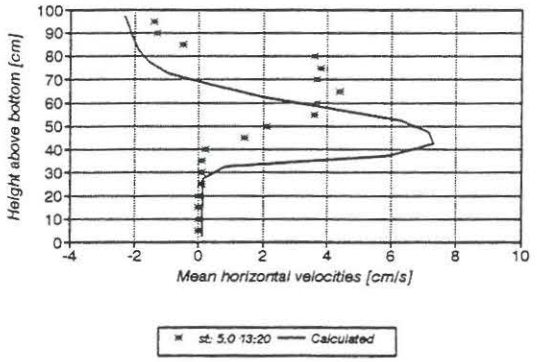

Experiment 2. 160692
Velocity profiles st. 5.0

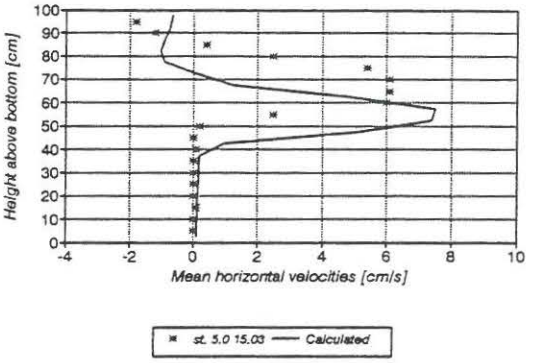

Experiment 2. 160692
SS concentration profiles st. 5.0

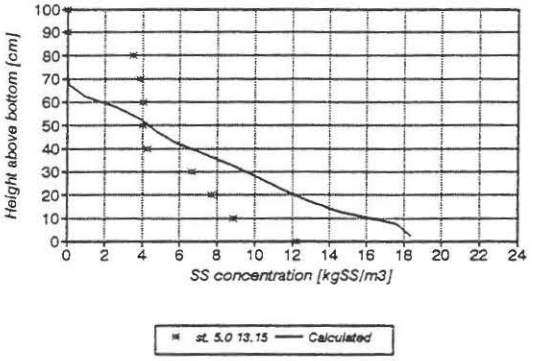

Experiment 2. 160692
SS concentration profiles st. 5.0

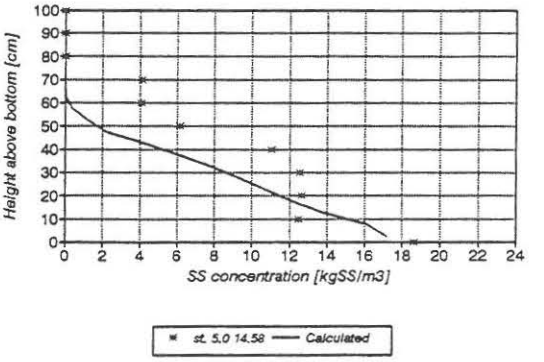

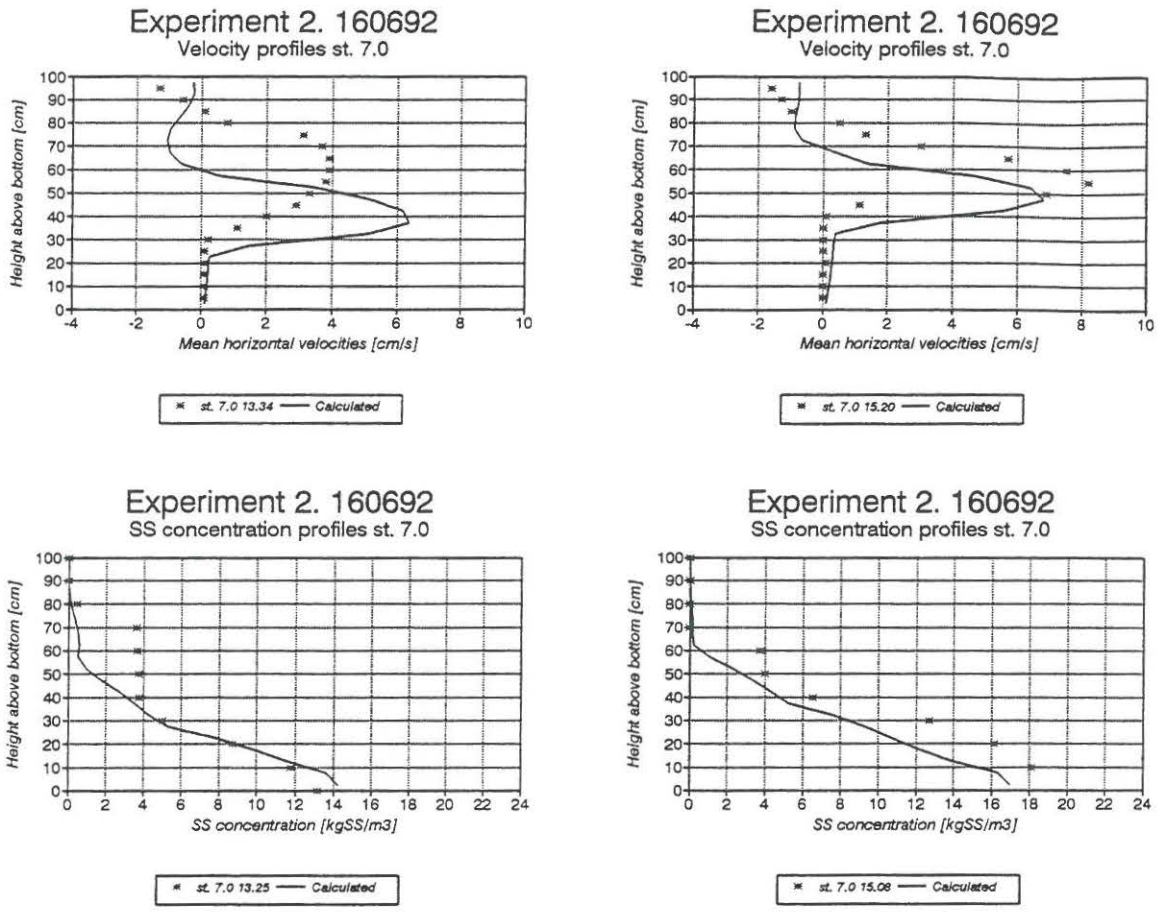

Fig. 6.21. Simulation results compared with measurement 16069202.

Especially for this measurement a difference is seen between the simulated and measured sludge concentration profiles. The measurements in the first series shows a concentration equal to the influent concentration in most of the density current. This is not the case for the simulated results. An explanation can be that the numerical model is more sensitive to backward velocities at the top of the model tank, and in some cases therefore predict a too high zone of backward velocities. This causes increased mixing with influent and decreases the concentration in the density current.

In enclosure 2 model simulation compared with the other measurements is presented. Despite the good model predictions of the measurements there were 2 measurements, 11069201 and 16069201 for which no good model prediction is found. These measurements were both for initial condition with inlet boards and the highest flow rates. The measurements

shows a large eddy in the inlet zone with forward velocities at the top and backward velocities at the bottom of the tank. See enclosure 1. This large motion the model simulation is not able to predict. The flow rate in both measurements can be considered as beyond the maximum flow rate expected in secondary settling tanks. Therefore, the problem with a model prediction of these measurements is not considered as critical.

6.6 Discussion

Basic measurements of relationship between, settling velocities and suspension density depending of the sludge concentration were made. From the calibration and validation of the numerical model in section 6.4 and 6.5, the comparison between model simulations and model tank measurements shows that the basic measurement procedures provided results which gives a good model prediction of the settling of sludge and buoyancy.

The microscopical examination of the activated sludge shows a high level of filamentous microorganisms with an Eikelboom index at 3 - 4. From chapter 3 filamentous microorganisms are known to influence the settling and the rheology of the activated sludge. For the settling is seen good settling characteristics despite of the high index, and for the rheological characteristics a very steady sludge blanket interface is seen as expected with a high level of filamentous microorganisms.

The calibration of the numerical model is made by comparing model simulations with model tank measurements and changing the relationship between the critical shear stress τ_y and the plastic viscosity η dependence of the sludge concentration. These parameters are calibrated to give the best agreement between simulation and measurements. The calibrated numerical model predicts the measurements well despite of the specialised calibration where the influent sludge concentration is included in the calibration of τ_y depending on the sludge concentration.

In the validation of the numerical model, where the model simulation is compared with new measurements, the numerical model predicts the measurements well. This means that the calibrated numerical model can simulate dynamic changes where the sludge accumulated in the model tank increases during a measurement and can simulate different inlet geometries and different hydraulic and sludge loads.

7. FULL SCALE MEASUREMENTS AND SIMULATIONS

The purpose of the full scale measurements was to provide measurements for validation of the numerical model for full scale settling tanks. In the full scale measurements, different loads were used, some with steady and some with unsteady conditions. To examine the flexibility of the model, two different wastewater treatment plants were chosen. The first was the Lynetten wastewater treatment plant of 1 mill. PE which is a mechanical and biological treatment plant without denitrification and phosphorus removal. The second was the Slagelse wastewater treatment plant of 125,000 PE which is a mechanical, biological and chemical treatment plant with both removal of nitrogen and phosphorus. In section 7.1 the Lynetten measurements and the model simulation are described. It includes a description of the measurement set-up, the measurement procedures, basic measurements and full scale measurement results and finally model simulation and validation. A similar description for Slagelse is presented in section 7.2.

7.1 Lynetten wastewater treatment plant

This section describes the measurements carried out in one of the secondary settling tanks at the Lynetten wastewater treatment plant.

7.1.1 Outline of the settling tank

The secondary settling tank is 60 m long, 8 m wide and 3 m deep, with weir scrapers. Fig. 7.1 shows the settling tank.

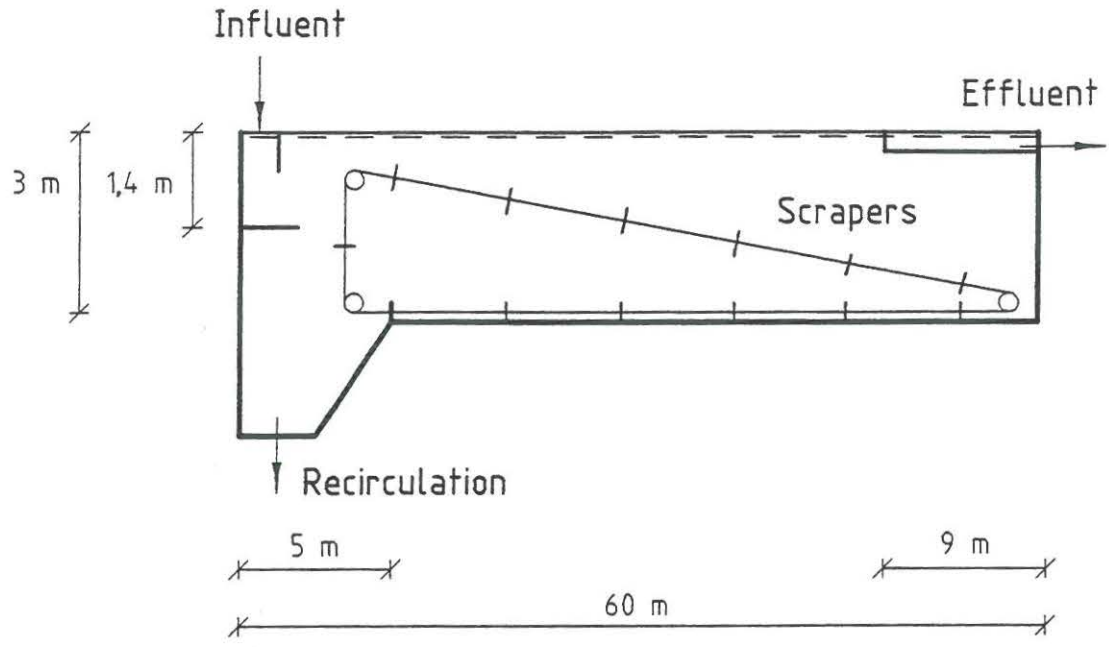

Fig. 7.1. Secondary settling tank, Lynetten.

Fig. 7.1 shows that the influent is guided by baffles to prevent the influent from going down directly into the recirculation pit. At the outlet end of the tank the water is drawn from the tank at the surface of the last 9 m by effluent weirs. The recirculation flow is pumped out of the tank from the recirculation pit.

In the measurements, the settling tank was simplified to a two-dimensional system which means that measurements were taken only in the middle of the tank on a line from the inlet to the outlet end. On this line 4 measurement stations were established by bridges over the settling tank as seen on the photo in Fig. 7.2.

Fig. 7.2. Bridges over settling tank, Lynetten.

The distance between the bridges is shown in Fig. 7.3. The 1st bridge was placed close to the inlet baffles for measuring the influent there. The 4th bridge was placed just before the effluent weirs and the 2nd and 3rd bridges in between.

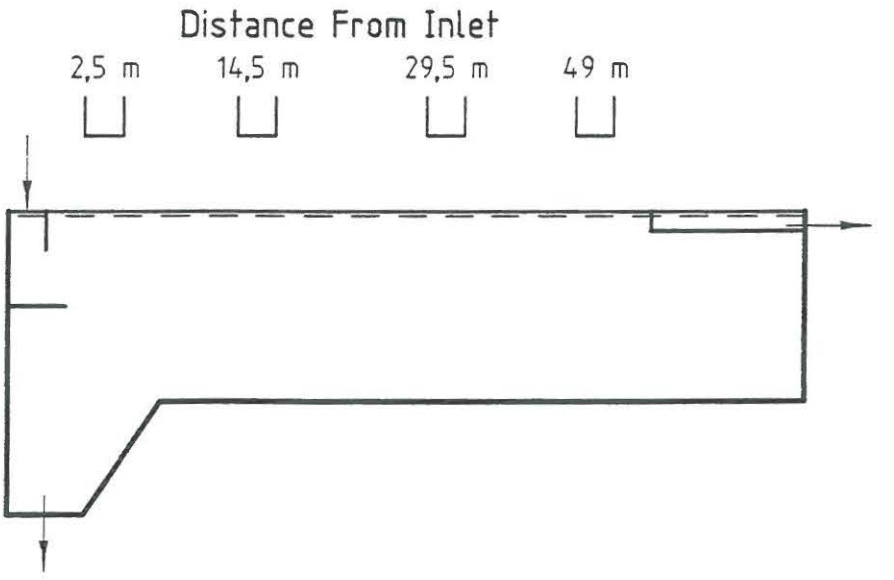

Fig. 7.3. Distance between measurement section.

The measurements carried out from the bridges were profiles of the mean, horizontal velocity and the sludge concentration. The measurement instruments and procedure were described in section 5.1. To measure the mass balance of sludge in the settling tank, sludge concentration was measured at the influent, recirculation flow and effluent. The recirculation flow was measured on-line in the pipe from the recirculation pump. The flow through the tank was calculated by integration of the measured velocity profiles. From a distribution channel 16 settling tanks are fed. To control the influent to each tank controllable inlet boards are present in each tank. See Fig. 7.4.

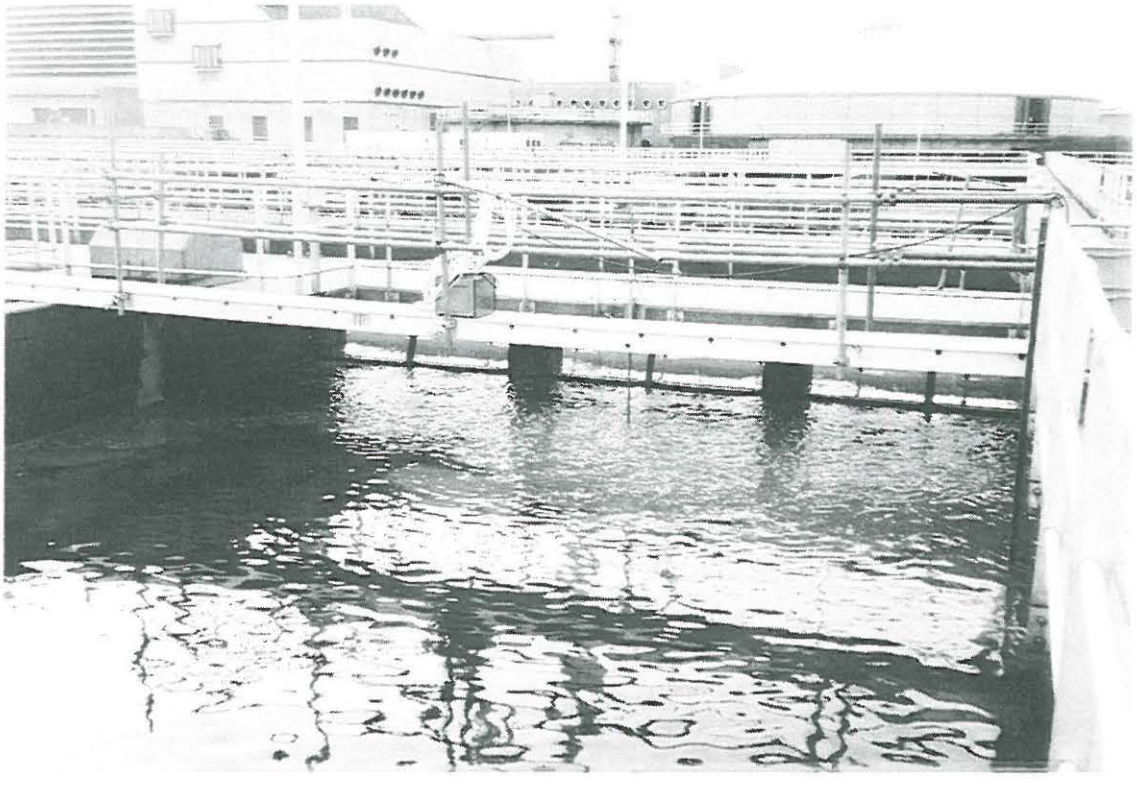

Fig. 7.4. Photo of controllable inlet board.

The influent could thus be controlled within a range which was large enough for the measurements decided upon. Furthermore, the recirculation flow could be controlled by a valve near the recirculation pump.

Full scale measurement procedures

Two different types of measurements were carried out in the settling tank. First, a steady measurement where the influent was kept as steady as possible. After a steady state condition was reached, velocity and sludge concentration profiles were measured from each bridge. After-

wards, a tracer measurement was made as described in section 5.1.3. The second measurement type were unsteady. They started with a steady measurement and after the first profile measurements at each bridge, the influent was increased. Hereafter, the changes in the profiles at each bridge were followed. Furthermore, the sludge concentration in the influent, recirculation flow and effluent for the mass balances was followed during the whole measurement.

A total of six different measurements, three steady and three unsteady, were carried out at Lynetten. Table 7.1 shows the influent and influent sludge concentration for each measurement, named with the date of the measurement. Furthermore, it must be noted that the slash means a change in influent.

	Influent Q m^3/h	Recirc. flow Q_r m^3/h	$SS_{influent}$ $kgSS/m^3$
140493	356/631	175	3.15
150493	498/908	147	3.00
160493	519	149	3.20
190493	414	147	2.60
200493	588	147	2.75
210493	596/1060/459	140	2.96

Table 7.1. Flows and influent sludge concentration conditions for the Lynetten measurements

7.1.2 Results of basic measurements

With the measurement procedures described in section 5.2 basic measurement was carried out for measuring, free settling velocities and flocculation, hindered settling velocities, density of suspension and finally a microscopical examination.

The measurement for examining the free settling velocities and flocculation at different turbulence conditions was used for two different, initial sludge concentrations and five different turbulence levels. An example of the results from one measurement is seen in Fig. 7.5. The first graph is the direct measurement of the sludge concentration changes at one point and the second graph shows the differences in settling velocities.

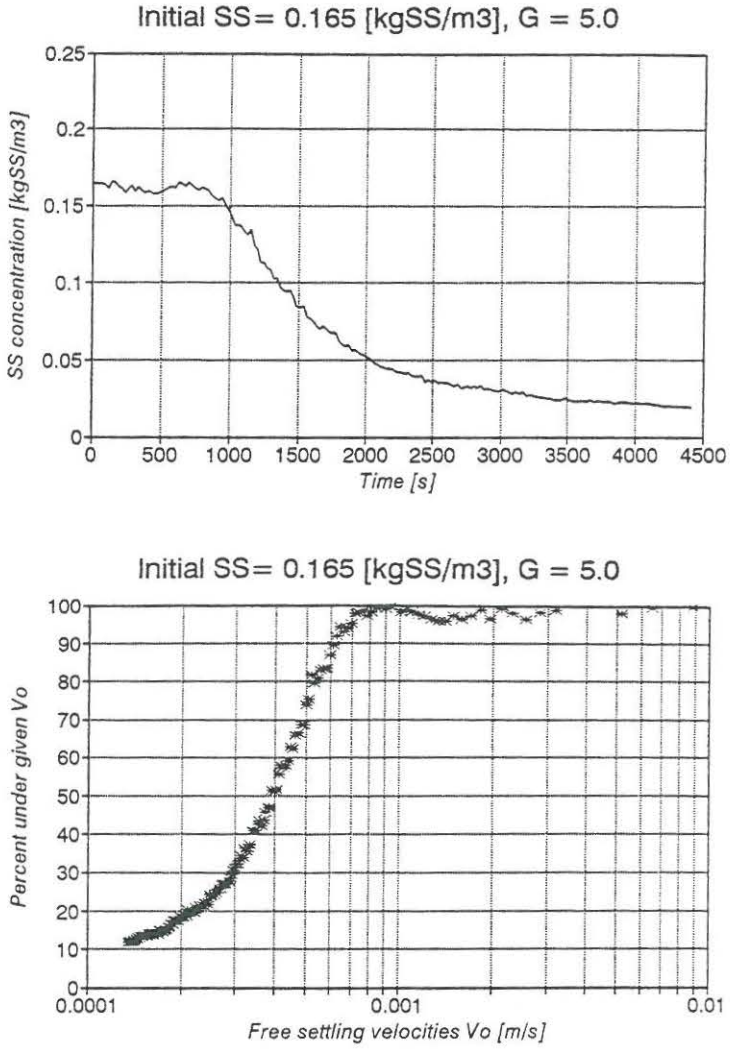

Fig. 7.5. a. Sludge concentration changes in one point of the settling column. b. Percentage of initial sludge with settling velocities under a given velocity.

In Fig. 7.5 two parameters can be seen directly. The first parameter is the mean free settling velocity defined as the velocity where 50% of the settleable part of the sludge is settled past the measuring point. The second parameter is the percentage of the sludge which is non-settleable within the duration of the measurement. From section 3.4 the settleable sludge is defined as the sludge flocs and the non-settleable sludge at dispersed particles. Fig. 7.6.a and b show these parameters for the different turbulence levels characterised by the parameter G and for the initial sludge concentration.

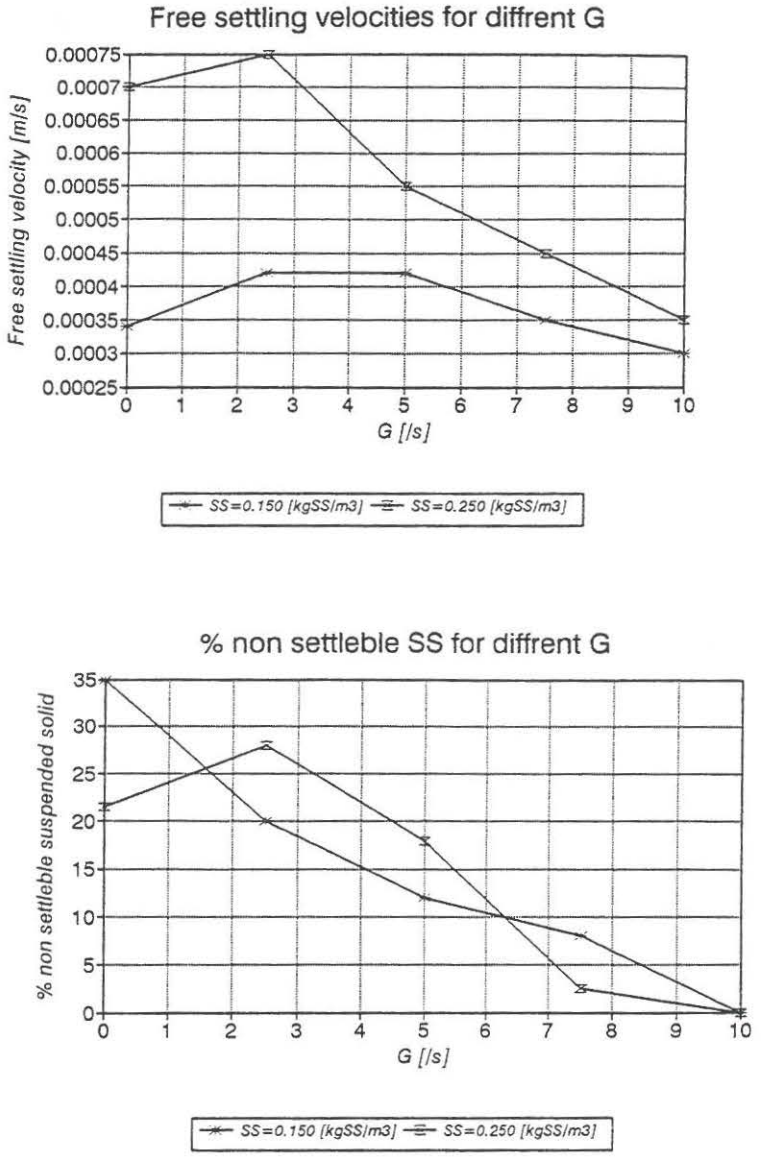

Fig. 7.6. a. Mean free settling velocity for different turbulence levels.
b. Percentage of non-settleable sludge for different turbulence levels.

In Fig. 7.6.a it is seen that the mean settling velocities are highest with a value of G at 2.5 and that the highest initial sludge concentration give higher mean settling velocities than the low concentration for all values of G. This means that the best floc settling occurs at G = 2.5 and that the sludge concentration influences the flocculation efficiency. Fig. 7.6.b shows that the percentage of the initial sludge which is non-settleable is to a great extent dependent on the turbulence level.

The high turbulence levels with G > 2 only occur just at the inlet zone of the settling tank where free settling does not occur. Therefore, the description of free settling velocities is not modelled as depending on the turbulence levels but only depending on the sludge concentrations. As

settling velocities for 150 mgSS/l and 250 mgSS/l the velocities for G = 1 at 0.000375 m/s and 0.000725 m/s are used.

In Fig. 7.6.b it is seen how the percentage of non-settleable sludge decreases with increased turbulence level. To determine the flocculation model to these results, a one-dimensional numerical model for simulation of the settling and flocculation measurement in the column is used. In the model simulation of the column measurement the measured mean settling velocities for each measurement are used. Either 35% or 45% of non-settleable sludge are used as initial condition for the measurement with 150 mgSS/l or 250 mgSS/l, respectively. These values is the measured or expected values for G = 0.

The constants K_A and K_B in the flocculation model are then calibrated to fit the percentage of non-settleable sludge at the end of the measurements. Fig. 7.7 shows the simulated results compared with the measured results with the calibrated constants at $K_A = 1.5 \cdot 10^{-3}$ and $K_B = 1.0 \cdot 10^{-6}$.

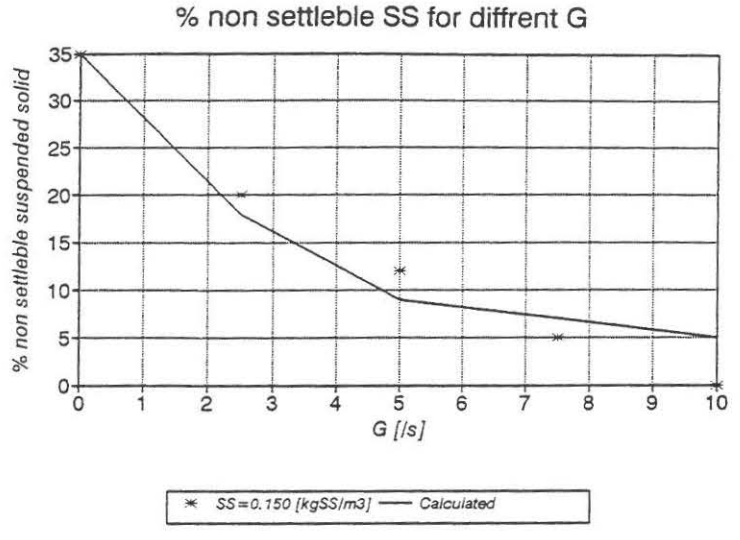

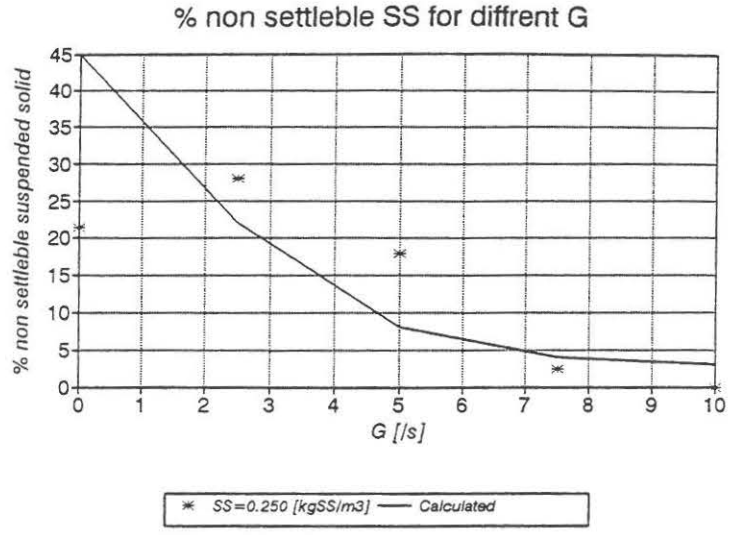

Fig. 7.7. Simulated percentage of non-settleable sludge for different G compared with measurements for two initial sludge concentrations.

The measurement result for G=0 for the initial concentration at 250 mgSS/l is expected to be an error so the selected initial condition in the simulation is chosen to give the best adjustment to the other measured results. Despite this difference the simulated result shows the same decreasing percentage of non-settleable sludge for increased G value as the measured results.

For the hindered settling regime nine measurements are carried out with different initial sludge concentrations. In Fig 7.8 the measured settling velocities is shown for different sludge concentrations. Furthermore, the measured free settling velocities and the description used in the numerical model are shown.

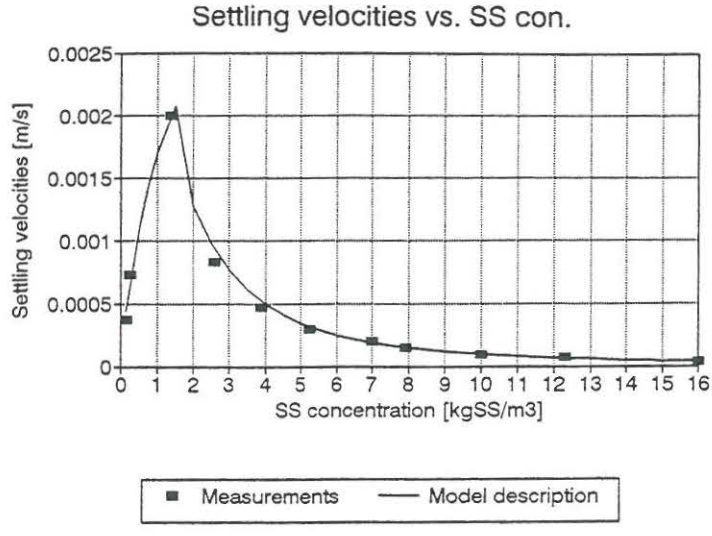

Fig. 7.8. Measured settling velocities depending on sludge concentrations and model description used.

The model description seen in Fig. 7.8 is constructed by a curve fitting in two intervals 0 - 1.5 kgSS/m3] and 1.5 - 16.0 kgSS/m^3.

The relationship between the sludge concentration and the density of the suspension was measured twice. Fig. 7.9 shows one of the measurement results with a slope of the linear approximation at 0.30 where the second measurement shows a slope at 0.33.

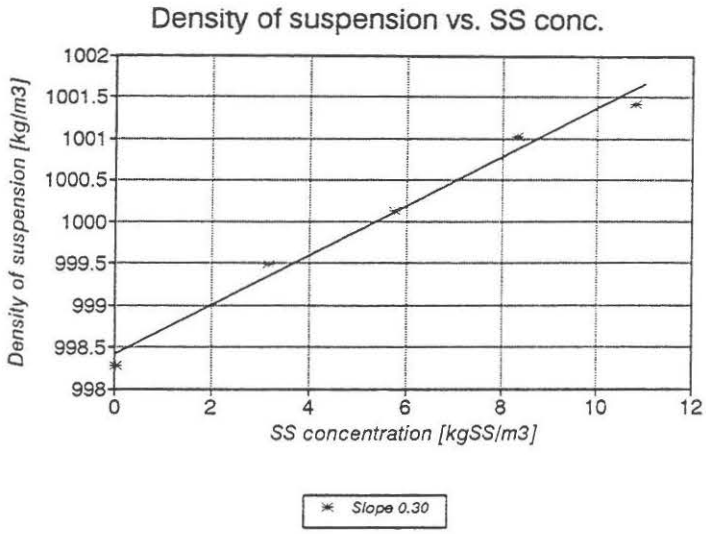

Fig. 7.9. Relationship between sludge concentration and the density of the suspension.

Enclosure 3 includes the results from the microscopical examination presented. As can be seen from the measurement report there are very few filament microorganisms characterised as 1 on the Eikelboom index which also can be seen on the photo. The floc structure can be characterised as weak and rounded with small flocs. Another characteristic is many free cells. The sludge is settling well but the supernatant is unclear owing to many small flocs and free cells.

7.1.3 Results of full scale measurements

From the six different measurements on the secondary settling tank at Lynetten two is chosen to be presented here. The two measurements are one steady and one unsteady. The results from the four other measurements are presented in enclosure 4. Fig. 7.10 presents the results from measurement 150493.

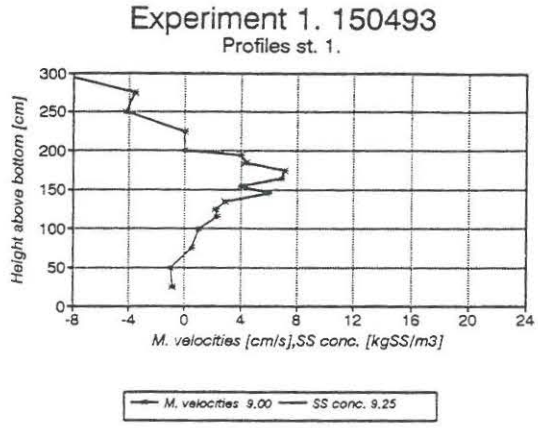

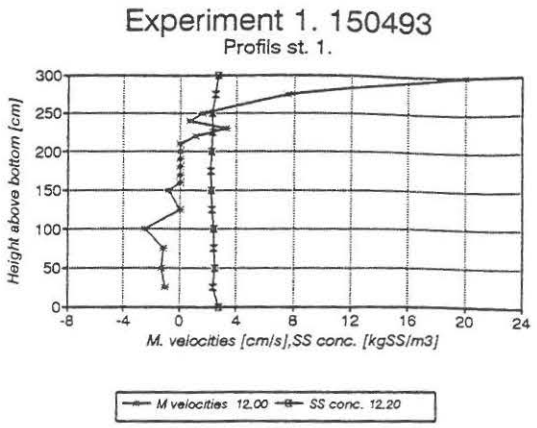

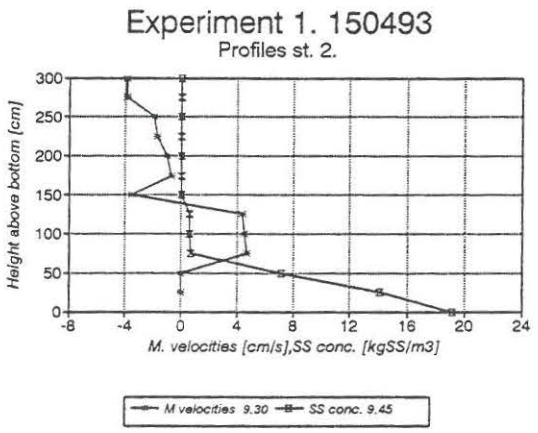

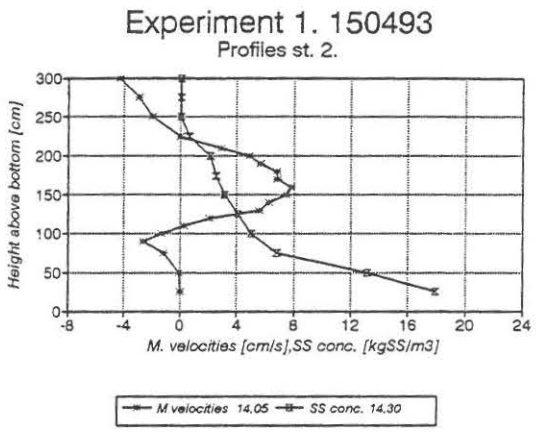

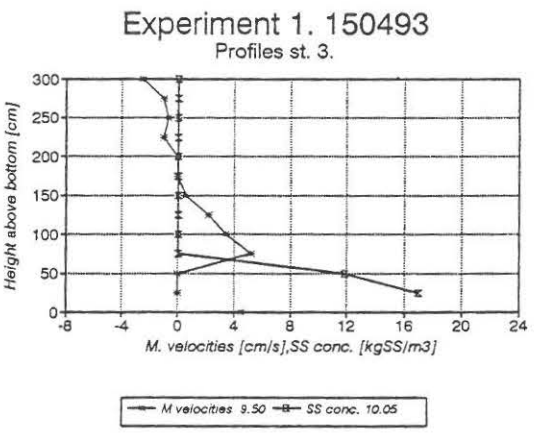

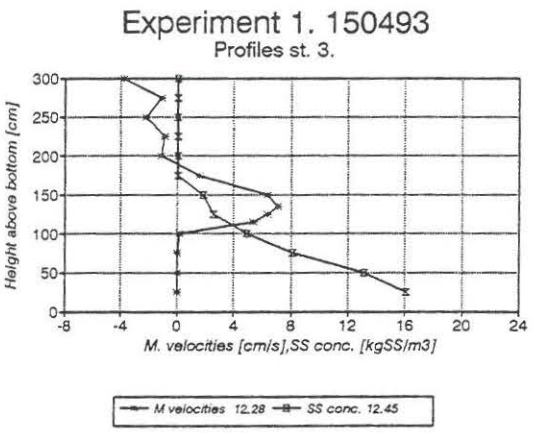

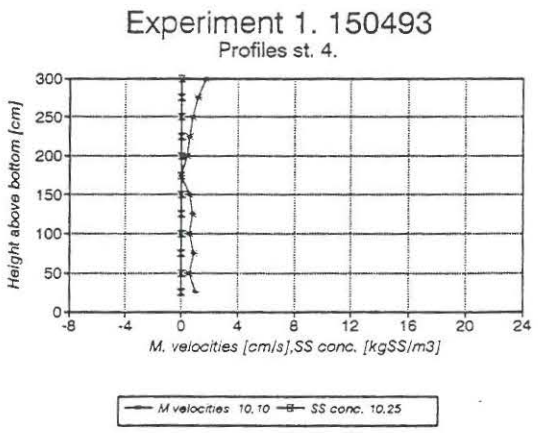

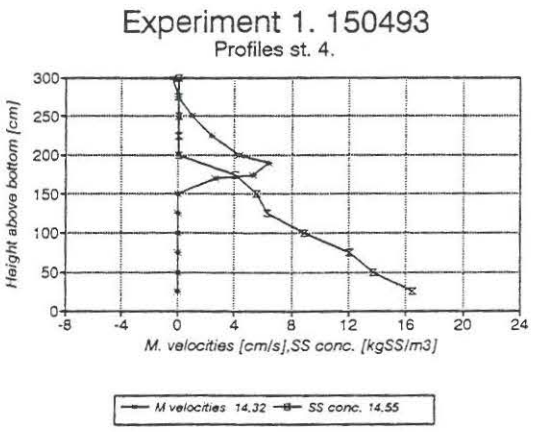

Fig. 7.10. Mean horizontal velocities and sludge concentration profiles for measurement 150493.

Fig. 7.10 shows the profiles from the 4 bridges at two different times each. The measuring time is presented in the legends of each profile. For the velocity measurements from the first bridge the instrument, which is a one-direction instrument, had trouble measuring in the highly turbulent regime with velocities downwards towards the recirculation zone. Thus, the velocity profiles from bridge 1 are often incorrect for large parts of the profile. Otherwise, one can see a similar picture of the relationship between the velocity and sludge concentration profiles as for the model tank measurements described in chapter 6. For the first steady state conditions at the measuring stations, the amount of accumulated sludge is low so that no sludge is found at bridge 4.

The second series of profiles from each bridge was measured at a different period of time after an increase in the influent. At the time 10.30 the influent was increased by lowering the inlet board. The amount of accumulated sludge then started to increase as shown in Fig. 7.10 and the velocity profiles followed the sludge concentration profiles. Especially, at the measuring station 4 a large difference is seen in accumulated sludge, from none to a level where the density current reaches the water surface. Fig. 7.11 shows the development in the effluent and recirculation sludge concentrations during the measurement.

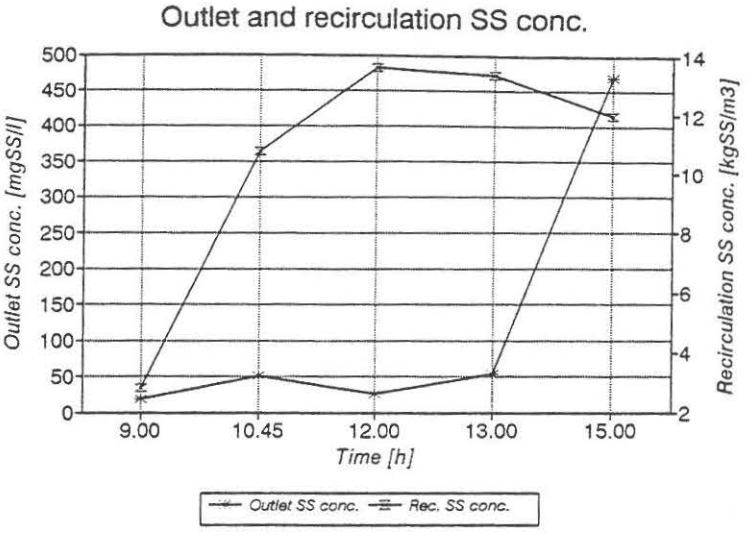

Fig. 7.11. Effluent and recirculation sludge concentrations.

As seen from Fig. 7.11, the effluent concentration is very high at the end of the measurement. Furthermore, the demand to the effluent concentration at 25 mgSS/l is exceeded twice during the measurement. At the time 10.45 no specific reason is found owing to the low accumulation of sludge at the time. But for the time 13.00 it is a result of the higher hydraulic load and sludge accumulation as seen in the second series of profiles.

The whole measurement shows how an increase in the hydraulic load will increase the sludge accumulation in the settling tank. In this case, the load was too high and a high amount of sludge started to escape from the settling tank. Fig. 7.12 shows the profiles from the steady measurement 160493.

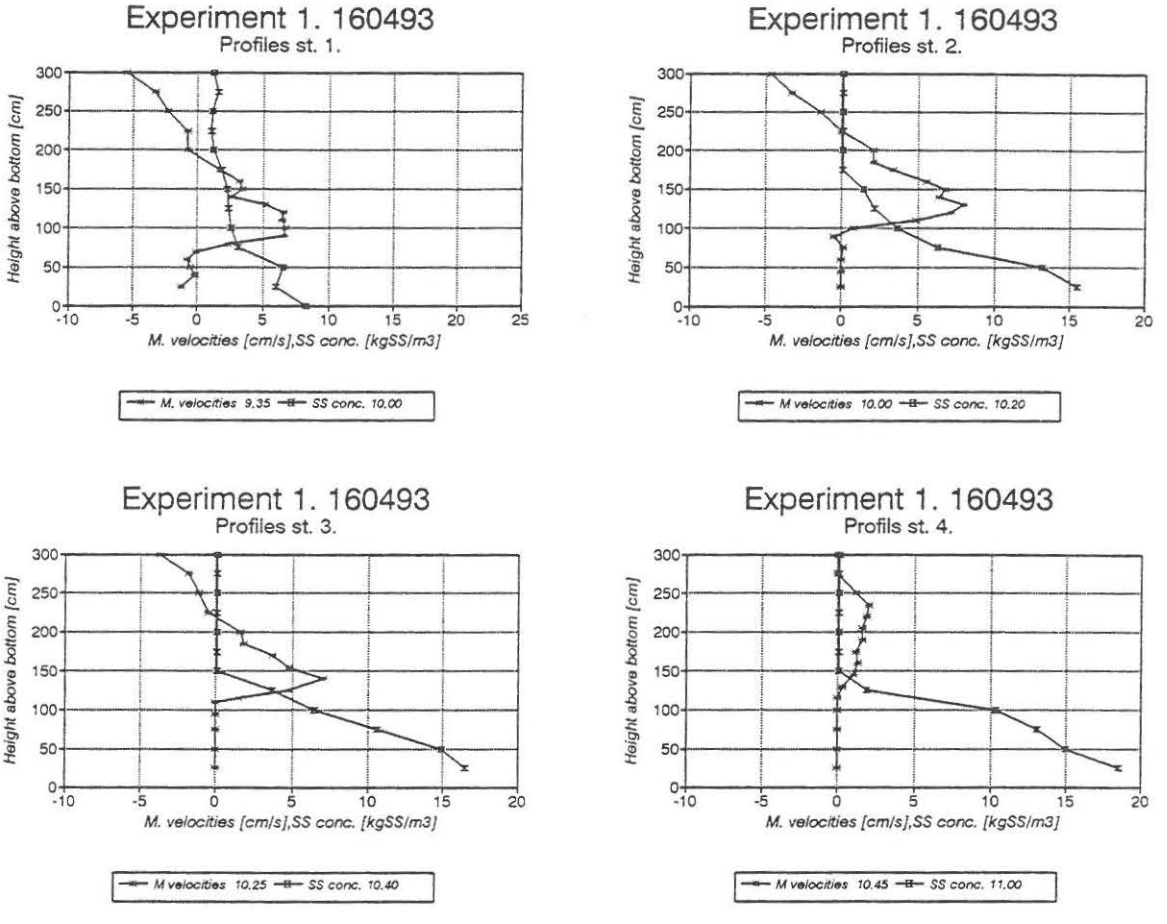

Fig. 7.12. Mean horizontal velocities and sludge concentration profiles for measurement 160493.

The profiles in Fig. 7.12 also show the typical relationship between the velocity on concentration profiles. The sludge settles out of the density current and just before the effluent weirs, almost all sludge have settled towards the sludge blanket. Table 7.2. shows the measured effluent and recirculation sludge concentration.

Time	Effluent kgSS/m^3	Recirculation kgSS/m^3
9.35	0.030	14.26
11.15	0.025	14.25

Table 7.2. Effluent and recirculation sludge concentrations.

The steady state conditions can be seen in these measured concentrations. After measuring the steady state condition a tracer measurement followed in order to measure the retention time. The measured concentrations are averaged to give a more smooth curve as seen in Fig. 7.13.

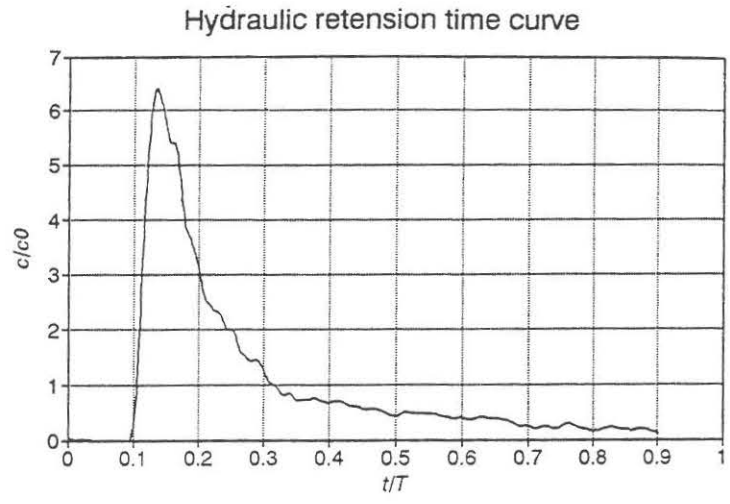

Fig. 7.13. Retention time curve for measurement 160493.

The retention time curve is shown with normalised time (t/T) as the x-axis and normalised concentration (C/C_0) as the y-axis where T is the mean retention time and C_0 is the concentration for full mixing. Due to a loss of tracer through the recirculation flow C_0 is calculated by a integration of the measured concentrations in the effluent. The retention time curve describes the flow field in the settling tank by some key parameter which can be compared with modelling results. The following key parameters are found and the values for measurement 160493 are shown in Table 7.3.

- $(t/T)_i$ initial arrival time
- $(t/T)_{50}$ time when 50% of the tracer has passed
- $(t/T)_{max}$ arrival time for $(C/C_0)_{max.}$
- $(C/C_0)_{max}$ maximum normalised concentration

$(t/T)_i$	$(t/T)_{50}$	$(t/T)_{max}$	$(C/C_0)_{max}$
0.096	0.203	0.134	6.40

Table 7.3. Key parameter from retention time curve for measurement 160493.

From Table 7.3. it is seen that low values of $(t/T)_i$ and $(t/T)_{max}$ indicate short circuiting through the settling tank which is known to be caused by the density current.

The mean flow velocity for travelling the 60 m long settling tank at the time $(t/T)_i$ can be calculated to 6.25 cm/s. Comparing this velocity with the velocities measured in the density current in Fig. 7.12, it is seen that the velocities are almost the same. The high $(C/C_0)_{max}$ value also indicates a high degree of short circuiting and the relatively low $(t/T)_{50}$ value indicates a low degree of mixing through the tank.

7.1.4 Simulation, comparison and validation

The geometry of the settling tank at Lynetten is modelled with the description shown in Fig. 7.14.

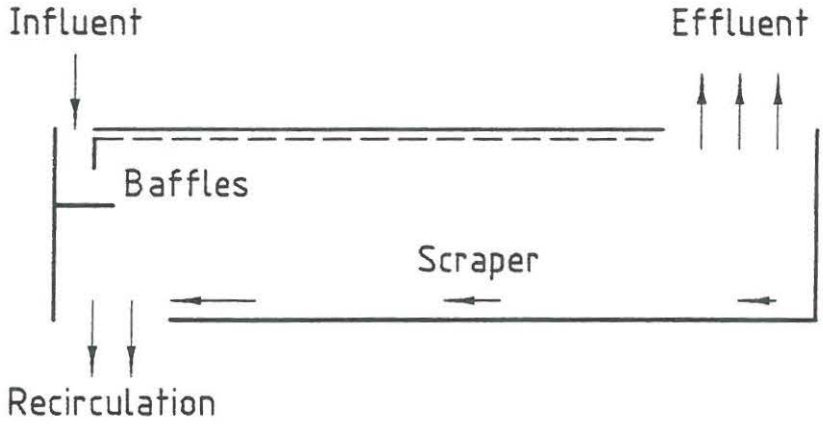

Fig. 7.14. Model description of settling tank geometry.

Fig. 7.14 shows that the influent comes from the overflow of the inlet board and is guided by the baffles. The effluent is drawn of at the surface in the effluent end. For the scrapers, no specific knowledge is found for the flow field created by the scrapers. The scraper nevertheless transport sludge from the whole settling tank bottom towards the recirculation pit. The scrapers are modelled by increasing the velocity linear from zero at the effluent end towards the recirculation zone, which created a uniform vertical velocity in the settling tank towards the scrapers. At the recirculation zone, the recirculation flow is drawn of. With this model geometry and the basic measurement results described in section 7.1.2 the inlet condition for the flocculation model is needed. From Das et al. (1993) it is found that the percentage of dispersed particles to secondary settling tanks varies between 0.07 - 3.71 percent of the sludge in 15 different treatment plants. A mean value of 1.5 percent is used as the inlet condition in the model simulations. As a beginning the Bingham plastic calibrations from the model tank simulations are used. Fig. 7.15 shows the flow field and concentration field regarding a simulation of measurement 160493.

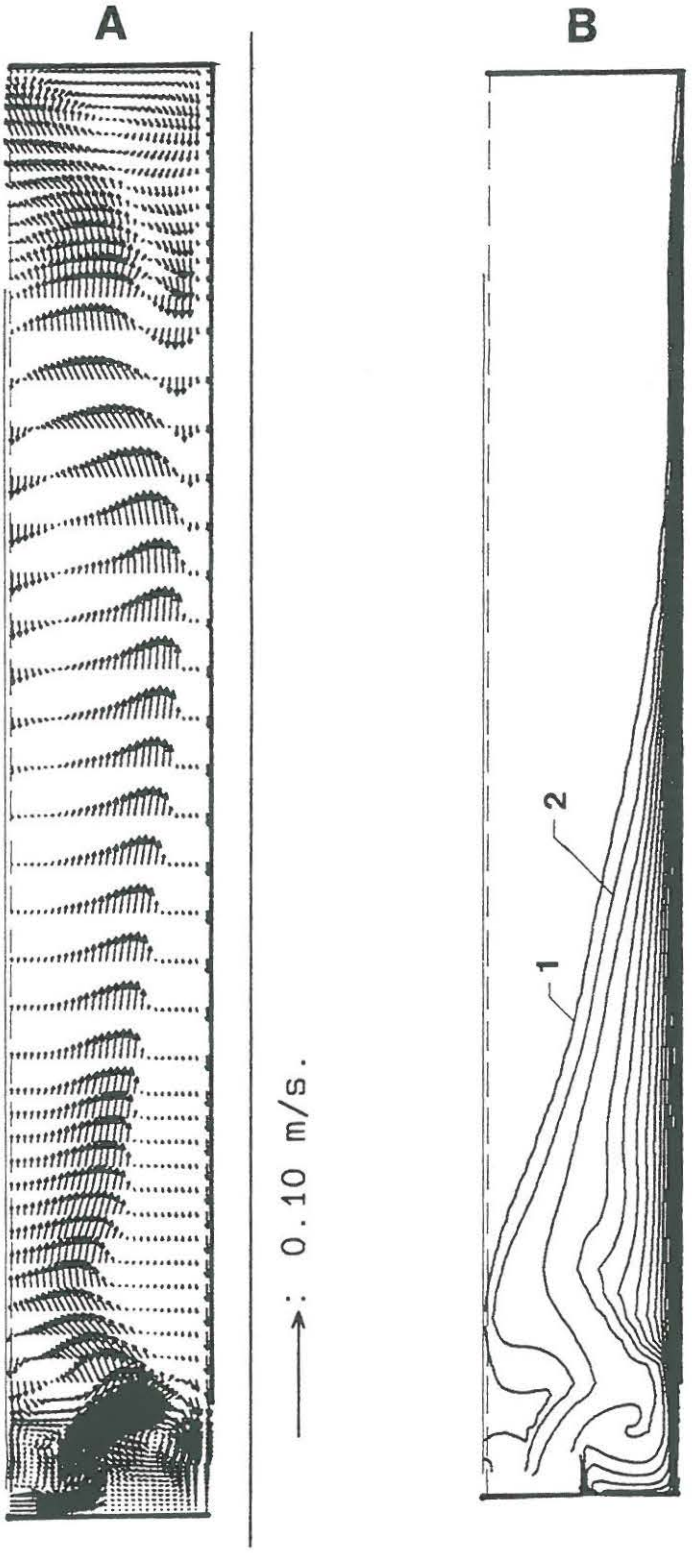

Fig. 7.15. Simulation results for measurement 160493. a. Flow field, b. Concentration field with 1 kgSS/m3] iso-concentration curves for the interval 0 - 16 kgSS/m^3.

In the flow field it is seen how the influent jet falls down towards the bottom and the recirculation flow owing to buoyancy effects. The influent jet erodes down in the sludge blanket and is divided in a short circuited

flow towards the recirculation zone and the main flow through the settling tank. This main flow reached an established sludge blanket and is directed towards the surface. In the flow towards the surface the velocities decreases, and the viscosity increases due to the Bingham plastic description and amplified the velocity decreasing. Several attempts are made by changing calibration parameters and the description of the scrapers, but the results are the same. Despite the mentioned problem, the model simulation showed the characteristic steady sludge blanket and high velocity gradient to the density current. In the density current it is seen how the sludge concentration decreased along the tank due to settling. Backwards velocities are seen in the effluent end of the tank.

Another approach for modelling the rheology of the suspension is made by describing the kinematic viscosity ν as a function of only the sludge concentration as described in equation (3.7) in section 3.3.

Equation (3.7) is used with the constant at 0.132 as seen and with constants at higher values. The best prediction is reached with a constant at 0.28. In Fig. 7.16 the flow and concentration fields are shown.

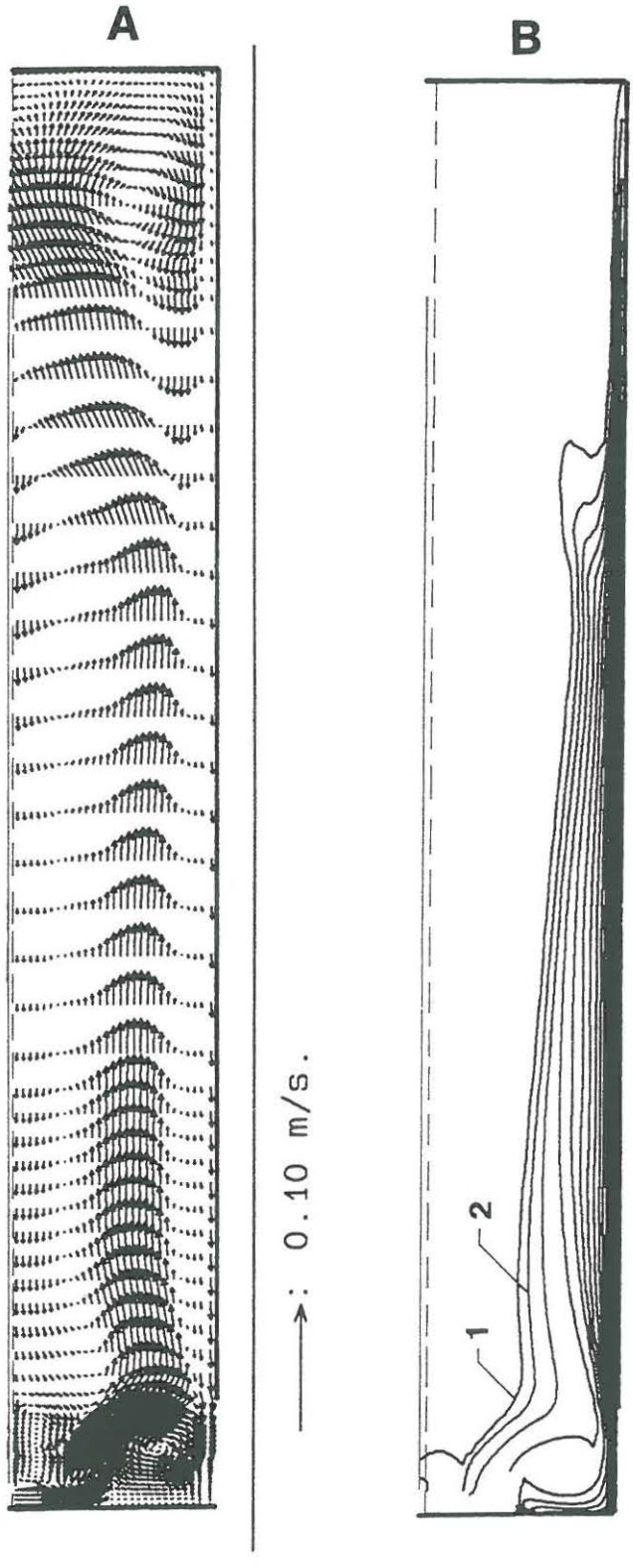

Fig. 7.16. Simulation results for measurement 160493 using equation 3.7. a. Flow field. b. Concentration field with 1 kgSS/m^3 iso-concentration curves for the interval 0 - 16 kgSS/m^3.

Fig. 7.16 shows a creation of a density current above a steady sludge blanket and backwards velocity at the surface in most of the settling tank.

This flow field have much more likeness to the measurement results shown in Fig. 7.12 than the simulation results in Fig. 7.15. The flow field differs from the measurement results by the velocities in the density current and in the backward flow. The maximum velocity in the simulation of the density current is approximately 4.5 cm/s where the maximum measured velocity is approximately 7.5 cm/s. Furthermore, the simulated density current is higher than the measured. These differences result in more time in the simulation for the sludge to settle in the first part of the settling tank. Therefore, the accumulation of sludge become too high predicted in the first part and too low in the effluent end of the tank. An attempt is made to increase the velocities in the density current by limiting the description of rheology changes to suspension with sludge concentration higher than the influent concentration. This results in a simulation of the density current with a viscosity equal to pure water. These changes have now affect on the prescription of the density current.

Due to the described problems with the prediction of velocities and accumulation of sludge in the tank, the measurement results are not compared with simulation results for different measurements. Despite the problems with the model simulation, the model results from the simulation in Fig. 7.16 for the low concentration of the sludge, non-settleable dispersed particle concentration and the eddy viscosity ν_t are presented in Fig. 7.17.

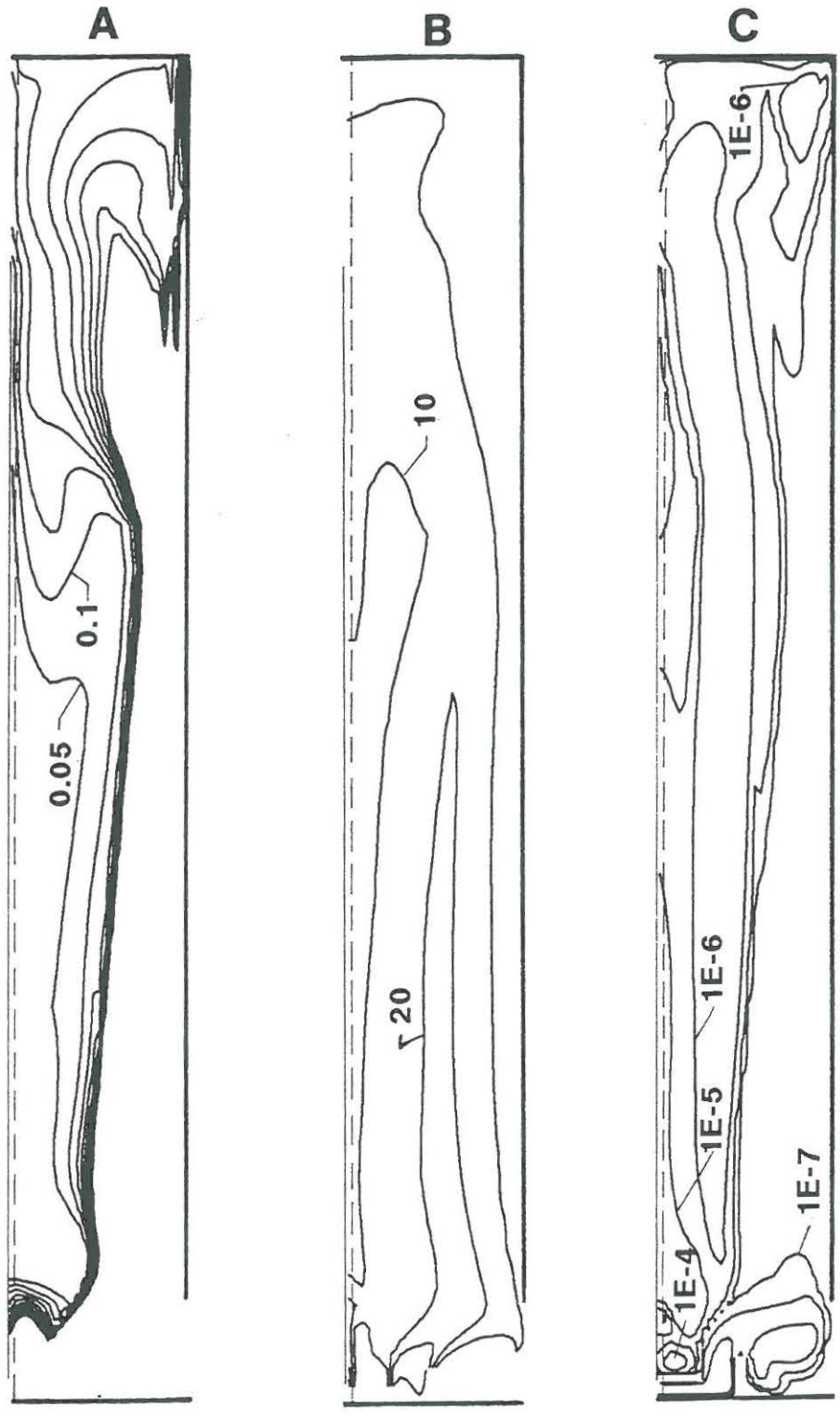

Fig. 7.17 a. Settleable sludge with 0.05 kgSS/m^3 iso-concentration curves. b. Non-settleable sludge with 0.01 kgSS/m^3 iso-concentration curves. c Eddy viscocity iso-curves.

Looking at the concentration field for the settleable sludge, it is seen that the effluent concentration is between 150 - 200 mgSS/l. This high effluent concentration is not seen in the measurement and can indicate

that the settling velocities for low concentrations are too low in the model description of the settling. Fig. 7.17 shows how the concentration of non-settleable dispersed particles in the effluent is between 10 - 20 mgSS/l. With an influent concentration of non-settleable dispersed particles at 48 mgSS/l some of the dispersed particles flocculated with the settleable sludge. As regards the eddy viscosity describing the turbulence, higher values are seen at the inlet and recirculation zones. Lower values are found in the density current and the backward flow, and the turbulence disappears in the sludge blanket due to density gradient effects on the dissipation of turbulence.

The numerical model simulations shows results for the different model variables which have good likeness with the measured results and the description of processes in the system analysis. Nevertheless, the model simulations can not predict the correct values for all the variables.

7.2 Slagelse wastewater treatment plant

This section describes the measurements carried out on one of the secondary settling tanks at Slagelse wastewater treatment plant.

7.2.1 Outline of the settling tank

The secondary settling tank is of a new design, 45 m long, 7 m wide and 4 m deep with weir scrapers. Fig. 7.18 shows the settling tank.

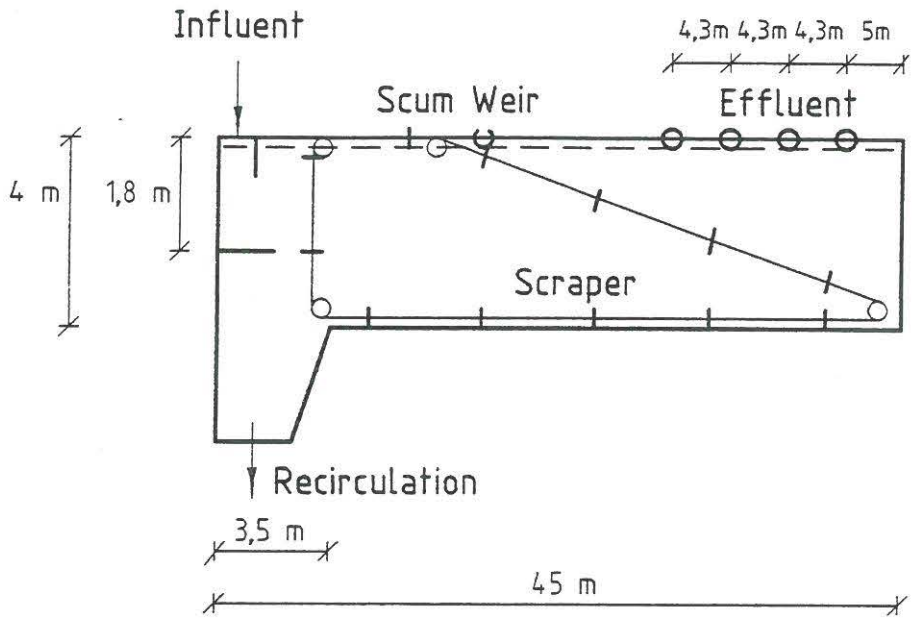

Fig. 7.18. Secondary settling tank, Slagelse.

This settling tank is different from the settling tank at Lynetten in some areas. Especially, the Slagelse tank is not as long as the Lynetten tank, and the design of effluent weirs is totally different. The measuring stations were also established with bridges as seen in Fig. 7.19 where the distance between the bridges is shown as well.

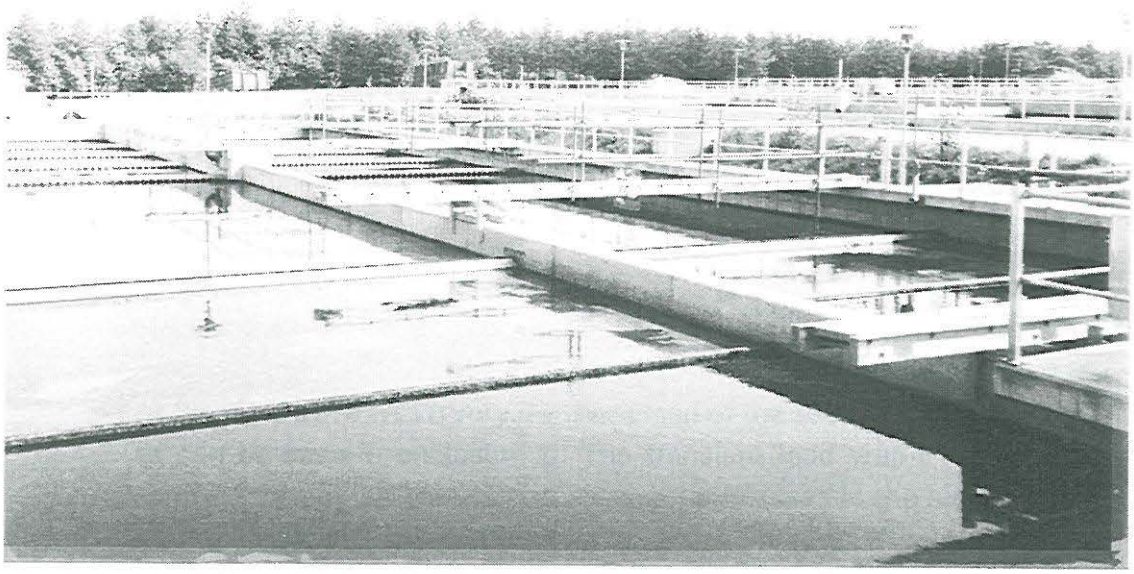

Fig. 7.19. Bridges over settling tank, Slagelse.

From a distribution building 7 secondary settlings are fed. The influent to the measurement tank could therefore only be changed by blocking the influent to some of the other settling tanks. The recirculation flow is controlled by movable Thomson weirs as seen in Fig. 7.20.

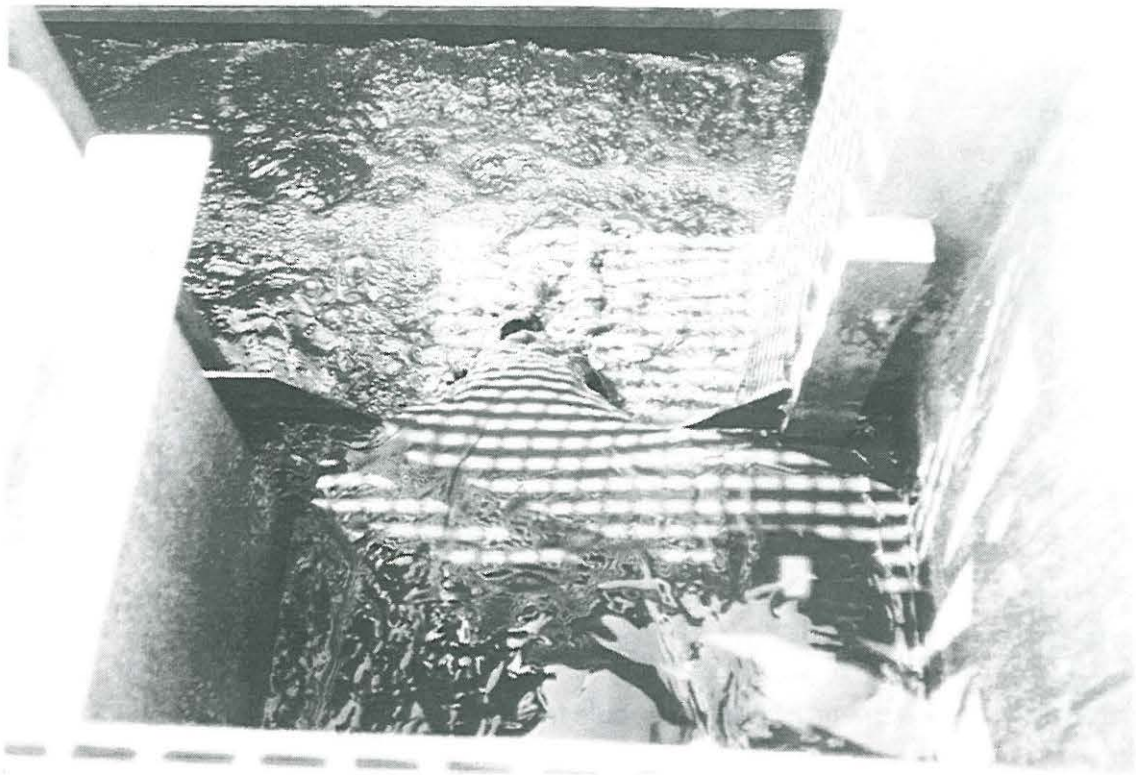

Fig. 7.20. Control of recirculation flow by Thomson weirs.

The control of the recirculating flow is on-line by measuring the water surface constantly and thus calculating the flow from a known formula. The Thomson weirs can then be moved until the wanted flow is reached. Due to problems with this on-line control, the Thomson weirs were kept at a steady position. This means that the recirculation flow changes during the measurements but an attempt was made to measure the mean flow for each measurement. Otherwise, the measurement configuration was similar to the Lynetten measurements.

Full scale experimental procedures.

At Slagelse there was a very transient load of the secondary settling tanks as can be seen in enclosure 5. The transient load was a result of the control strategy for the change between processes in the biological part of the treatment plant. Due to this transient load it was difficult to describe the hydraulic conditions in the settling tank. Therefore, no steady measurements followed by tracer measurements was carried out as at Lynetten. So only unsteady measurements were made at Slagelse, but

also here the transient load affected the measurements of the mean horizontal velocity profiles. This effect will be discussed later. The mass balance of sludge for the settling tank was followed during the measurements. To describe the mean influent for the measurement the measurements of the total flow to the treatment plant were used, which can be seen in enclosure 5 as well. At the distribution building where the flow to each settling tank could be controlled, a distribution factor to each tank was known. From these factors the flow to the measurement settling tank could be calculated. Table 7.4 shows the influent and influent sludge concentrations and the recirculation flow for each measurement which was named by the date of the measurement.

	Influent Q m^3/h	Recirc. flow Q_r m^3/h	$SS_{influent}$ $kgSS/m^3$
030593	56/96	114	(5.5)
040593	70/205	33	5.5
050593	67/205	33/147	5.4
060593	70/416/93	154	5.3

Table 7.4. Flow and influent sludge concentration conditions for the 4 measurements.

Due to measurement error the influent sludge concentration for measurement 030593 was not measured. With the steady concentrations for the other measurements a concentration at 5.5 $kgSS/m^3$ was expected.

7.2.2 Results of basic measurements

With the measurement procedure described in section 5.2 basic measurements were carried out for measuring free settling velocities and flocculation, hindered settling velocities, density of suspension and finally a microscopic examination.

To examine the free settling velocities and flocculation, measurements were made with two different initial sludge concentrations and five different turbulence levels. Fig. 7.21.a shows the direct measurement of one measurement of the sludge concentration changes at the measuring point, and Fig. 7.21.b shows the differences in settling velocities.

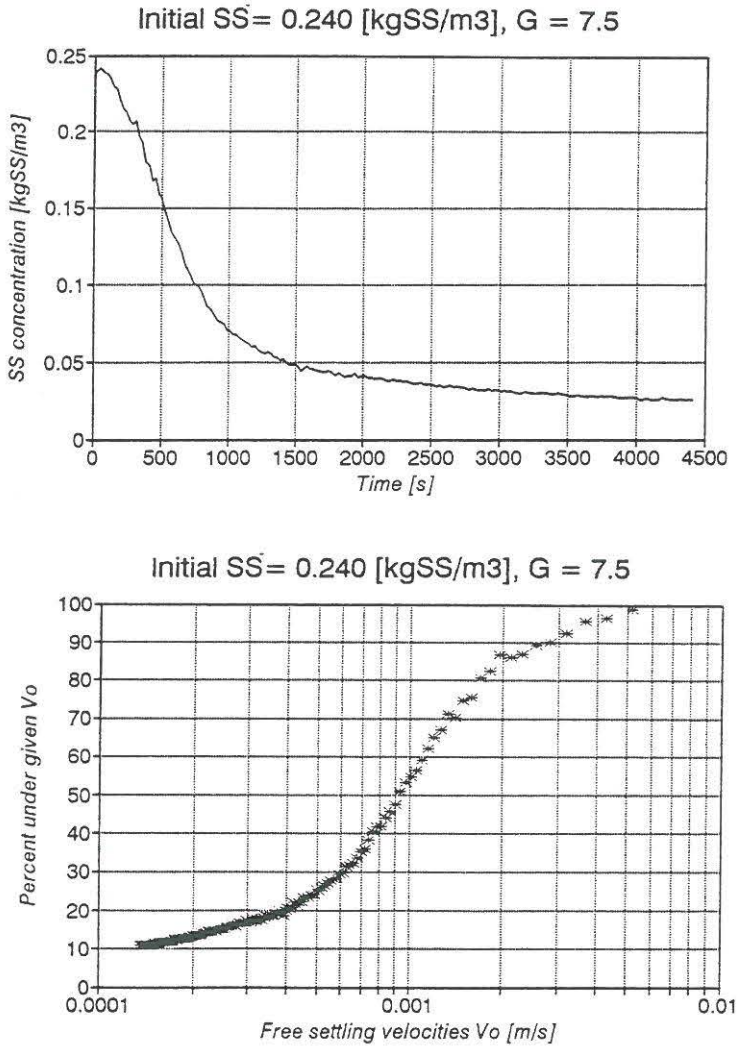

Fig. 7.21. a. Sludge concentration changes in one point of the settling column. b. Percentage of initial sludge with settling velocities under a given velocity.

The two parameters, the mean free settling velocity and the percentage of non-settleable initial sludge can be found from the results in Fig. 7.21.a.b. From section 3.4 the settleable sludge is defined as the sludge flocs and the non-settleable sludge as dispersed particles. Fig. 7.22.a and b. shows these parameters for the different turbulence levels, characterised by the parameter G, and the initial sludge concentration.

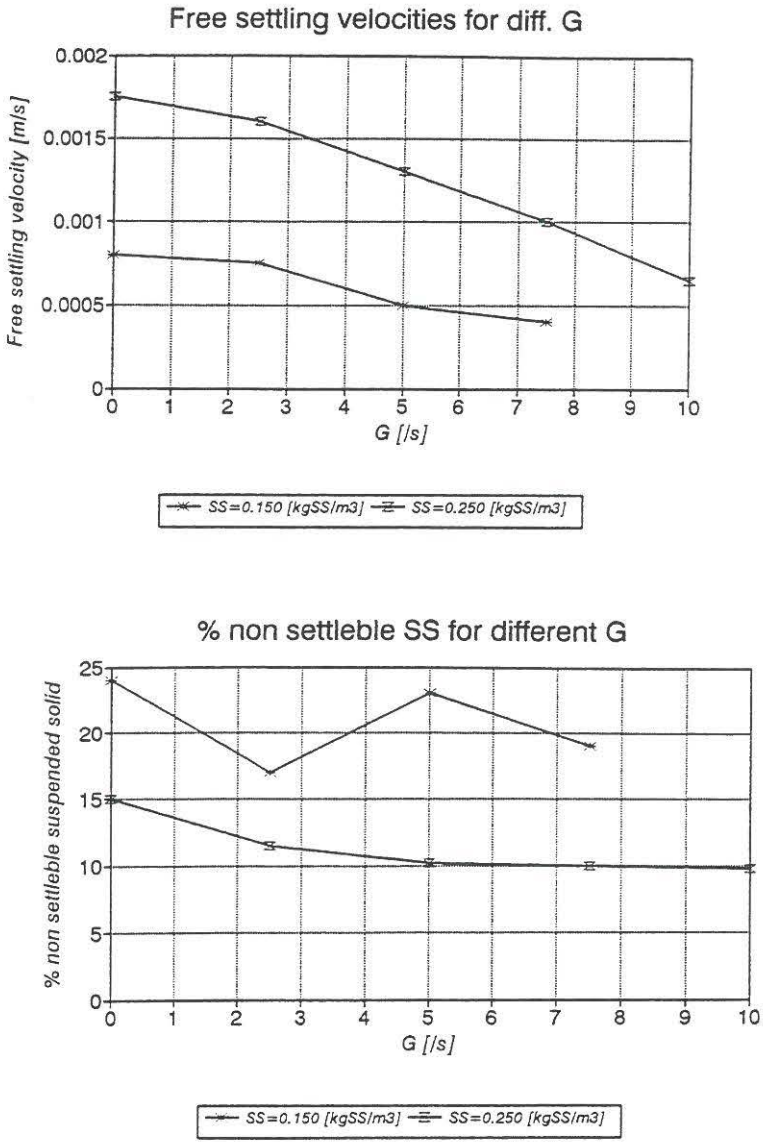

Fig. 7.22. a. Mean free settling velocity for different turbulence levels. b. Percentage of non-settleable sludge for different turbulence levels.

In Fig. 7.22 it is seen that the measurement with low initial sludge concentration and G = 10 is missing due to errors in initial concentrations. Fig. 7.22.a shows that the mean free settling velocities decreases with high turbulence levels and that the measurements with the higher initial concentrations shows the highest mean settling velocities. The percentage of non-settleable sludge seen in Fig. 7.22.b shows only small variations for different turbulence levels but a dependence on the initial concentration.

The high G value only occurs in the influent zone of the settling tank so the free settling velocities are only modelled as depending on the

concentrations with G = 1. The settling velocities are then 0.000775 m/s for 150 mgSS/l and 0.0017 m/s for 250 mgSS/l.

The parameters K_A and K_B in the flocculation model is found with the same one-dimensional model used for the Lynetten data. Fig. 7.23 presents the measured and calculated percentage of non-settleable sludge for different G values.

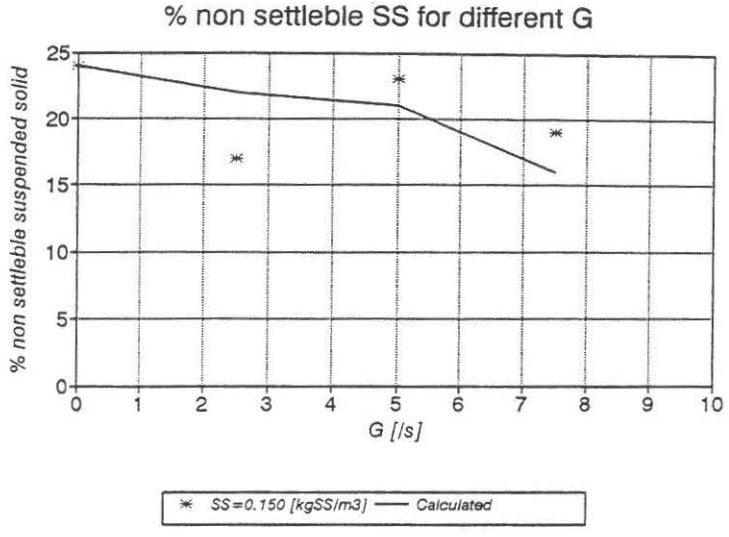

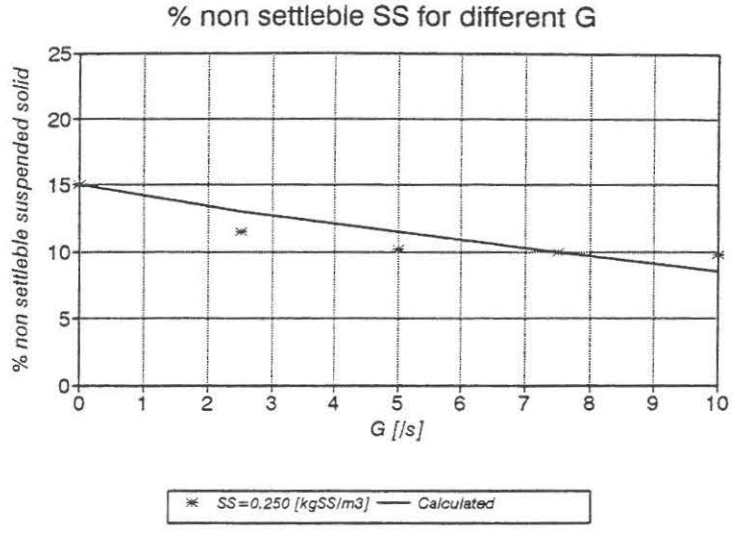

Fig. 7.23. Percentage of non-settleable sludge for simulation compared with measurement.

The calibration constants are found to be $K_A = 6.0 \cdot 10^{-4}$ and $K_B = 1.0 \cdot 10^{-6}$.

In the hindered settling regime 14 measurements were carried out with different initial sludge concentrations. Fig. 7.24 shows the measured

settling velocities for different concentrations. Furthermore, the measured free settling velocities and the used relationship in the numerical model are shown.

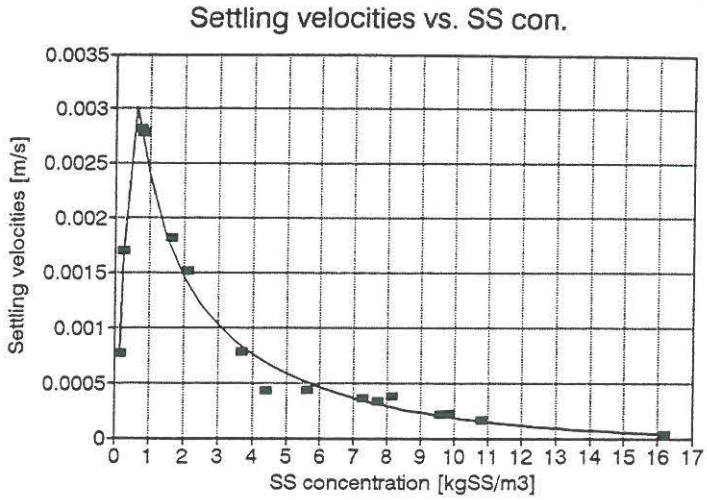

Fig. 7.24. Measured settling velocities depending on sludge concentrations and used model description.

The relationship between the density of the suspension and the sludge concentration was measured and the results are seen in Fig. 7.25.

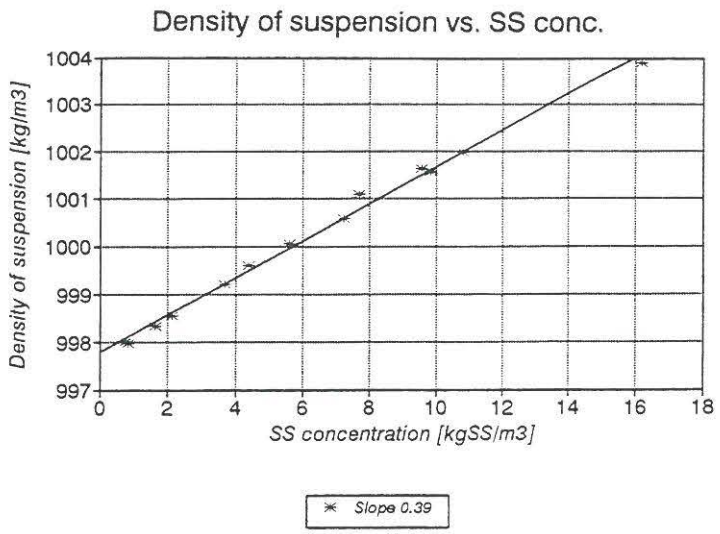

Fig. 7.25. Relationship between density of suspension and sludge concentrations.

The model description of this relationship is constructed linear with the density of clean water as reference density and a slope for the relationship at 0.39 found in the measurements.

In enclosure 3 the results from the microscopical examination are presented. There is a normal number of filamentous microorganisms

characterised by an Eikelboom index of 2. The sludge flocs are of normal sizes with filamentous microorganisms in the flocs and with a firm but irregular structure. Comparison of these characteristics with the free settling and flocculation measurement results shows that the filamentous microorganisms give the flocs a higher shear strength than is seen for the Lynetten measurements resulting in higher settling velocities due to larger flocs. But still, the floc sizes also depends on the turbulence level.

7.2.3 Result of full scale measurements

Two of the four measurements in the secondary settling tank at Slagelse are presented and discussed here. In enclosure 6 the results from the other measurements are presented. Fig. 7.26 shows the profiles of the mean horizontal velocities and the sludge concentration for measurement 040593. The profiles are shown at different times in the measurement and at the four measurement stations shown in Fig. 7.19.

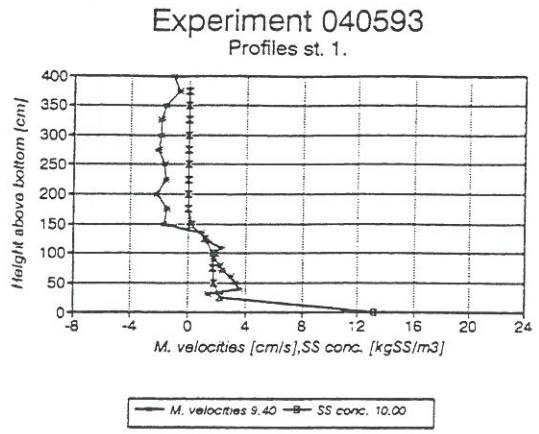

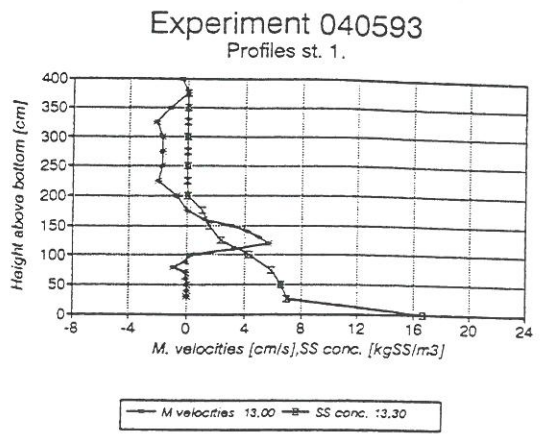

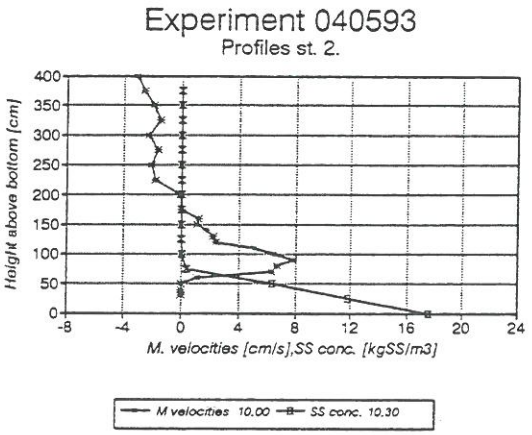

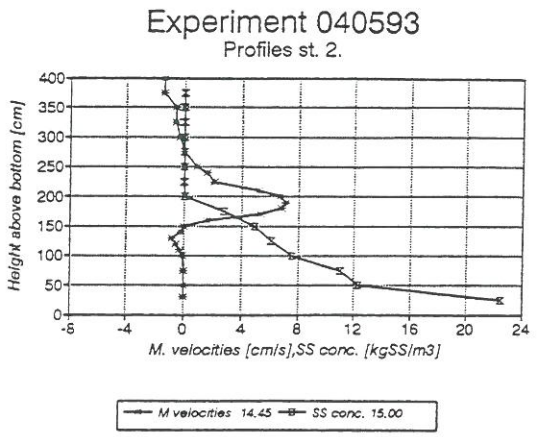

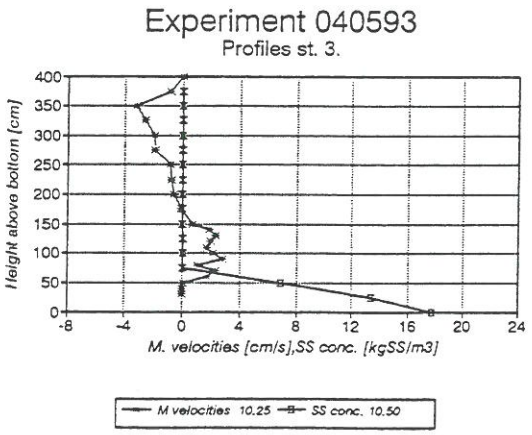

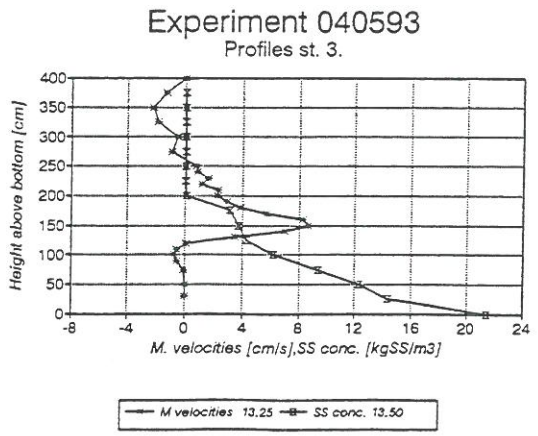

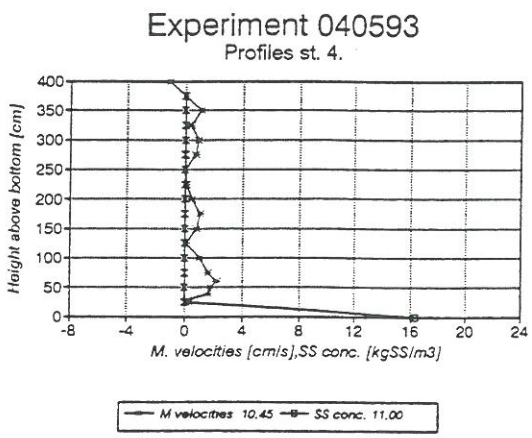

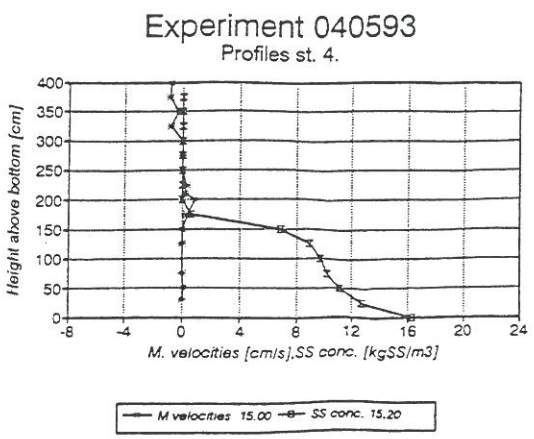

Fig. 7.26. Mean horizontal velocities and sludge concentration profiles for measurement 040593.

Owing to the previously mentioned transient load in the settling tank, changes in the flow field sometimes occurred when measuring a velocity profile. An example is the first profile from measurement station 3 where the flow decreased during the measuring so that an integration of the velocity profile gives a negative flow. Sometimes, the flow almost disappeared as seen in the last profile in station 4.

Despite these changes in the velocities, the measurements are very much like the Lynetten measurements with the density current and the steady sludge blanket and backward velocities above the density current. Furthermore, the increased accumulation of sludge in the settling tank is seen with the increased hydraulic load. Fig. 7.27 shows the changes in the effluent and recirculation sludge concentrations during the measurement.

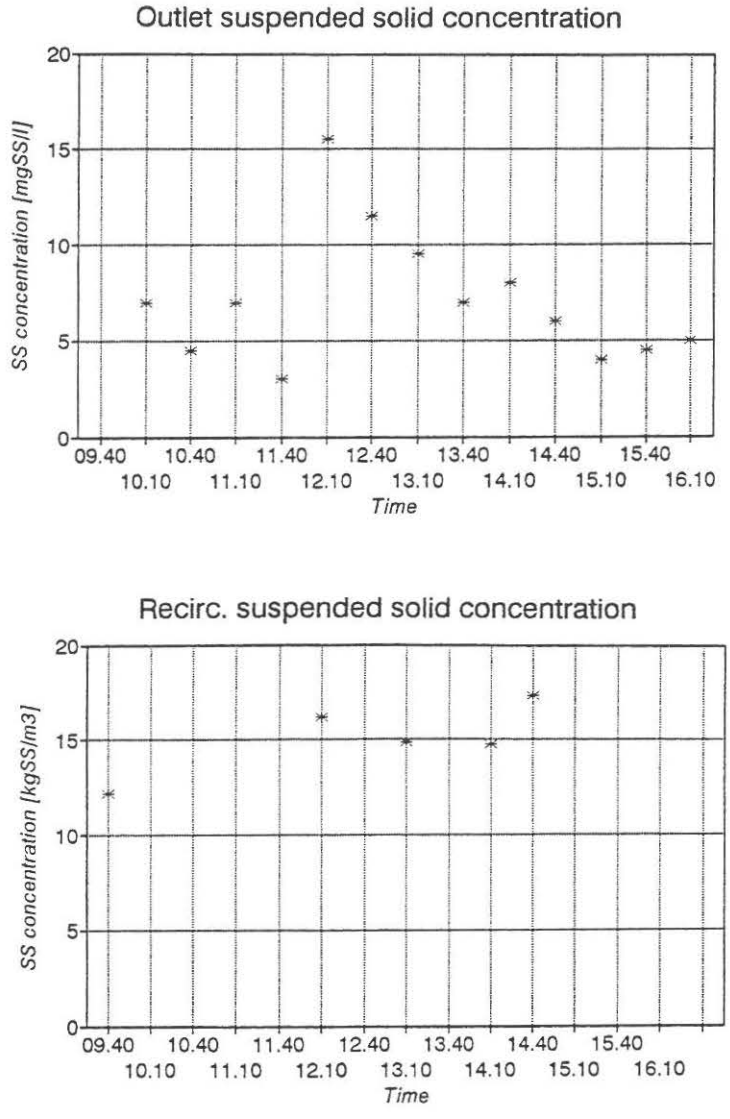

Fig. 7.27. a. Effluent sludge concentrations during measurement 040593. b. Recirculation sludge concentration during measurement 040593.

The effluent concentration is very low during the whole measurement and shows a good effluent quality despite the increased accumulation of sludge. From the recirculation concentrations an increased concentration is seen owing to the increased accumulation of sludge but only little variation after the increase. Fig. 7.28 shows the measured profiles from measurement 050593.

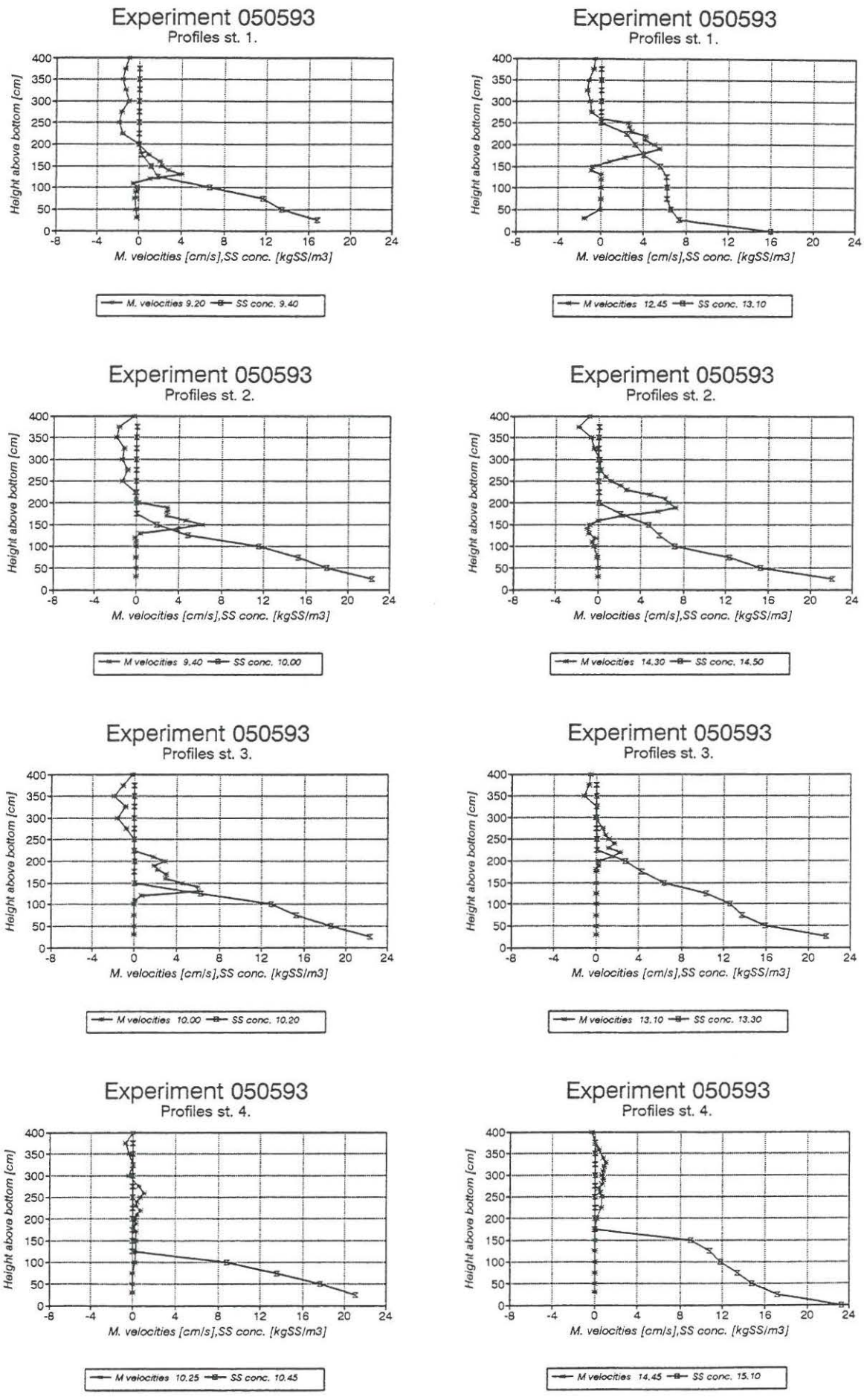

Fig. 7.28. Mean horizontal velocities and sludge concentration profiles for measurement 050593.

Measurement 050593 differs from measurement 040593 by a higher accumulation of sludge in the settling tank for initial condition. The explanation of this higher accumulated sludge is a decreased recirculation flow in the night between measurement 040593 and 050593. Fig. 7.29 shows the effluent and recirculation sludge concentrations for measurement 050593.

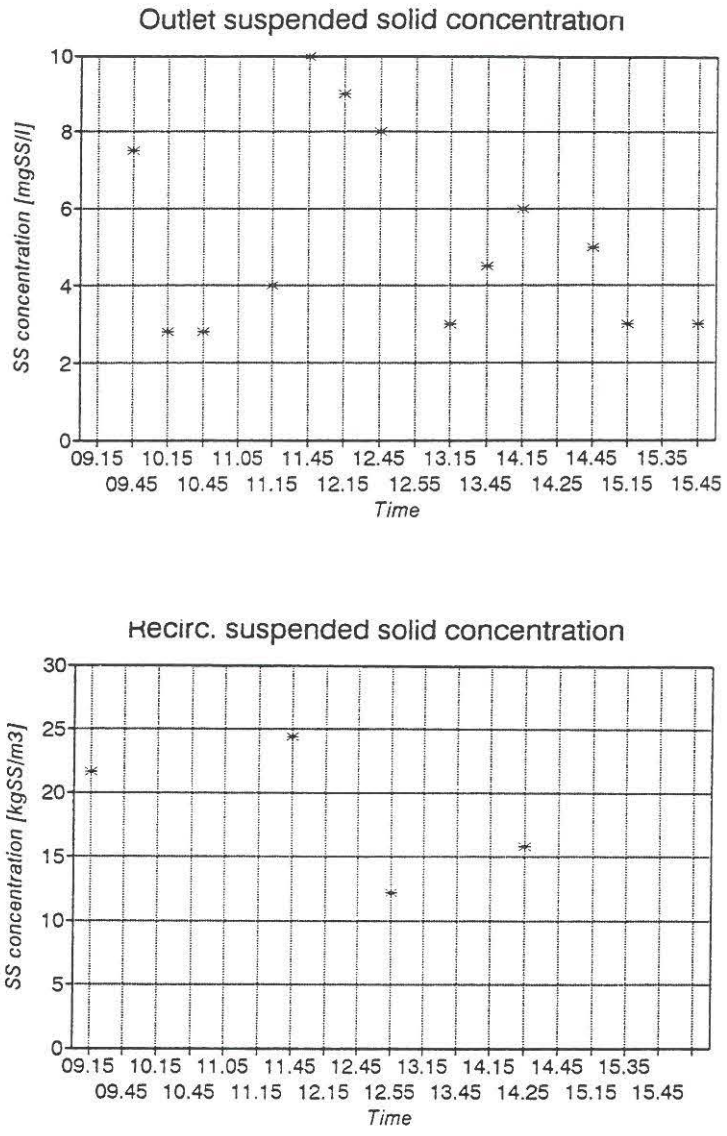

Fig. 7.29. a. Effluent sludge concentration during measurement 050593. b. Recirculation sludge concentration during measurement 050593.

Also in measurement 050593 low effluent concentrations is seen during the entire measurement. The variations can be due to the transient load to the settling tank, but no immediate relationship can be identified. No explanation is found to the variation of the recirculation concentration. It shall be noted that some measurements are lacking for the whole measurement due to concentrations exceeding the measuring range of the instrument used for sludge concentration measurements.

7.2.4 Simulation, comparison and validation

The model description of the geometry of the settling tank at Slagelse is as shown in Fig. 7.30.

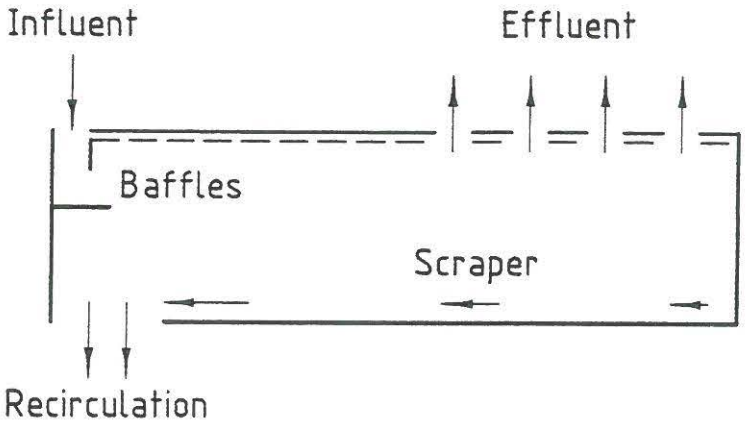

Fig. 7.30. Model description of settling tank geometry.

For the calibration of the Bingham plastic model description, similar problems arose to the ones described in section 7.1.4 regarding simulating the Lynetten tank. Therefore, equation (3.7) with a constant of 0.28 is also used in the model simulation of the settling tank at Slagelse. Fig. 7.31 and 7.32 show the simulation results for a simulation of measurement 050593 with the high flow condition. The sludge concentrations for the recirculation flow are 14.4 kgSS/m^3 and for the effluent 0.06 kg SS/m^3.

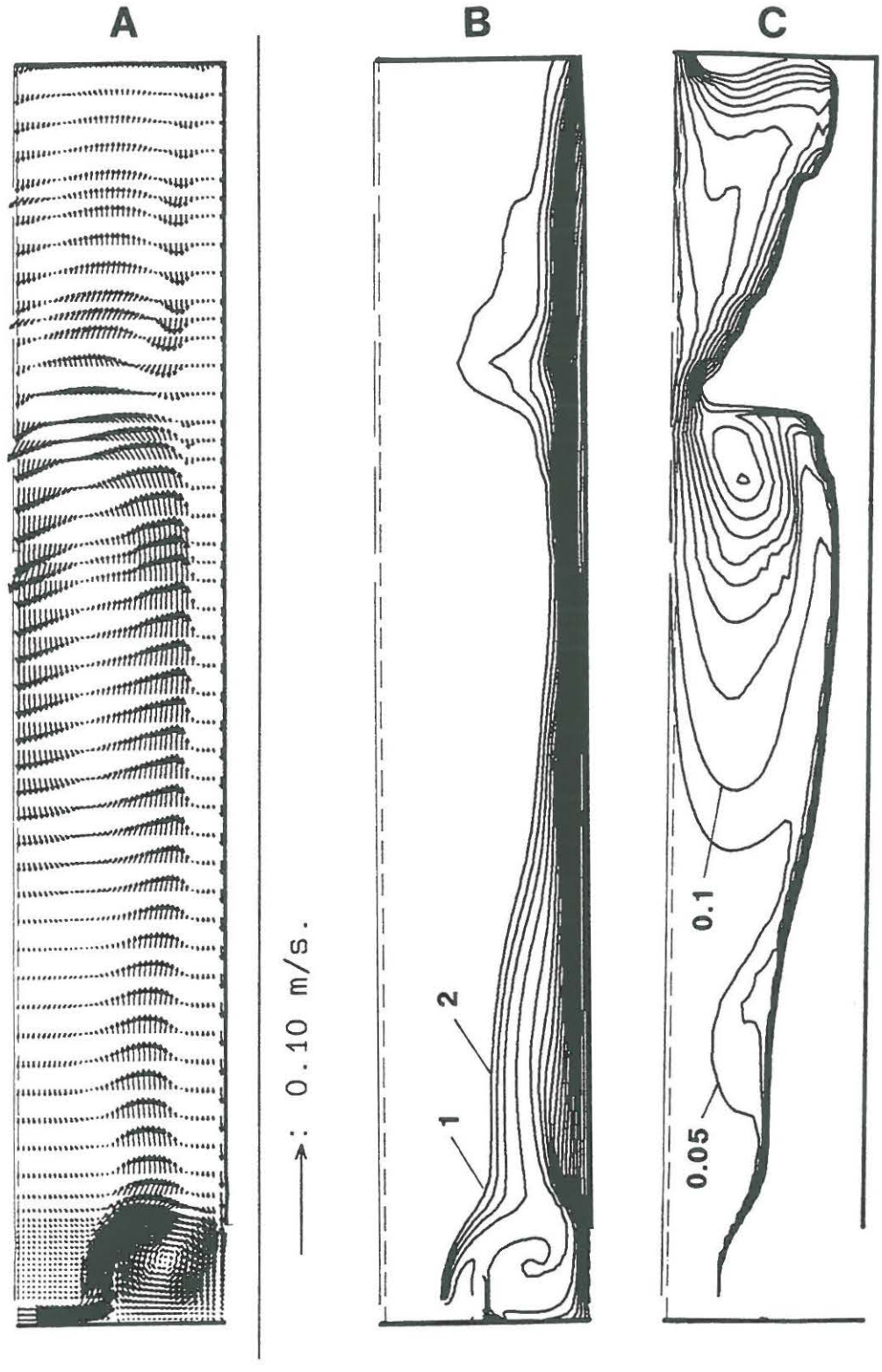

Fig. 7.31. Simulation results for measurement 050593 with high flow condition. a. Flow field. b. and c. Settleable sludge with 1 kgSS/m^3 and 0.05 kgSS/m^3 iso-concentration curves, respectively.

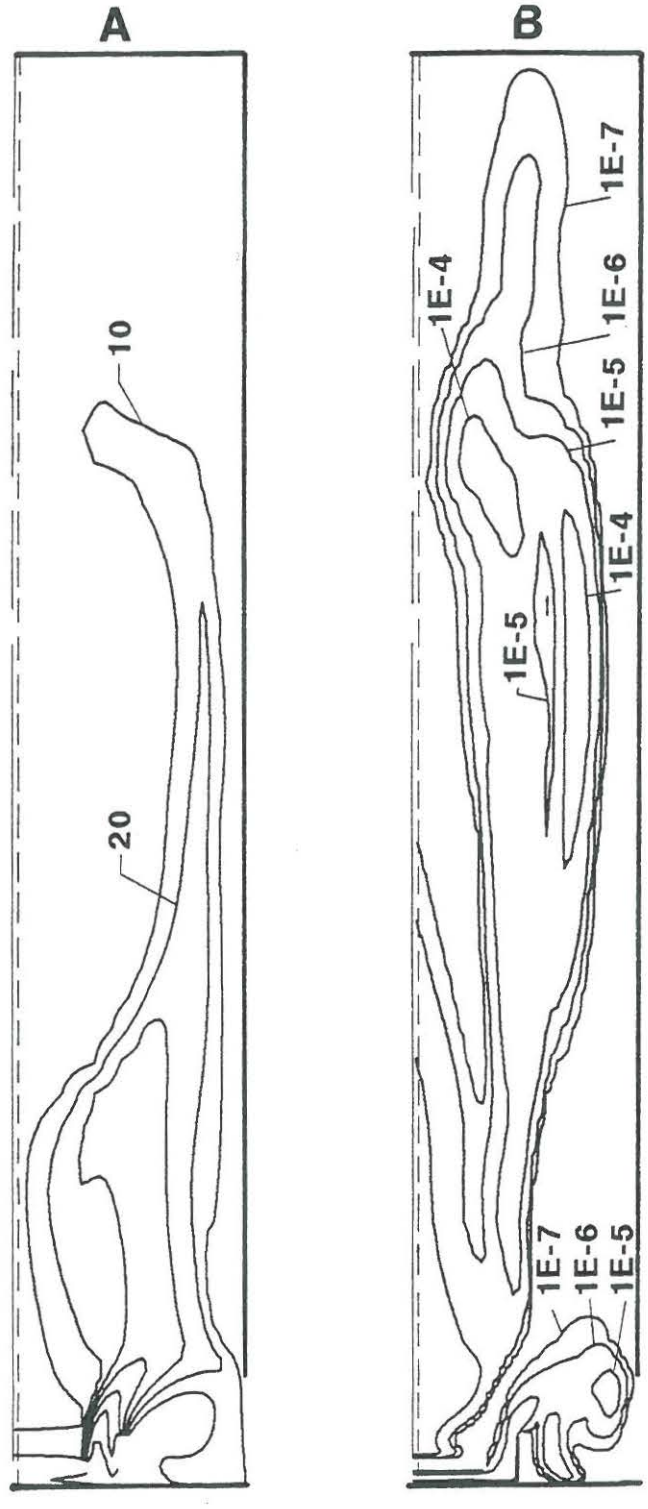

Fig. 7.32. Simulation results for measurement 050593 with high flow conditions of a. Non-settleable sludge with 0.01 kgSS/m^3 iso-concentration curves. b. Eddy viscosity iso-curves.

Fig. 7.31.a shows a density current, a steady sludge blanket and a backwards flow at the surface. Comparing the simulated velocities with

the measurements in Fig. 7.28 shows higher measured velocities both in the density current and in the backwards flow. Similar to the Lynetten measurements there is no direct comparison between simulation and measurement results due to the difference in velocities. Fig. 7.31.b shows how the sludge concentration increases rapidly in the sludge blanket. Furthermore, it is seen how the flow towards the effluent weirs withdraw some of the sludge. Fig. 7.31.c shows how the withdrawal of sludge results in concentration of 50 - 100 mgSS/l near the effluent weirs. Fig. 7.32.a shows how the concentration of non-settleable sludge decreases through the tank due to flocculation and gives only very low concentrations near the effluent weirs. From the eddy viscosity the higher values are seen above the sludge blanket near the effluent weirs and in the short circuit flow towards the recirculation pit. The eddy viscosity disappears in the sludge blanket due to the effects of density differences.

Despite the mentioned simulation problems the simulation did show the correct large scale motions in the settling tank and correct behaviour of the model variables in each of the 4 different submodels.

7.3 Conclusion on validation

The Lynetten measurements consisted of the basic measurements, steady measurements with measurement of retention time and unsteady measurements where the effects of a change in the influent was measured. The full scale measurements, where profiles of the mean horizontal velocity and the sludge concentration are measured, shows that the expected relationship between these two profiles is similar to the model tank measurements.

For the calibration of the rheology is first used the model tank calibrations for Bingham plastic characteristic. The Bingham plastic description proved unable to describe the mixing zone where the influent divides into the density current and a short circuit flow and where the scraper and the withdrawal to the recirculation flow, transports sludge from the sludge blanket towards the recirculation pit. A new approach where the viscosity of the suspension only depends on the sludge concentration shows a better description of the mentioned mixing zones. The calibrated model can not predict the exact values of the model variables in comparison with the measurements, but can predict the large scale motion and shows the expected behaviour for each of the 4 submodels.

In the Slagelse measurements problems arose with regard to the transient load of the secondary settling tanks. Therefore, the measurements were only unsteady where the effect of a change in the influent was followed and also here the transient load affected the quality of the measurements.

In the simulation of the measurements at Slagelse, the numerical model is calibrated with the same approach as for Lynetten. Similar to the simulation of the Lynetten measurements, the model can not predict the exact values of the model variables for the measurements at Slagelse. But the full scale motion can be predicted to some extend.

The validation of the numerical model to full scale measurements shows that the combination of an advanced numerical model, basic measurements and full scale measurements results in a model which can describe the different processes in a settling tank. The description of the different processes shows the right pattern, but is not precise enough to give the correct values of the model variables.

8. IMPROVEMENT OF A SECONDARY SETTLING TANK USING THE NUMERICAL MODEL

In this chapter the numerical model is used to examine the effects of changes in a settling tank on the efficiency of the tanks. Despite the problems with the model simulation described in chapter 7 the settling tank at Lynetten is used as an example. The initial conditions is the same as the conditions used for simulation of the settling tank at Lynetten except for the effluent weirs which are extended to the double length. The effluent weirs are thus placed over the last 18 m of the settling tanks. The new simulation results are shown in Fig. 8.1 and Fig. 8.2 and the effluent concentration is found to be 0.167 kgSS/m^3 and the recirculation concentration is 13.0 kgSS/m^3.

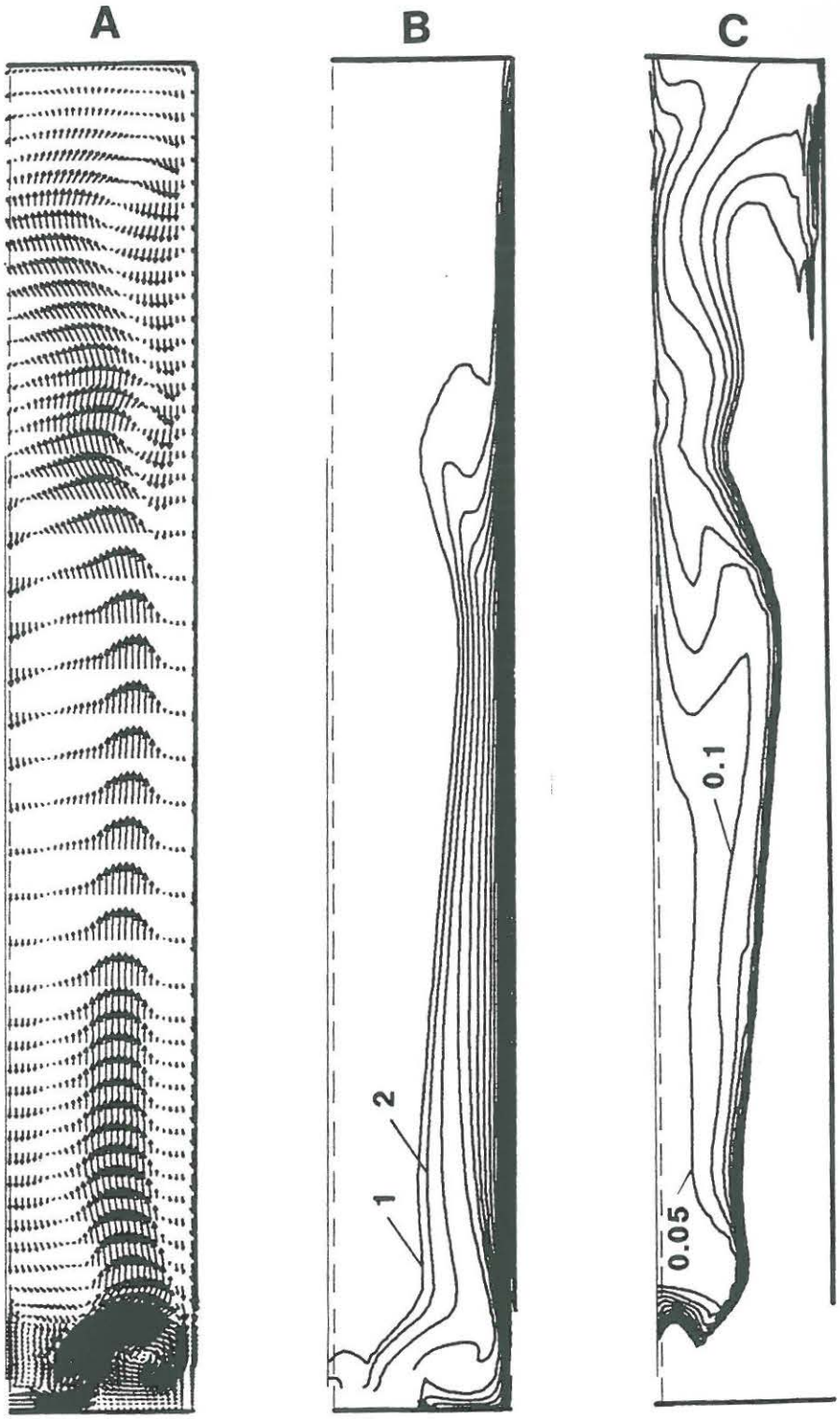

Fig. 8.1. a. Flow field. b and c. Settleable sludge with 1.0 kgSS/m^3 and 0.05 kgSS/m^3 iso-concentration curves, respectively.

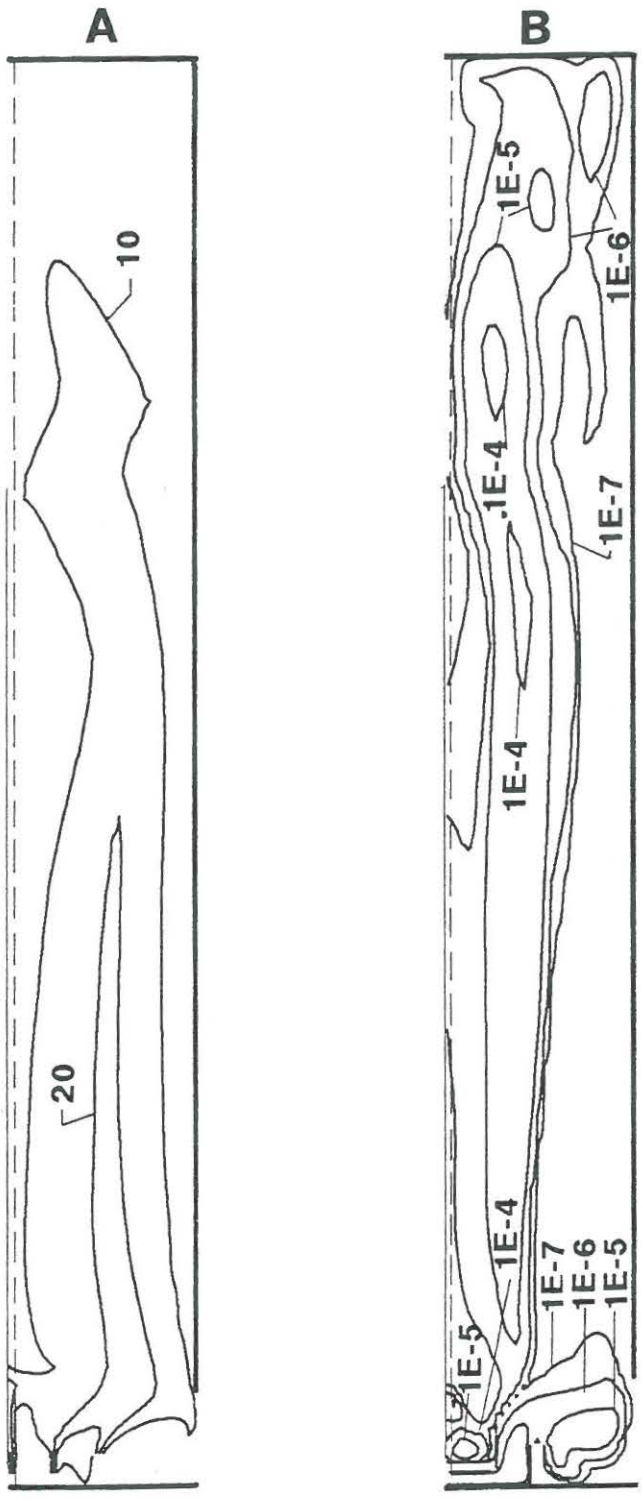

Fig. 8.2. a. Non-settleable sludge with 0.01 kgSS/m^3 iso-concentration curves. b. Eddy viscosity iso-curves.

The main result is a small improvement of the effluent quality of 0.012 kgSS/m^3 which is equal to a 7% improvement. This improvement is a result of small flow velocities towards the effluent weirs due to a larger area with effluent weirs. Fig. 8.1.a shows the larger area from the flow field. Otherwise the changes are very small. A numerical model can thus be used to examine different kinds of changes in a settling tank.

9. FINAL DISCUSSIONS AND CONCLUSIONS

The aim of the present work was to develop a numerical model for simulation of secondary settling tanks. The numerical model comprises 4 submodels which describe the prevailing processes pointed out in the system analysis: hydrodynamic, turbulence, transport and flocculation in settling tanks. The most general conclusions that emerge from this study can be summarised in the following way:

- In the existing design practice of secondary settling tanks many of the physical processes which are important to the flow and sludge transport in the settling tanks were not included directly.

- Despite some problems with simulation of full scale tanks, the numerical model could be used for predicting a relative improvement of a settling tank by changing the effluent weirs. The existing numerical model can thus be used to examine relative changes, but not yet for actual design of secondary settling tanks.

The more specific conclusions can be outlined in the following way:

- The developed basic measurement procedures provided measurements of settling velocities, flocculation and density which gave a reasonably good model description of these physical processes.

- In the results from the model tank and full scale measurements agreement with pictures discussed in the system analysis was seen for the large scale motions. The measurements showed the characteristic density current, a steady sludge blanket and countercurrent velocities above the density current.

- Through a calibration of the parameters in the Bingham plastic model description, the numerical model simulated the model tank measurements with reasonable agreement. Also for the validation, in which the model simulation was compared with new measurement, the numerical model predicted the measurements reasonably well.

- In the validation of the numerical model for full scale secondary settling tanks a poorer reproduction of the measurements was found by the model simulations. The model simulations could predict the large scale motion, but not giving the correct values for all the model variables. The critical point in the numerical model was found to be the model description of the Bingham plastic suspension.

Visions

In order to use the numerical model for predicting the effect of modifications to improve the performance of existing settling tanks and for developing new design practices for settling tanks, it is necessary to improve some model descriptions.

- Especially the model description of the Bingham plastic characteristic can be improved to enable the numerical model to better predict the large scale motions. A better large scale prediction is fundamental to improve the numerical model

- Furthermore, an improvement of the measurements and model description of flocculation and settling still remain, both in the free and hindered settling regimes. The physical effect of the sludge collection system on the flow field near the bottom of the settling tank is not described well in the literature. Therefore, the present description of scrapers can therefore be improved, when more knowledge is available.

LIST OF SYMBOLS

Symbol	Unit	Description
$(\tilde{})$		Instantaneous value
$(\bar{})$		Time average value
$(\,)'$		Fluctuation value
α		Measured angle or constant
δ_{ij}		Kronecker delta
η	kg/s	Plastic viscosity
$\dot{\gamma}$	s^{-1}	Velocity gradient
$\dot{\gamma}^*$	s^{-1}	Velocity gradient at last time step
κ		von Kármáns's constant
λ	m^2/s	Molecular diffusion coefficient
μ	kg/s	Dynamic viscosity
ν	m^2/s	Kinematic viscosity
ν_t	m^2/s	Eddy viscosity
ρ	kg/m^3	Density
ρ_r	kg/m^3	Reference density
σ_t		Turbulent Pradtl number for matter
σ_k		Turbulent Pradtl number for kinetic energy
σ_ϵ		Turbulent Pradtl number for dissipation
Ω		Short circuit factor
τ	N/m^3	Shear stress
τ_y	N/m^2	Critical shear stress or yield strength
ϵ	m^2/s^3	Dissipation
η	kg/ms	Bingham plastic viscosity
Φ	m^3/m^3	Volumetric concentration
Φ_p	kg/ms^3	Work of shear per unit of volume per unit of time
Φ_m	kg/ms^3	Mean of Φ_p in a volume
A	m^2	Area
C	kg/m^3	Dissolved substance concentration
C_f	kg/m^3	Floc concentration
C_P	kg/m^3	Dispersed particle concentration
C_0	kg/m^3	Tracer concentration for full mixing
c_D		Empirical constant in 1-eqn. turbulence model
c_μ		Empirical constant in 2-eqn. turbulence model
$c_{1\epsilon}$		Dissipation generation constant, do.
$c_{2\epsilon}$		Dissipation decay constant, do.
$c_{3\epsilon}$		Richardson constant, do.
D	m	Diameter
E		Roughness parameter
G	s^{-1}	Root mean-square (rms) velocity gradient
G_k	m^2/s^3	Buoyancy production/destruction rate of k
G_p	s^{-1}	Velocity gradient at one point

G_m	s^{-1}	Mean of G_p in a volume
g	m/s^2	Gravitational acceleration
H	m	Height
HOB	m/h	Hydraulic surface load
i		Tensor indices
j		Tensor indices
K_A		Flocculation constant
K_B		Disintegration constant
k	m^2/s^2	Turbulent kinetic energy
L	m	Length scale
MLSS	$kgSS/m^3$	Suspended sludge concentration in process tank
P	N/m^2	Pressure
P_k	m^2/s^3	Production rate of k
Q	m^3/h	Flow rate
Q_r	m^3/h	Recirculation flow rate
R		Recirculation factor
R_f	$kgSS/m^3s$	Flocculation rate
R_P	$kgSS/m^3s$	Disintegration rate
S	$kgSS/m^3s$	Source term, settling
S_f	$kgSS/m^3s$	Source term, flocculation of flocs
S_p	$kgSS/m^3s$	Source term, flocculation of dispersed particles
SS	$kgSS/m^3$	Suspended sludge or solid concentration
SVI	ml/g	Sludge volume index
T	s	Mean retension time
t	s	Time
t_a	s	Averaging time
t_e	s	Sludge concentration time
U	m/s	Velocity component in numerical model
U_f	m/s	Resultant friction velocity
U_i	m/s	Cartesian velocity component
U_{res}	m/s	Resultant velocity parallel to the bottom
V	m/s	Velocity component in numerical model
$\hat{V}$	m/s	Velocity scale
v	m/s	Settling velocity
v_i	m/s	Settling velocity for the i'th fraction of the sludge
v_o	m/s	Settling velocity in free settling regime
v_s	m/s	Settling velocity in hindered settling regime
x	m	Cartesian space co-ordinate
y	m	Distance from wall to first grid point
y*		Dimensionless wall distance

LIST OF REFERENCES

Adams E.W. and Rodi W., 1990. Modelling flow and mixing in sedimen tation tanks. *Hyd. Eng.* Vol. 116, No. 7, pp. 895-913.

Andreasen K, Nielsen P.H., Jørgensen P.E, Sigvardsen L. and Holm G., 1990, in Danish. Let slam - et problem i danske renseanlæg. *Vand og Miljø*, No. 8, pp. 283-286.

ATV-Arbeitsberichte 1988. Schlamräumungssysteme für Nachklärbeck en von Belebungsanlagen. *Korrespondenz Abwasser*, 3/88, 35. Jahrgang.

ATV-Regelwerk, 1991. Bemessung von einstufigen Belebungsanlagen ab 5000 Einwohnewerten. *Abwasser-Abfall*, DK 628.356:62832.001.2 (083) Arbeitsblatt A131 Februar.

Billmeier E., 1988. The influence of blade height on the removal of sludge from activated sludge settling tanks. *Wat. Sci. Tech.*, Vol. 20, No. 4/5, pp 165-175.

Bokil S.D. and Bewta J.K., 1972. Influence of Mechanical Blending on Aerobic Digestion of Waste Activated Sludge. *6th Int. Conf. on Water Pollution Research*, Jerusalem, Israel, pp. 421-438.

Buscall B. and White L.R., 1987. The Consolidation of Concentrated Suspensions. *J. Chem. Soc.*, Faraday Trans. 1, 83, pp 873-891.

Cailleaux C., Pujol E. deDianous F. and Druoton J.C., 1992. Study of weighted flocculation in view of a new type of clarifier. *J. Water SRT-Aqua*, Vol. 41, No. 1, pp. 18-27.

Camp T.R. and Stein P.C., 1943. Velocity gradients and internal work in fluid motion. *J. Boston Soci. Civ. Eng.*, Vol. 30, No. 4, pp. 219-237.

Camp T.R., 1946. Sedimentation and the design of settling tnaks. *Transaction, ASCE,* Paper No. 2285, Vol. 111, pp. 895-937.

Campbell H. and Crescuolo P.J., 1982. The use of rheology for sludge characterization. *Wat. Sci. Tech.*, Vol. 14, Capetown, pp. 475-489.

Celik I., Rodi W. and Stamou A.I., 1985. Prediction of Hydrodynamic Characteristics of Rectangular Settling Tank. *Proc. Int. Symp. on Refined Flow Modelling and Turbulence Measurements*. Iowa City, Iowa, pp. C12-1 - C12-11.

Cordaba-Molina F.T., Hudgins R.R. and Silveston P.L, 1979. The gravity clarifier as a stratified flow phenomenon. *The Canadian J. of Che. Eng.*, Vol. 57, June, pp. 249-254.

Dahl C.P., Kjelds J.T. and Sørensen H.R., 1990, (in Danish). Numerical Modelling of a secondary clarifier. *University of Aalborg, Master Thesis in Environmental Engineering.*

Daigger G.T. and Roper R.E. jr., 1985. The relationship between SVI and activated sludge settling characteristics. *Journal WPCF*, Vol. 57, No. 8, pp. 859-866.

Das D., Keinath T.M., Parker D.S. and Wahlberg E.J., 1993. Floc breakup in activated sludge plants. *Wat. Envir. Res.*, Vol. 65, No. 2, pp. 138-145.

Dammel E.E. and Schroeder E.D., 1991. Density of activated sludge solids. *Wat. Res.*, Vol. 25, No. 7, pp. 841-846.

De Vantier B.A. and Larock B.E., 1987. Modelling sediment induced density currents in sedimentation basins. *J. of Hydr. Eng.*, Vol. 113, No. 1, pp. 80-93.

Dich R.I. and Buck J.H., 1985. Measurement of activated sludge rhe ology. *Proceeding of the Environmental Engineering Division, ASCE*, Vol. 111, pp. 539-545.

Dich R.I. and Ewing B.B., 1967. The rheology of activated sludge. *Journal WPCF*, Vol. 39, No. 4, pp. 543-560.

Esteban G., Tellez C. and Bautista L.M., 1991. Dynamic of ciliated protozoe communities in activated sludge process. *Wat. Res.*, Vol. 25, No. 8, pp. 967-972.

Eikelboom D.H. and Buijsen H.J.J., 1981. Microscopic Sludge Investiga tion Manual. *Report A94a*, IMG-TMO Delft.

Imam E. and McCorquadale I.A., 1983. Simulation of flow in rectangular Clarifiers. *J. of Envir. Eng.* Vol. 109, No. 3, pp. 713-730.

Imam E., McCorquodale I.A. and Bewta I.K., 1983. Numerical Modelling of Sedimentation Tanks. *J. of Hydr. Eng.*, Vol. 109, No. 12, pp. 1740-1754.

Javaheri A.R. and Dick R.I., 1969. Aggregate size variations during thickening of activated sludge. *journal WPCF*, Vol. 41, No. 5 Part 2, pp. R197-R214.

Koopman B. and Cadee K., 1983. Prediction of thickening capacity using diluted sludge volume index. *Wat. Res.*, Vol. 7, No. 10, pp. 1427-1431.

Krebs P., 1991. Modellierung und Verbesserung der Strömung in Nachklärbecken. *Dissertation No. 9486*, Swiss Federal Institute of Technology (ETH) Zürich, Switzerland.

Krüger, 1993. Design af efterklaringstanke. *Internal Notes not official.* T1020.DK.

Larock B.E., Chun W.K.C. and Schamber D.R., 1983. Computation of sedimentation basin behaviour. *Wat. Res.* Vol. 17, No. 8, pp. 861-867.

Larsen P., 1977. On the hydraulics of rectangular settling basin, Experi mental and theoretical studies. *Rapport No. 1001, Department of Water Resources Engineering, Lund Institute of Technology*, Lund, Sweden.

Lavelle J.W., 1978. Effects of hindered settling on sediment concen tration profiles. *J. of Hydr. Res.*, Vol. 16, No. 4, pp. 347-355.

Li D-H. and Ganczarczyk J.J., 1986. Physical Characteristics of activated sludge flocs. *Critical Reviews in Env. Cont.*, Vol. 17, Issue 1, pp. 53-87.

Li D-H. and Ganczarczyk J.J., 1987. Stroboscopic determination of settling velocity, size and porosity of activated sludge flocs. *Wat. Res.* Vol. 21, No. 3, pp. 257-262.

Li D-H. and Ganczarczyk J.J., 1991. Size distribution of activated sludge flocs. *Res. Journal WPCF*, Vol. 63, No. 5, pp. 806-814.

Lumley D.J., 1985. Settling of activated sludge. A study of limiting Factors and Dynamic Response. *Dept. of San. Eng., Chalmer Univ. of Techn.*, Sweden, Publication 6:85.

Lumley D.J. and Balmér P., 1987. Full scale investigation of secondary settler dynamics. *Proc. 10th Symp. on Wastewater Treatment*, Montreal, 10.-11. Nov.

Lumley D.J. and Horkeby G., 1988a. Detention time distribution of sludge in rectangular secondary settler. *Poster presented at IAWPRC 14th Bien. Conf. & Exh. on Wat. Pollut. Control*, Brighton. (To be publ. in Wat.Sci.Tech.).

Lumley D.J., Balmér P. and Adamsson J., 1988b. Investigation of Secondary Settling at a Large Treatment Plant. *Wat. Sci. Tech.*, Vol. 20, No. 4/5, pp. 133-142.

Lumley D.J. and Balmér P., 1990. Solids transport in rectangular secondary settlers. *Wat. Supply*, Vol. 8, Jönköping, pp. 123-132.

Mandersloat W.G.B., Scott K.J. and Geyer C.P., 1986. Sedimentation in the hindered settling regime. *Advance in Soil - Liquid Separation edited by H.S. Muralidhara*. Betelle Memorial Institute, Ohio.

O'Melia, C.R., 1985. The influence of coagulation of the fate of particles, associated pollutants, and nutrients in lakes. *Chemical Processes in lakes*, pp. 208-224, Werner Stum (ed.), John Wiley and Sons.

Palm J.C. and Jenkins D., 1980. Relationship between organic loading, dissolved oxygen concentration and sludge settleability in the completely mixed activated sludge process. *Journal WPCF*, vol. 52, No. 10, pp. 2484-2506.

Parker D.S., 1970. Characteristics of biological flocs in turbulence regimes. *Thesis presented to the University of California, at Berkeley, Calif. in 1970*, in partial fulfilment of the requirements for the degree of Doctor of Philosophy.

Parker D.S., Kaufman W.J. and Jenkins D., 1972. Floc breakup in tur bulent flocculation processes. *J. of the San. Eng. Div. Proc. of the ASCE*, Vol. 98, No. SA1, pp. 79-99.

Patankar S.V., 1980. Numerical heat transfer and fluid flow. *Hemi sphere Publishing Corporation*, xii + 197 pp.

Petersen O., 1992. Application of turbulence models for transport of dissolved pollutants and particles. *ph.D. Thesis, Dept. of Civil. Engrng.*, University of Aalborg.

Pitman A.R., 1984. Settling of nutrient removal activated sludge. *Wat. Sci. Tech.*, Vol. 17, Amsterdam, pp. 493-504.

Rachwall A.J., Johnstone D.W.M., Hanhury M.J. and Critchard G.J., 1982. The application of settleability tests for the control of activated

sludge plants. Bulking of activated sludge -Preventative and remedial methods, pp. 224 Chapter 13. *Process Eng. Wat. Res. Centre*, Stevenage Laboratory, Herefordshire.

Rodi W., 1984. Turbulence models and their application in hydraulics - A state of the art review. IAHR Delft. The Netherland, Second revised edition.

von Smoluchowski M., 1916. Drei Vorträge über Diffusion, Brownsche Molekularbewegung und Koagulation von Kolloidteilchen. *Physih. Z.* 17 pp. 557-585.

von Smoluchowski M., 1918. Versuch einer Mathematischen Teorie der Koagulationskenetic Kolloide Lösungen. *Z. Physih. Chem.* 92, pp. 155.

Spalding, D.B, 1989. The PHOENICS beginners' guide. CHAM TR/100. *CHAM Ltd.*, Wilbledon, London.

Stamou, A.I. and Adams E.W., 1988. Study of the Hydraulic Behaviour of a Model Settling Tank using Flow Through Curves and Flow Patterns. *Sonderforschungsbereich 210*, Universität Karlsruhe.

Stamou A.I., Adams E.W. and Rodi W., 1989. Numerical modelling of flow and settling in primary rectangular clarifiers. *J. of Hydr. Res.*, Vol. 27, No. 5, pp. 665-682.

Svensson M., 1985. Numerical modelling of environmental two-phase flows. *Lecture presented at LSPRA courses on nuclear science and techn.*

Vesilind, P.A., 1968. The Influence of Stirring in the Thickening of Biological Sludge. *Ph.D. Dissertion, Dept. of Environmental Sciences and Engineering*, University of North Carolina, Chapel Hill, N.C.

Wahlberg E.J. and Keinoth T.M., 1988. Development of steeling flux curves using SVI. *Journal WPCF*, Vol. 60, No. 12, pp. 2095-2100.

White M.J.D., 1976. Design and Control of Secondary Settlement Tanks. *I. Inst. Wat. Pollut. Control*, pp. 464.

Wood R.F. and Dick R.I., 1975. Some effects of sludge characteristics on dissolved air flotation. *Prog. in Wat. Tech.*, Vol. 7, No. 2, pp. 173-182.

Ødegaard H., 1979. Orthokinetic flocculation of phosphate precipitates in a multicompartment reactor with non-ideal flow. *Prog. Wat. Tech.*, Suppl. 1, pp. 61-88.

APPENDIX 1

A.1 Hydrodynamic, turbulence, transport and flocculation theory

The following appendix describes the theory behind the governing partial differential equation for the numerical models. The used equations are a result of the choices for the numerical models described in section 3.4.

A.1.1 Hydrodynamic and transport models

First, the governing equations for the mean flow quantities are presented. For the conservation of mass a continuity equation is formed presuming that mass and velocity are continuous functions in space and time. For a field volume and incompressible fluid the density is constant and the conservation of mass is reduced to conservation of volume. In tensor notations the equation yield.

Continuity equation (Mass conservation):

$$\frac{\partial \tilde{U}_i}{\partial x_i} = 0 \qquad \text{(A1.1)}$$

Here $\tilde{U}_i$ denotes the instantaneous velocity component and x_i is a cartesian spatial coordinate. An equation for conservation of momentum can be found by applying Newton's 2nd law on an elementary volume of fluid. Assuming that the fluid is isotropic and incompressible and using Boussinesq's approximation, that assume that variation in density are small compared to the absolute value the equation yield.

Navier-Stokes equations (Momentum conservation):

$$\frac{\partial \tilde{U}_i}{\partial t} + \tilde{U}_j \frac{\partial \tilde{U}_i}{\partial x_j} = -\frac{1}{\rho_r}\frac{\partial \tilde{P}}{\partial x_i} + \nu \frac{\partial^2 \tilde{U}_i}{\partial x_j \partial x_j} + g_i \frac{\rho - \rho_r}{\rho_r} \qquad \text{(A1.2)}$$

t denotes the time, ρ_r is the reference density, ρ is the local density, $\tilde{P}$ is the instantaneous pressure and g_i is the gravitational acceleration component. Combining Fick's 1st law and the conservation of mass for an elementary volume of fluid yields an equation for conservation of concentration.

Transport/dispersion equation (Concentration conservation):

$$\frac{\partial \tilde{C}}{\partial t}+\tilde{U}_j\frac{\partial \tilde{C}}{\partial x_j}=\lambda\frac{\partial^2 \tilde{C}}{\partial x_j \partial x_j}+S \qquad \text{(A1.3)}$$

where $\tilde{C}$ is the instantaneous species concentration, λ is the diffusivity and S is a source term for e.g. settling.

Most flows of practical interest are influenced by turbulence. In theory equation (A1.1) - (A1.3) form a close set and are able to describe all details of the turbulent motion. But in practice, computer storage capacity and available computer simulation time is at present far from what is necessary for the use of these exact equations to describe turbulent motion. The reason is that turbulent motion contains motion in a very small scale, typically 10^{-3} of the extent of the flow domain. To set-up a numerical grid to cover these small turbulent motions is totally unrealistic. Another approach is therefore needed to describe turbulent motion (Rodi 1984).

In order to reduce the amount of information a statistical approach is called for and the instantaneous values of $\tilde{U}_i$, $\tilde{P}$ and $\tilde{C}$ are separated into mean $\bar{U}_i$, $\bar{P}$ and $\bar{C}$ and fluctuating u'_i, p' and c' quantities.

$$\tilde{U}_i=\bar{U}_i+u_i' \qquad \tilde{P}=\bar{P}+p' \qquad \tilde{C}_i=\bar{C}+c' \qquad \text{(A1.4)}$$

Equation (A1.4) has been developed with the assumption of isotropic turbulence. The mean quantities are defined as shown for $\bar{U}_i$

$$\bar{U}_i=\frac{1}{t_a}\int_0^{t_a}\tilde{U}_i dt \qquad \text{(A1.5)}$$

and the time mean of the fluctuation is zero by definition.

$$\frac{1}{t_a}\int_0^{t_a}u_i' dt=0 \qquad \text{(A1.6)}$$

where the averaging time t_a is long compared to the time scale of the turbulent motion.

Inserting (A1.4) in (A1.1) - (A1.3) using the average from (A1.5) and (A1.6) gives the following equations.

Continuity equation:

$$\frac{\partial U_i}{\partial x_j}=0 \tag{A1.7}$$

Momentum equation:

$$\frac{\partial U_i}{\partial t}+U_j\frac{\partial U_i}{\partial x_j}=-\frac{1}{\rho_r}\frac{\partial P}{\partial x_i}+\frac{\partial}{\partial x_j}\left(\nu\frac{\partial U_i}{\partial x_j}-\overline{u_i'u_j'}\right)+g_i\frac{\rho-\rho_r}{\rho_r} \tag{A1.8}$$

Transport dispersion equation:

$$\frac{\partial C}{\partial t}+U_j\frac{\partial C}{\partial x_j}=\frac{\partial}{\partial x_j}\left(\lambda\frac{\partial C}{\partial x_i}-\overline{u_j'c'}\right)+S \tag{A1.9}$$

Where U_i, P and C now are the mean quantities. These equations are also exact as no assumptions are made, but they do no longer form a closed set of equations due to unknown correlations $\overline{u_i'u_j'}$ and $\overline{u_i'c'}$. The quantity $\overline{u_i'u_j'}$ becomes either normal stresses when (i = j) and shear stresses when ($i \neq j$). These stresses are called Reynold-stresses. Similar to a laminar flow Boussinesq assumed in analogy with Newton's formula for viscous shear, that a linear relation exists between the turbulent stresses and the mean velocity gradients. For general flow situation this eddy viscosity concept gives.

$$-\overline{u_i'u_j'}=\nu_t\left(\frac{\partial U_i}{\partial x_j}+\frac{\partial U_j}{\partial x_i}\right)-\frac{2}{3}k\cdot\delta_{ij} \tag{A1.10}$$

where ν_t is the turbulent eddy viscosity, k is the kinetic energy and δ_{ij} is the Kronecker delta ($\delta_{ij} = 1$ for i = j and $\delta_{ij} = 0$ for $i \neq j$). The second term on the right side of (A1.10) is included to make the expression applicable also to normal stresses. The first term on the right side of (A1.10) yield for normal stresses (one direction as an example).

$$\overline{u_i'^2}=-2\nu_t\frac{\partial U_1}{\partial x_1} \tag{A1.11}$$

The sum of the all normal stresses are zero to satisfy the continuity equation (A1.7). However, by definition all normal stresses are positive, and the sum is twice the kinetic energy.

$$k=\frac{1}{2}\left(\overline{u_1'^2}+\overline{u_2'^2}+\overline{u_3'^2}\right) \qquad \text{(A1.12)}$$

In order to ensure this definition, the second term on the right hand side in (A1.10) is included. Nevertheless, this term can be absorbed by the pressure gradient term with the pressure at P + ⅔ k. Therefore, with the assumption in (A1.10) the unknown Reynolds stresses are reduced to one unknown parameter the eddy viscosity ν_t.

The shear stresses τ in turbulent motion is for both laminar and turbulent sheer stresses from (A1.8) equal to

$$\tau=\mu\frac{\partial U_i}{\partial x_j}-\rho\overline{u_i'u_j'} \qquad \text{(A1.13)}$$

where μ is the dynamic viscosity. The laminar sheer stresses are negligible to turbulent sheer stresses in turbulent flows except from the viscose boundary layers. But in a description of a Bingham plastic suspension, the laminar sheer stresses excite the turbulent sheer stresses in some cases. Both sheer stresses are therefore taken into account in the following equation. By including (A1.10) and (A1.11) in (A1.7) - (A1.9), the following equations with only the mean quantities are formed.

Continuity equation

$$\frac{\partial U_i}{\partial x_i}=0 \qquad \text{(A1.14)}$$

Momentum equation

$$\frac{\partial U_i}{\partial t}+U_j\frac{\partial U_i}{\partial x_i}=-\frac{1}{\rho_r}\frac{\partial P}{\partial x_i}+\frac{\partial}{\partial x_j}\left((\nu_t+\nu)\frac{\partial U_i}{\partial x_j}\right)+g_i\frac{\rho-\rho_r}{\rho_r} \qquad \text{(A1.15)}$$

Transport/dispersion equation

$$\frac{\partial C}{\partial t}+U_j\frac{\partial C}{\partial x_i}=\frac{\partial}{\partial x_i}\left((\nu_t+\nu)\frac{\partial C}{\partial x_i}\right)+S \qquad \text{(A1.16)}$$

A.1.2 Turbulence model

With (A1.14) - (A1.16) the eddy viscosity ν_t is the only parameter to be determined to close the set of equations. ν_t is in turbulence models used

as the parameter for the turbulent motion. The eddy viscosity ν_t is in contrast to the molecular viscosity ν not a fluid property but depends strongly on the state of the turbulence and may vary considerably over the flow field. The close analogy between the laminar and turbulence stresses which is the basis of the eddy viscosity concept has been criticised for the physical differences. Further, it is important to note that turbulence models do not describe the details of the turbulent fluctuations but only the average effects of these terms on the mean quantities. Nevertheless, the eddy viscosity concept has proven to give good results for various kinds of flows because ν_t as defined in equation (A1.10) can be determined to good approximations.

The eddy viscosity ν_t is proportional to a velocity scale $\hat{V}$ and a length scale L characterising the large scale turbulent motion.

$$\nu_t \propto \hat{V} \cdot L \tag{A1.17}$$

Actually, it is the distribution of these scales which can be approximated reasonably well in many flows. As the turbulence model, the k-ϵ model is chosen due to its ability to describe the transport/dispersion of the turbulent motion. The kinetic energy of the turbulent motion (per unit masse) k is from (A1.12) seen to be a natural scala for the turbulent fluctuations where

$$\hat{V} = \sqrt{k} \tag{A1.18}$$

Including (A1.17) in (A1.18) the following relations occur in the eddy viscosity relation.

$$\nu_t = c'_\mu \sqrt{k} L \tag{A1.19}$$

where c'_μ is an empirical constant.

For turbulent motion the large eddies interact with the mean flow and thereby extracting kinetic energy from the mean motion and feeding it into large scale turbulent motion. The eddies can be considered as vortex elements which stretch each other. Due to this, energy is passed on to smaller and smaller eddies until viscose forces became active and dissipate the energy into heat. This process is called energy cascade. The dissipation rate of turbulence ϵ is therefore depending on the large scale motion although dissipation takes place in the smallest eddies. The dissipation process is usually modelled by the expression

$$\epsilon = c_D \frac{k^{3/2}}{L} \tag{A1.20}$$

By including (A1.20) in (A1.19) the ϵ is included in the eddy viscosity relations by

$$\nu_t = c_\mu \frac{k^2}{\epsilon} \tag{A1.21}$$

where $c_\mu = c'_\mu \cdot c_D$ is empirical constants. Equation (A1.21) forms together with transport/dispersion equations for k and ϵ based on Naviere-Stokes equation the so called k-ϵ turbulence model.

$$\frac{\partial k}{\partial t} + U_i \frac{\partial k}{\partial x_i} = \frac{\partial}{\partial x_i}\left(\frac{\nu_t}{\sigma_k}\frac{\partial k}{\partial x_i}\right) + P_k + G_k - \epsilon \tag{A1.22}$$

$$\frac{\partial \epsilon}{\partial t} + U_i \frac{\partial \epsilon}{\partial x_i} = \frac{\partial}{\partial x_i}\left(\frac{\nu_t}{\sigma_\epsilon}\frac{\partial \epsilon}{\partial x_i}\right) + c_{1\epsilon}\frac{\epsilon}{k}P_k + c_{1\epsilon}\frac{\epsilon}{k}(1 - c_{3\epsilon})G_k - c_{2\epsilon}\frac{\epsilon^2}{k} \tag{A1.23}$$

where σ_k and σ_ϵ are empirical diffusion constants (Prandtl numbers) and $c_{1\epsilon}$, $c_{2\epsilon}$ and $c_{3\epsilon}$ are empirical constants. P_k is the production of kinetic energy from the mean flow defined as:

$$P_k = \nu_t \left(\frac{\partial U_i}{\partial x_J} + \frac{\partial U_j}{\partial x_i}\right)\frac{\partial U_i}{\partial x_j} \tag{A1.24}$$

G_k is the production/destruction of kinetic energy from density differences defined as

$$G_k = \frac{g}{\rho}\frac{\nu_t}{\sigma_t}\frac{\partial \rho}{\partial x_i} \tag{A1.25}$$

where g is the gravitational acceleration. To the standard k-ϵ model the values of constants are shown in Table (A1.1) (Rodi, 1984).

c_μ	$c_{1\epsilon}$	$c_{2\epsilon}$	σ_k	σ_ϵ	σ_t	$c_{3\epsilon}$
0.09	1.44	1.92	1.0	1.3	1.0	0.8

Table A1.1. Values of constants in the k-ϵ model.

The values in Table A1.1 have been found by calibration between a number of well-documented laboratory shear flows and model prediction to give the best overall agreement.

Boundary equations

For wall boundaries very steep gradients in velocity prevail in the viscose sublayer so that many grid points must be used for a proper solution. Furthermore, viscose effects are important in this layer so that high reynolds-number turbulence models as the k-ϵ model are not applicable. By empirical laws the wall conditions can be connected to the dependent variables just outside the viscose sublayer. The universal law of the wall may be expressed as.

$$\frac{U_{res}}{U_f} = \frac{1}{\kappa} \ln(y^* \cdot E) \qquad \text{(A1.26)}$$

where U_{res} is the resultant velocity parallel to the wall, U_f is the resultant friction velocity, $y^* = (y \cdot U_f)/\nu$ is a dimensionless wall distance, κ is the von Kármán constant and E is a roughness parameter (E = 9 for hydraulic smooth walls).

In the sublayer local equilibrium prevails and the turbulence production P_k is equal to the dissipation ϵ. The boundary equations for k and ϵ is.

$$\frac{k}{U_f^2} = \frac{1}{\sqrt{c_\mu}} \qquad \text{(A1.27)}$$

$$\epsilon = \frac{U_f^3}{\kappa y} \qquad \text{(A1.28)}$$

A.1.3. Flocculation model

A two fraction flocculation model is chosen to describe the relationship between dispersed particles and flocs. The flocculation rate R_f and the disintegration rate R_P are shown in equations (A1.29) and (A1.30)

$$R_f = K_A \cdot C_P \cdot C_f \cdot G \qquad \text{(A1.29)}$$

$$R_P = K_B \cdot C_f \cdot G^2 \qquad \text{(A1.30)}$$

where

$$G = \sqrt{\frac{\epsilon}{\nu}} \qquad \text{(A1.31)}$$

is the rms velocity gradient, K_A and K_B are constants and C_f, C_P are concentration of flocs and dispersed particles, respectively. The flocculation and disintegration balance between dispersed particles and flocs is found in all points and the source terms S_p and S_f for the dispersed particles and flocs, respectively is found.

$$S_f = R_f - R_p \qquad \text{(A1.32)}$$

$$S_p = R_p - R_f \qquad \text{(A1.33)}$$

A transport/dispersion equation as (A1.17) are used for each of the two fractions of sludge dispersed particles and flocs. The source terms are included in these equations.

APPENDIX 2

A.2 Numerical solutions

This appendix describes the numerical solution used in the numerical model, developed in the program PHOENICS. When using PHOENICS, different numerical schemes can be chosen, but the default scheme gives the best solution with respect to fluid flow problems like secondary settling tanks (Spalding, 1989). The default scheme is the implicit Hybrid scheme, which will be described in the following using a one-dimensional conversion and diffusion equation as an example.

A.2.1. Forms of discretisation

First of all, this subsection describes the form or term used in the following subsections for discretisation, giving the equation

$$\frac{d}{dx}\left(K\frac{dT}{dx}\right)+S=0 \qquad \text{(A2.1)}$$

Integration of (A2.1) over the control volume in Fig. A.2.1 gives.

$$\left(K\frac{dT}{dx}\right)_e - \left(K\frac{dT}{dx}\right)_w + \int_w^e S dx = 0 \qquad \text{(A2.1)}$$

The discretisation of this equation with piecewise linear profile discretisation according to the grid in Fig. A.2.1 gives

$$\frac{K_e(T_E-T_p)}{(\delta x)_e} - \frac{K_w(T_P-T_w)}{(\delta x)_w} + \bar{S}\Delta x=0 \qquad \text{(A2.3)}$$

where $\bar{S}$ is the mean of S in the control volume.

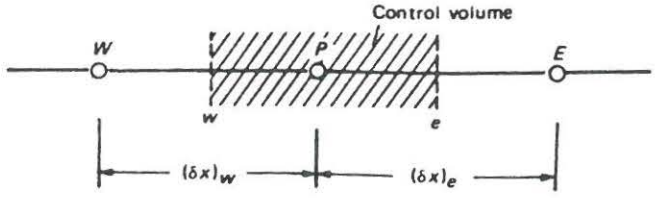

Fig. A2.1. Grid point cluster for the one-dimentional problem (Patankar, 1980).

(A2.3) can be rearranged to the form used in the following section:

$$a_P T_P = a_E T_E + a_W T_W + b \tag{A2.4}$$

$$a_E = \frac{K_e}{(\delta x)_e} \tag{A2.4a}$$

$$a_W = \frac{K_w}{(\delta x)_w} \tag{A2.4b}$$

$$a_P = a_E + a_W \tag{A2.4c}$$

$$b = \overline{S}\,\Delta x \tag{A2.4d}$$

A.2.2 Central difference scheme

To illustrate the different discretisation schemes a one-dimensional conversion and diffusion equation is used.

$$\frac{d}{dx}(\rho u \phi) = \frac{d}{dx}\left(\Gamma \frac{d\phi}{dx}\right) \tag{A2.5}$$

Integration of (A.2.5) over the control volume shown in Fig. A.2.1 gives the following:

$$(\rho u \phi)_e - (\rho u \phi)_w = \left(\Gamma \frac{d\phi}{dx}\right)_e - \left(\Gamma \frac{d\phi}{dx}\right)_w \tag{A2.6}$$

with piecewise linear profile discretisation

$$\frac{1}{2}(\rho u)_e(\phi_E+\phi_P)-\frac{1}{2}(\rho u)_w(\phi_P+\phi_W)=$$

$$\frac{\Gamma_e(\phi_E-\phi_P}{(\delta x)_e}-\frac{\Gamma_w(\phi_P-\phi_W)}{(\delta x)_w} \qquad \text{(A2.7)}$$

where the factor ½ arises from the acceptance of the interface to the control volume being midway between the grid points. Another integration factor would otherwise be used. Two new symbols are defined to.

$$F=\rho u \qquad D=\frac{\Gamma}{\delta x} \qquad \text{(A2.8)}$$

where F indicates the strength of the convection (or flow), while D is the diffusion conductance.

Using (A2.8) and rearranging (A.2.7) to the forms described in subsection A.2.1 the following set of equations occur for the central difference scheme.

$$a_P\phi_P=a_E\phi_E+a_W\phi_W \qquad \text{(A2.9)}$$

where

$$a_E=D_e-\frac{F_e}{2} \qquad \text{(A2.9a)}$$

$$a_W=D_w+\frac{F_w}{2} \qquad \text{(A2.9b)}$$

$$a_P=a_E+a_W+(F_e-F_w) \qquad \text{(A2.9d)}$$

By continuity $F_e = F_w$ and $a_P = a_E + a_W$ (Patankar, 1980).

A.2.3. Upwind difference scheme

The upwind scheme corrects a weak point in the central scheme with the assumption that the averaged property Φ_e at the interface is the average

of Φ_E and Φ_P and propose a better description (Patanker, 1980). The diffusion terms are untouched. The value of Φ at an interface is equal to the value of Φ at the grid point on the upwind side of the face, which gives:

$$\phi_e=\phi_P \quad if \quad F_e>0 \tag{A2.10a}$$

$$\phi_e=\phi_E \quad if \quad F_e<0 \tag{A2.10b}$$

an equal for Φ_w. Note that F_e can be both positive and negative due to the definition depending on the direction of u. Using the term $[\![A.B]\!]$, which denotes the greatest of A and B (A.2.10) can be compressed to:

$$F_e\phi_e=\phi_P [\![F_e,O]\!] - \phi_E [\![-F_e,O]\!] \tag{A2.11}$$

and the discretisation equation for the upwind difference scheme becomes:

$$a_P\phi_P=a_E\phi_E+a_W\phi_W \tag{A2.12}$$

where

$$a_E=D_e+[\![-F_e,O]\!] \tag{A2.12.a}$$

$$a_W=D_w+[\![F_w,O]\!] \tag{A2.12.b}$$

$$a_P=a_E+a_W+(F_e-F_w) \tag{A2.12.c}$$

The construction of the upwind scheme results in a scheme where the fluid would not know anything about the volume which it is heading for. This gives a physical realistic solution, but not always as close to the exact solution as other schemes (Patankar, 1980).

A.2.4. The hybrid difference scheme

To describe the hybrid difference scheme, the new symbol P_e the Peclet number is defined by

$$P_e=\frac{F}{D} \tag{A2.13}$$

The hybrid scheme is developed as a combination of the central difference scheme and the upwind difference scheme as will be shown. The whole idea is to create a scheme close to the exact solution for all P_e (Patankar, 1980). The use of the dimension form a_E/D_e as a function of P_e is shown in Fig. A.2.2, where the central difference scheme is used for $-2 \leq P_e \leq 2$ and the upwind difference scheme outside this P_e interval and with the diffusion set equal to zero (Patankar, 1980).

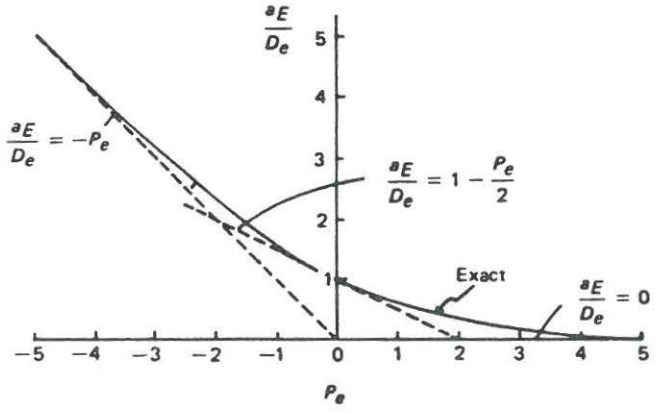

Fig. A.2.2. a_E/D_e as a funktion of P_e for hybrid difference scheme (Patankar, 1980).

The three lines in Fig. A.2.2 describing the hybrid difference scheme can be described by:

For $P_e < -2$

$$\frac{a_E}{D_e} = -P_e \tag{A2.14}$$

For $-2 \leq P_e \leq 2$

$$\frac{a_E}{D_e} = 1 - \frac{P_e}{2} \tag{A2.15}$$

For $P_e > 2$

$$\frac{a_E}{D_e} = O \tag{A2.16}$$

The discretisation equation for the hybrid differences scheme becomes:

$$a_P\phi_P = a_E\phi_E + a_W\phi_W \tag{A2.17}$$

where

$$a_E = [\![-F_e, D_e - \frac{F_e}{2}, O]\!] \tag{A2.17a}$$

$$a_W = [\![F_w, D_w + \frac{F_w}{2}, 0]\!] \qquad \text{(A2.17b)}$$

$$a_P = a_E + a_W + (F_e - F_w) \qquad \text{(A2.17c)}$$

Fig. A.2.3 shows how the hybrid difference scheme makes a close description of the exact solution for all P_e and therefore becomes a very stable scheme.

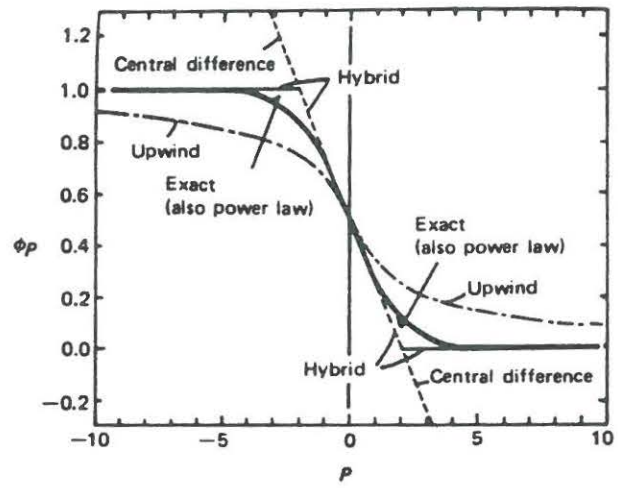

Fig. A.2.3 Φ_P predicted by different schemes for a range of P_e (Parankar, 1980).

From Fig. A.2.3 is also seen that the hybrid difference scheme uses the most exact parts of the central and upwind difference scheme (Patankar, 1980).

Krüger Systems

RAPPORTDATABLAD

Titel:	Numerical modelling of flow and settling in secondary settling tanks.
Nøgleord:	Efterklaringstanke, systemanalyse, numerisk modellering, målemetoder, modeltank, fuldskalamålinger.

Udgivelsesdato:	08.11.1993		
Selskab:	KSY	**Afd.:**	082
Forfatter(e):	Claus Dahl		

Sekretær:	BJ
Rapport mrk.:	FD82-5
Antal sider:	150 + bilag
Rapport udsendt til:	ATV, EB, KNJ, censorer: Torben Larsen, AUC, Ole Petersen, AUC, Poul Harremoës, LTH, BEN.

Rapport findes på biblioteket Ja/Nej: Nej

Rekvirent:	ATV
Finansiering:	ATV + IK
Kontonummer:	4082-908235
Bemærkninger:	Erhvervsforskerprojekt

CPD0095/BJ

30. november 1993